TCF-7 is dispensable for anti-tumor response but required for persistent function of mature CD8 T cells

Rebecca Harris[1*], Mahinbanu Mammadli[1*], Shannon Hiner[1], Liye Suo[2], Qi Yang[3], Jyoti Misra Sen[4,5], Mobin Karimi[1ℜ]

[1]Department of Microbiology and Immunology, SUNY Upstate Medical University, Syracuse, NY 13210.

[2]Department of Pathology, SUNY Upstate Medical University, Syracuse, NY 13210.

[3]Department of Pediatrics, Rutgers Robert Wood Johnson Medical School
Rutgers Child Health Institute of New Jersey New Brunswick, NJ 08901

[4]National Institute on Aging-National Institutes of Health, 08C218, Biomedical Research Center, 251 Bayview Boulevard, Suite 100, Baltimore, MD 21224.

[5]Immunology Program, Department of Medicine, Johns Hopkins School of Medicine, Baltimore, MD 21224.

Rebecca Harris[1*]and Mahinbanu Mammadli[1*] equally contributed to this manuscript

To whom correspondence should be addressed ℜ:
Mobin Karimi
Assistant Professor of Immunology and Microbiology
SUNY Upstate Medical University,
766 Irving Ave Weiskotten Hall Suite 2281,
Syracuse, NY 13210
Office Phone: 315-464-2344
Laboratory Phone: 315-464-7652
Email: karimim@upstate.edu

Conflict of interest statement: The authors have declared that no conflict of interest exists

Abstract

T Cell Factor-1, encoded by *TCF-7,* is a transcription factor that plays an essential role during T cell development and differentiation. In this manuscript we utilized a pre-clinical model provided evidence that *TCF-7* is dispensable for the anti-tumor response, and that *TCF-7* suppresses key transcriptional factors Eomes and T-bet and molecules responsible for peripheral CD8 T cell cytolytic function. We discovered that *TCF-7* regulates NKG2D expression on naïve and activated mouse CD8 T cells, and that peripheral CD8 T cells from *TCF-7* cKO utilize NKG2D to clear tumor cells.

We also provide evidence that *TCF-7* regulates key signaling molecules, including LCK, LAT, ITK, PLC-γ1, P65, ERKI/II, and JAK/STATs required for peripheral CD8 T cell persistent function. Our data transcriptomic and protein data uncovered the mechanism of how *TCF-7* impacting peripheral CD8 T cell inflammatory cytokine production, CD8 T cell activation, and apoptosis. Our pre-clinical model showed that CD8 T cells from *TCF-7* cKO mice did not cause GVHD, but effectively cleared primary tumor cells.

64 **Introduction**

65 T Cell Factor-1 (*TCF-7*), a major T cell developmental transcription factor, is involved in the
66 Wnt signaling pathway, and is critical for T cell development as well as activation (Escobar et
67 al., 2020; Ma et al., 2012). Dysfunction of the Wnt/β-catenin/*TCF-7* signaling pathway leads to
68 immune deficiency or autoimmunity (Shi et al., 2016). It is well known that *TCF-7* is involved in
69 the regulation of cell proliferation and survival during later T cell development (Kim et al.,
70 2020). In the absence of *TCF-7*, T cell development is completely blocked after early thymocyte
71 progenitor (ETP) cells, which suggests that *TCF-7* is also important in T cell lineage
72 specification (Germar et al., 2011; Weber et al., 2011). Several studies have shown that *TCF-7* is
73 critical for controlling viral infection (He et al., 2016; Im et al., 2016; Utzschneider et al., 2016).
74 Furthermore, *TCF-7* + CD8+ T cell have self-renewal capacity, while CD8+ T cells lacking
75 *TCF-7* do not (Utzschneider *et al.*, 2016; Wu et al., 2016). Overwhelming evidence has
76 suggested that *TCF-7* is critical for CD8 T cell persistence and capacity to control viral infection
77 (Kurtulus et al., 2019; Miller et al., 2019; Siddiqui et al., 2019; Wu *et al.*, 2016). While
78 investigating the role of *TCF-7* in viral infection, single cell RNA sequencing data uncovered
79 that CD8 T cells expressing higher levels of *TCF-7* are quiescent and tissue resident, while CD8
80 T cells expressing higher levels of *TCF-7* in periphery are highly proliferative, and that *TCF-7*
81 negative T-bet^{hi} CD8 T cells are transitory effector cells. *TCF-7*$^{-}$ Eomes^{hi} CD8 T cells are not
82 proliferative and express higher levels of immune checkpoint receptors, but maintain effector
83 function (Beltra et al., 2020; LaFleur et al., 2019; Zander et al., 2019). Studies have also reported
84 that *TCF-7*+ CD8 T cells with stem-like abilities expresses low levels of PD-1 and Tim
85 checkpoint receptors, further providing evidence that *TCF-7* is required for CD8 T cell formation
86 and persistent function (Kurtulus *et al.*, 2019; Siddiqui *et al.*, 2019; Utzschneider *et al.*, 2016).
87 Studies have demonstrated that dysfunctional virus-specific CD8 T cells transplanted into naïve

88 mice give rise to *TCF-7*-negative CD8 T cells (Utzschneider et al., 2013). However, tumor-
89 specific CD8 T cells transferred to naïve mice might give rise to *TCF-7*+ CD8 T cells,
90 demonstrating the differential role of *TCF-7* in viral infection and tumor (Schietinger et al.,
91 2016). These differences could be due to the differences between microenvironments in viral
92 infection and in tumors (Philip et al., 2017). Whether *TCF-7*+ cells will give rise to *TCF-7*+ or
93 *TCF-7*- cells will be dependent on internal and external signaling. Some studies have shown that
94 both the long (p45) and the short (p33) *TCF-7* isoform are expressed by CD8 T cells that will
95 give rise to stem-like CD8 T cells during viral infection, and it has been shown that the long
96 isoform of *TCF-7* is capable of promoting stem-like CD8 T cell formation during viral infection
97 by regulating genes like CD127, CXCR5 and cMyb (Chen et al., 2019). Currently, the role of
98 long and short *TCF-7* isoforms is largely unknown.

99 Studies of T cells as immunotherapy in both human and mice showed that for a superior
100 anti-tumor response, less differentiated cells are more favorable than a more differentiated subset
101 of CD8 T cells (Gattinoni et al., 2011; Im *et al.*, 2016; Lugli et al., 2013). Ideal CD8 T cells for
102 immunotherapy have been shown to exhibit stem-like abilities (such as those obtained by
103 inducing *ex vivo* cell growth with IL-17, IL-15, IL-21) and higher expression of *TCF-7*, Eomes,
104 and Bcl6 (Cieri et al., 2013; Cui et al., 2011). Thus, the suitability of *TCF-7* as a target for
105 immunotherapy to clear viral infection and cancer might also indicate considerable consequences
106 for autoimmune diseases.

107 To study the role of *TCF-7* in a clinically relevant model, we utilized allogeneic
108 hematopoietic stem cell transplantation (allo-HSCT). In allo-HSCT, mature peripheral donor T
109 cells found in the graft become alloactivated upon recognition of host HLA as non-self. These T
110 cell activities help to clear residual malignant cells, which is called the graft-versus-leukemia

111 effect (GVL) (Balassa et al., 2019; Giralt and Bishop, 2009; Hall and Shenoy, 2019). On the
112 other hand, alloactivated T cells also target healthy recipient tissues, an effect known as graft-
113 versus-host disease (GVHD) (Mavers and Bertaina, 2018). We used a unique mouse strain which
114 has deletion of *TCF-7* in mature T cells, rather than a global deletion (Xing et al., 2016). This
115 *TCF-7* flox/flox x CD4cre mouse experiences deletion of *TCF-7* in all T cells at the double-
116 positive phase of development, when all T cells express CD4 (Wang et al., 2019b). This allows
117 us to overcome the severe T cell developmental defect that occurs in global *TCF-7* deletion, as
118 *TCF-7* is critical for the double-negative stage of development (Yang et al., 2019).
119 Using a mouse model of GVHD and GVL following allo-HSCT, we were able to study all
120 of the major T cell functions, as well as phenotype, clinical outcomes, and gene expression, in a
121 single model. In this model, we transplanted CD8 T cells from either WT or *TCF-7* cKO mice
122 into irradiated BALB/c mice ($H2K^b \rightarrow H2K^d$) (Mammadli et al., 2021a; Mammadli et al., 2021c;
123 Mammadli et al., 2021d). Using allogenic pre-clinical model, we have shown that CD8 T cells
124 from *TCF-7* cKO effectively clear tumor cells without inducing GVHD by producing
125 significantly less inflammatory cytokines as proinflammatory cytokines are con sidered the
126 hallmark of allo-immunity (Ju et al., 2005; Seif et al., 2017). Our data also uncovered that CD8 T
127 cells from *TCF-7* cKO mice cause significantly less tissue damage in GVHD target organs
128 (Bleakley et al., 2012; Breems and Lowenberg, 2005). Molecular analysis showed that CD8 T
129 cells from *TCF-7* cKO mice significantly showed reduction in key molecules required for CD8 T
130 cell persistent function (Germar *et al.*, 2011; Giralt and Bishop, 2009; Gounari and Khazaie,
131 2022). CD8 T cells from *TCF-7* cKO mice exhibited innate memory-like phenotype by
132 upregulating CD122, CD44, and effector and central memory phenotypes in mature CD8 T cells
133 critical for GVHD development (Dutt et al., 2011; Huang et al., 2013). We also uncovered that

134 CD8 T cells from *TCF-7* cKO mice significantly upregulated Eomes and T-bet, two downstream
135 transcription factors which are known to be involved in GVL (Mammadli *et al.*, 2021a; Weeks et
136 al., 2021; Zhou et al., 2010). Our data demonstrated that naïve CD8 T cells from *TCF-7* cKO
137 mice upregulated NK cell type 2 receptor (NKG2D). NKG2D, encoded by *Klrk1*, is an activating
138 cell surface receptor that is predominantly expressed on Natural killer cells (Larson et al., 2006;
139 Wensveen et al., 2018). While naïve human $CD8^+$ T cells express NKG2D, in mice CD8 T cells
140 only upregulate NKG2D upon activation (Hu et al., 2016; Maasho et al., 2005). Upregulation of
141 Granzyme B on CD8 T cells from *TCF-7* cKO mice was also observed. The loss of *TCF-7* also
142 led to upregulation of NK cell type 2 receptor (NKG2D). NKG2D, encoded by *Klrk1*, is an
143 activating cell surface receptor that is predominantly expressed on Natural killer cells (Larson *et*
144 *al.*, 2006; Wensveen *et al.*, 2018). NKG2D is abundantly present on all NK cells, NKT cells, and
145 subsets of γδ T cells (Stojanovic et al., 2018). While naïve human $CD8^+$ T cells express NKG2D,
146 in mice CD8 T cells only upregulate NKG2D upon activation (Hu *et al.*, 2016; Maasho *et al.*,
147 2005). Upregulation of Granzyme B on CD8 T cells from *TCF-7* cKO mice was also observed.
148 Our molecular and animal data were confirmed by transcriptomic analysis.
149 Altogether, our data demonstrate that loss of *TCF-7* in mature murine CD8 T cells
150 enhanced Eomes and T-bet expression and reduced TCR-signaling, resulting in less severe
151 GVHD. Our data demonstrated that *TCF-7*-deficient CD8 T cells utilized NKG2D receptors to
152 kill tumor targets. These findings will have a considerable impact on developing strategies to
153 uncouple GVHD from GVL, and for developing therapeutic interventions for T cell-driven
154 autoimmune disorders.
155

156 **Results**

157 **Loss of *TCF-7* in donor CD8 T cells reduced severity and persistence of GVHD symptoms,**
158 **increased survival from lethal GVHD, and retained anti-tumor capabilities for the GVL**
159 **effect.** Most of the previous research on *TCF-7* utilized a global *TCF-7* knockout because the
160 primary focus was on *TCF-7's* role as a developmental factor (Gounari and Khazaie, 2022;
161 Weber *et al.*, 2011). However, we wanted to study the role of *TCF-7* in mature T cells. Global
162 loss of *TCF-7* results in minimal T cell production from the thymus, because *TCF-7* is critical for
163 DN stages of development (Johnson et al., 2018). Therefore, we obtained mice with a T cell-
164 specific knockout for *TCF-7* (Tcf7 flox/flox x CD4cre, called *TCF-7* cKO here (Xing *et al.*,
165 2016). This allowed us to study mature T cells that developed normally in the thymus, then lost
166 expression of *TCF-7* at the DP phase (Berga-Bolanos et al., 2015).

167 To determine whether *TCF-7* plays a role in mature alloactivated T cell regulation, which
168 is currently unknown, we used a mouse model of MHC-mismatched allo-HSCT leading to
169 GVHD and GVL. Briefly, BALB/c mice (MHC haplotype d) were lethally irradiated and
170 transplanted with wild-type (WT) bone marrow and C57Bl/6-background (MHC haplotype b)
171 donor CD8 T cells (Mammadli *et al.*, 2021c; Mammadli *et al.*, 2021d). The donor CD8 T cells
172 came from wild-type (WT), or *TCF-7*-deficient (*TCF-7* cKO) mice. Recipients were given
173 $1X10^6$ CD8 T cells and $10X10^6$ WT T cell-depleted bone marrow cells, as well as $2X10^5$
174 luciferase-expressing B-cell lymphoma (A-20) cells (Edinger et al., 2003a; Edinger et al., 2003b)
175 to assess GVL responses (Mammadli *et al.*, 2021a; Mammadli et al., 2021b; Mammadli *et al.*,
176 2021c; Mammadli *et al.*, 2021d). A20 cells are syngeneic to BALB/c mice and allogeneic to
177 C57BL/6 (B6) mice (Edinger *et al.*, 2003a; Edinger *et al.*, 2003b), meaning that the cells will not
178 be naturally rejected by the BALB/c hosts, but will be attacked by the transplanted donor T cells.
179 The MHC haplotype mismatch between host and donor cells drives alloactivation of donor T

180 cells, which in turn causes GVHD and GVL effects (Hoffmann et al., 2002). To examine disease
181 severity, progression, and recipient mouse survival, recipient mice were weighed and given a
182 clinical score three times per week following transplant, until about day 70 **(Fig. 1A-D)**. The
183 mice were scored based on six factors: skin integrity, fur texture, posture, activity level, weight
184 loss, and diarrhea (Cooke et al., 1996). Since the A20 cells express luciferase (called A20 luc)
185 (Mammadli *et al.*, 2021c), allowing us to track them by injecting D-luciferin into the recipient
186 mice and imaging them with an *in vivo* bioluminescence scanner (IVIS 50), the mice were
187 scanned one time per week with IVIS 50 until the end of the experiment **(Fig.1A, 1E).**
188 We found that mice who received WT donor CD8 T cells had a rapid increase in GVHD
189 severity, with a high score being reached by day 14, suggesting severe GVHD **(Fig. 1B)**. This
190 high score was maintained, suggesting persistent disease, and reached a high peak score at day
191 40 when the recipient mice died of disease burden **(Fig. 1B-D)**. WT-transplanted mice lost
192 weight initially and were unable to regain much weight (**Fig.1C)**. In contrast, mice given *TCF-7*
193 cKO CD8 T cells had much better survival, lower peak and average clinical scores, minimal
194 disease burden, and a gain in weight following the initial weight loss period **(Fig.1B-D).** In
195 addition, the clinical scores for *TCF-7* cKO CD8 T cells transplanted mice quickly reduced to
196 near-control levels following peak score at day 10 **(Fig. 1B)**, suggesting that disease does not
197 persist in these mice. Therefore, loss of *TCF-7* in donor T cells led to reduced GVHD severity
198 and persistence, with improved survival **(Fig.1D)**.
199 Regarding anti-tumor effects, we observed that over time, the group receiving only bone
200 marrow and tumor cells showed a large increase in tumor growth **(Fig. 1A, 1E)**, because no T
201 cells were present to control the tumor cells. In contrast, most mice given CD8 T cells from any
202 donor type along with the BM and A20 luc cells were able to clear the tumor cells by the end of

203 the experiment **(Fig. 1A, 1E)**. The GVL effect was maintained even in *TCF-7* cKO-transplanted
204 mice **(Fig. 1A, 1E)**. Altogether, these data show that *TCF-7* is dispensable for GVL effects, but
205 critical for GVHD. Therefore, loss of *TCF-7* in donor T cells provides a clinically optimal
206 phenotype, where GVHD severity is reduced but beneficial GVL effects are maintained.
207
208 **Loss of *TCF-7* drives changes to mature CD8 T cell phenotype which are primarily cell-**
209 ***extrinsic***. It has been shown that loss of *TCF-7* in late stages of T cell development led to
210 impaired output of CD4 T cells, and redirection of CD4 T cells to a CD8 T cell fate(Steinke et
211 al., 2014). To determine whether loss of *TCF-7* affected mature donor T cell phenotype, we
212 performed flow cytometry phenotyping on CD8 T cells **(Fig. 2)**. First, we confirmed the loss of
213 *TCF-7* expression in *TCF-7* cKO mice by flow cytometry **(Fig.2A).** Next, we examined whether
214 the loss of *TCF-7* also altered Eomesodermin (Eomes) and T-box transcription factor 21 (T-bet)
215 expression, both of which are downstream of *TCF-7* (Chen *et al.*, 2019). Some reports have
216 claimed that Eomes is activated by *TCF-7* (meaning loss of *TCF-7* reduces Eomes expression)
217 (Paley and Wherry, 2010). However, in our model of conditional *TCF-7* deletion, we found that
218 *TCF-7* cKO CD8 T cells had increased expression of Eomes compared to WT CD8 T cells **(Fig.**
219 **2B)**. Other reports have claimed that T-bet may be activated or not affected by *TCF-7* (Ma *et al.*,
220 2012), but we found that loss of *TCF-7* led to increased T-bet expression in CD8 T cells **(Fig.**
221 **2C)**. This suggests that *TCF-7* normally suppresses the expression of Eomes and T-bet in mature
222 CD8 T cells.
223 Some reports have suggested that $CD44^{hi}$ T cells do not cause GVHD or cause less severe
224 GVHD (Dutt *et al.*, 2011). Therefore, we wanted to examine CD8 T cells from *TCF-7* cKO mice
225 for activation markers like CD44 and CD122. Our data showed that CD8 T cells from *TCF-7*

226 cKO mice exhibit increased expression of CD122 and CD44 **(Fig. 2D-E)**. Next, using CD62L
227 and CD44 markers, we identified three major memory subsets: central memory ($CD44^{hi}$
228 $CD62L^{hi}$), effector memory ($CD44^{hi}$ $CD62L^{low}$), and naive ($CD44^{low}$ $CD62L^{hi}$) cells **(Fig.2F)**.
229 *TCF-7* cKO mice showed increased central memory CD8 T cell subsets and decreased naive
230 CD8 T cells **(Fig. 2F)**. Thus, loss of *TCF-7* results in a more memory-skewed phenotype for
231 CD8 T cells. Some reports have suggested that memory T cells delay induction of GVHD (Dutt
232 *et al.*, 2011; Mammadli *et al.*, 2021c), so this phenotypic change may be beneficial (Nakajima et
233 al., 2021).

234 Changes to cell phenotype in a knock-out mouse may be cell-intrinsic (due directly to
235 gene deficiency within the cell) or cell-extrinsic (due to changes in the microenvironment from
236 gene deficiency) (Decman et al., 2010; Mammadli *et al.*, 2021d). To determine whether the
237 phenotypic effects we observed were cell-intrinsic or cell-extrinsic, we developed a chimeric
238 mouse model. Briefly, we mixed bone marrow from WT and *TCF-7* cKO mice at a 1:4
239 (WT:TCF) ratio for a total of $50X10^6$ BM cells, then used this mixture to reconstitute lethally
240 irradiated Thy1.1 mice. We used a 1:4 ratio based on our previous published work (Mammadli et
241 al., 2020; Mammadli *et al.*, 2021d), to ensure survival of the KO cells (based on our initial
242 observations that *TCF-7* cKO T cells did not proliferate well in culture). At 9 weeks post-
243 transplant, blood was taken to ensure reconstitution and survival of both donor types in each
244 mouse. At 10 weeks, splenocytes were phenotyped by flow cytometry, with donor cells being
245 identified by $H2K^b$, CD45.1 (WT), and CD45.2 (*TCF-7* cKO) markers (Mammadli *et al.*, 2020).

246 First, we looked at the *TCF-7* expression in CD45.1+ (WT), and CD45.2+ (*TCF-7* cKO)
247 cells and confirmed that cells from *TCF-7* cKO mice did not express *TCF-7* in chimeric mice
248 **(Supp.Fig.1A).** We did see a statistically significant increase in T-bet expression in CD8 T cells

249 from *TCF-7* cKO donor cells compared to WT donor cells in chimeric mice, when we performed
250 a t-test (data not shown). However, when we compared the T-bet expression in chimeric versus
251 naïve CD8 T cells, we observed that T-bet expression in CD8 T cells from *TCF-7* cKO donor
252 mice was reduced to near-WT levels from elevated levels **(Supp. Fig. 1B).** This suggests that the
253 increased expression of T-bet seen in *TCF-7* cKO CD8 T cells from naive mice is a cell-extrinsic
254 effect. Interestingly, in the chimeric mice we observed that Eomes and CD122 expression levels
255 in WT CD8 T cells were significantly increased to near-*TCF-7* cKO levels, suggesting that the
256 increase in Eomes and CD122 expression in CD8 T cells from *TCF-7* cKO mice is primarily
257 cell-intrinsic **(Supp.Fig.1C-D).**
258 Next, we examined the expression of CD44 and central memory phenotype in chimeric
259 mice. We observed that while the frequencies of these subsets were lower in *TCF-7* cKO-derived
260 CD8 T cells compared to WT-derived CD8 T cells in the chimera (opposite of the trend observed
261 in naive mice), this was because the frequencies of CD44 and CM phenotype in WT cells was
262 enhanced to the levels expressed by *TCF-7* cKO cells from naive mice **(Supp. Fig. 1E-F).**
263 These results suggest that the effects of *TCF-7* deficiency on CD44 and CM phenotype
264 expression in naïve mice could be primarily cell-intrinsic, with cell-extrinsic elements as well.
265 Interestingly, effector memory phenotype in the chimeric mice we observed that levels in WT
266 CD8 T cells were significantly increased to near-*TCF-7* cKO levels, suggesting that the increase
267 in effector memory phenotype in CD8 T cells from *TCF-7* cKO mice is primarily cell-intrinsic
268 **(Supp. Fig. 1G).** Finally, the naïve CD8 T cell population in the chimera coming from *TCF-7*
269 cKO bone marrow was significantly increased compared to CD8 T cells from WT bone marrow
270 and compared to naïve *TCF-7* cKO mice (**Supp. Fig. 1H**). This suggests that the effect on naive
271 CD8 T cells in *TCF-7* cKO mice could be either cell-intrinsic or cell-extrinsic. Altogether, these

272 data suggest that the phenotypic changes seen in *TCF-7* cKO may be primarily cell-intrinsic,
273 with some additional cell-extrinsic effects being present.
274
275 **Loss of *TCF-7* alters cytotoxic mediator production in mature CD8 T cells.** Our data
276 demonstrated that the loss of *TCF-7* increases Eomes and T-bet expression in mature CD8 T
277 cells (**Fig. 2B-C**). Considering that Eomes and T-bet have been reported to play a central role in
278 anti-tumor responses, we hypothesized that by upregulating Eomes and T-bet, CD8 T cells
279 lacking *TCF-7* can maintain cytotoxicity, and that *TCF-7* is not required for CD8 T cell-
280 mediated cytolytic function (Zhu et al., 2010). We anticipated that CD8 T cells from *TCF-7* cKO
281 mice may have attenuated TCR signaling, so we examined this and other activating receptors by
282 flow cytometry. It is also known that Eomes and T-bet overexpression increases NKG2D
283 expression in NK cells (Kiekens et al., 2021). Considering that loss of *TCF-7* in mature T cells
284 led to upregulation of Eomes and T-bet expression, we hypothesized that loss of *TCF-7* may also
285 lead to upregulation of NKG2D expression in CD8 T cells and enhance the anti-tumor response.
286 Natural killer group 2 member D (NKG2D) is constitutively expressed on mouse NK
287 cells, NKT cells and some other cells (Abel et al., 2018; Al Dulaimi et al., 2018), but does not
288 get expressed on naïve mouse CD8 T cells (Prajapati et al., 2018). Human CD8 T cells always
289 express NKG2D on their surface, but mouse CD8 T cells only express it upon activation
290 (Wensveen *et al.*, 2018) NKG2D is activated by NKG2D ligands (Raulet et al., 2013), and
291 NKG2D ligands are relatively restricted to malignant or transformed cells (Raulet, 2003; Raulet
292 *et al.*, 2013). In order to determine whether loss of *TCF-7* affects NKG2D expression and anti-
293 tumor responses, we analyzed NKG2D expression in CD8 T cells. We measured NKG2D
294 expression by flow cytometry before and at different time points after CD3/CD28 activation

295 (Karimi et al., 2015). We found that CD8 T cells from *TCF-7* cKO mice had significantly
296 increased expression of NKG2D on the cells surface compared to CD8 T cells from WT mice,
297 before stimulation **(Fig.3A).** Next, we wanted to examine whether NKG2D expression was
298 further upregulated on CD8 T cells from *TCF-7* cKO mice compared to CD8 T cells from WT
299 mice after stimulation. CD8 T cells were cultured with 2.5ug/ml anti-CD3 and 2.5ug/ml anti-
300 CD28 antibodies for 24, 48, or 72 hours. These cultured cells were examined for NKG2D
301 expression by flow cytometry. We observed an increase in NKG2D expression on CD8 T cells
302 from both WT and *TCF-7* cKO mice in a time-dependent manner, and at all time points,
303 expression of NKG2D was higher for cells from *TCF-7* cKO mice **(Fig.3B).** There was no
304 difference in the viability of the cells or CD8 T cell numbers before or after the culture
305 **(Supp.Fig.2A-B).**
306 We also wanted to compare the Granzyme B expression in CD8+, NKG2D+ T cells from
307 *TCF-7* cKO and WT mice (Chu et al., 2013). We did not observe any Granzyme B expression in
308 CD8 T cells before stimulation **(Fig.3C).** Only 24 hours after stimulation, we observed
309 Granzyme B expression in T cells from both strains, peaking at 48 hours post-stimulation with
310 no difference between strains of mice **(Fig.3C)**. After 72 hours post-stimulation, CD8 T cells
311 from WT mice had significantly reduced Granzyme B expression compared to *TCF-7* cKO CD8
312 T cells **(Fig.3C)**. We also confirmed total Granzyme B expression in CD8 T cells from *TCF-7*
313 cKO mice, in the presence and absence of CD3/CD28 stimulation, using Western blotting. Total
314 Granzyme B expression was upregulated in CD8 T cells from *TCF-7* cKO mice compared to WT
315 mice **(Fig.3D-E).** These data demonstrated that CD8 T cells from *TCF-7* cKO mice may
316 maintain anti-tumor responses by killing the target cells with an NKG2D-mediated mechanism,
317 and by persistent upregulation of Granzyme B expression (Liu et al., 2022; Wang et al., 2022).

318 Next, we wanted to examine the functional consequences of upregulation of NKG2D
319 expression on CD8 T cells from *TCF-7* cKO mice. We utilized an in *vitro* cytotoxicity assay,
320 where we used anti-NKG2D neutralizing antibody. We isolated CD8 T cells from WT and *TCF-*
321 *7* cKO mice and cultured them for 48 hours with anti-CD3/anti-CD28 antibodies in order to
322 induce optimal NKG2D expression in CD8 T cells. CD8 T cells from *TCF-7* cKO and WT mice
323 were then cultured with tumor target A20 cells (Edinger *et al.*, 2003b) in a 40:1 ratio of tumor
324 cells to CD8 T cells, along with anti-NKG2D antibody or isotype control antibody for 4 hours.
325 We used the A20 cell line as a tumor target because it is known for expressing NKG2D ligands
326 including Rae1, H60, and MULT1(Karimi *et al.*, 2015; Nishimura et al., 2008). Triplicate wells
327 were averaged and percent lysis was calculated from the data using the following equation: %
328 specific lysis = 100 × (spontaneous death bioluminescence – test bioluminescence)/ (spontaneous
329 death bioluminescence – maximal killing bioluminescence) (Karimi et al., 2014).
330 Our data showed that the addition of anti-NKG2D antibody significantly reduced the
331 cytotoxicity of CD8 T cells from *TCF-7* cKO mice, whereas addition of isotype control had no
332 effect on cytotoxicity of the CD8 T cells from *TCF-7* cKO mice **(Fig.3F).** In contrast, the
333 addition of anti-NKG2D antibody (Karimi *et al.*, 2015) did not change cytotoxicity of the CD8 T
334 cells from WT mice **(Fig.3F).** These data further support the idea that *TCF-7* cKO CD8 T cells
335 maintain their anti-tumor activity through an NKG2D-mediated mechanism. Taking into account
336 that normal tissue does not express NKG2D ligands on the surface and that primarily malignant
337 and transformed cells upregulate these ligands, this could explain why CD8 T cells from *TCF-7*
338 cKO mice cause less GVHD but maintain their anti-tumor activity (Nishimura *et al.*, 2008).
339

340 **Loss of *TCF-7* alters cytokine production, chemokine expression, and expression of**
341 **exhaustion markers by mature CD8 T cells.** We confirmed that CD8 T cells from *TCF-7* cKO
342 mice mediate cytolytic function primarily through NKG2D. Next, we wanted to examine the
343 mechanism behind why CD8 T cells from *TCF-7* cKO mice induce less GVHD. One of the
344 hallmarks of GVHD is the release of pro-inflammatory cytokines by alloactivated donor T cells,
345 eventually leading to cytokine storm (Lynch Kelly et al., 2015; Mohty et al., 2005). We
346 examined whether loss of *TCF-7* in donor CD8 T cells led to changes in cytokine production,
347 thereby affecting GVHD damage. We allotransplanted lethally irradiated BALB/c mice as
348 described above. Recipient mice were transplanted with $1.5X10^6$ WT or *TCF-7* cKO CD8 donor
349 T cells. Recipients were sacrificed at day 7 post-transplant. Splenocytes were isolated and
350 restimulated by 6 hours of culture with PBS (control) or anti-CD3/anti-CD28 (stimulation),
351 along with Golgiplug. Afterwards, the cultured cells were stained with antibodies against $H2K^b$,
352 CD3, CD4, CD8, TNF-α, and IFN-γ. Our data showed that production of TNF-α by donor CD8
353 T cells trended toward decreasing when *TCF-7* was lost **(Supp. Fig. 3A)**. In contrast, IFN-γ
354 trended toward increasing upon loss of *TCF-7* in CD8 T cells **(Supp. Fig. 3B)**.
355 We also obtained serum from cardiac blood of recipient mice at day 7 post-transplant and
356 tested it with a mouse Th cytokine ELISA panel (LEGENDplex kit from Biolegend) (Mammadli
357 *et al.*, 2020; Mammadli *et al.*, 2021d). Levels of TNF-α and IFN-γ in serum of recipient mice
358 given *TCF-7* cKO CD8 T cells were lower than in mice given WT CD8 T cells at day 7 **(Fig.**
359 **4A)**. In contrast, the serum levels of IL-2 in mice given *TCF-7* cKO CD8 T cells was higher than
360 in mice given WT CD8 T cells at day 7 **(Fig. 4A)**. At day 14 post-transplant, the reduction in
361 TNF-α and IFN-γ levels observed at day 7 for *TCF-7* cKO-transplanted mice was preserved **(Fig.**
362 **4B)**. We observed a trend towards decreased serum levels of IL-2 in mice given *TCF-7* cKO

363 CD8 T cells compared with mice given WT CD8 T cells at day 14 post-transplant, opposite of
364 the effect observed on day 7 post-transplant **(Fig.4B)**. This suggests that *TCF-7* cKO CD8 T
365 cells may be capable of IFN-γ and TNF-α production at the same level as WT CD8 T cells when
366 restimulated, but in reality, produce less IFN-γ and TNF-α than WT cells when allotransplanted.
367 In order for GVHD to persist, donor T cells must proliferate in secondary lymphoid
368 organs and target organs (Beilhack et al., 2005; Ferrara, 2014). Naive and effector T cells drive
369 GVHD, but they are short-lived and must be replaced to maintain an alloresponse (Jiang et al.,
370 2021; Jiang et al., 2014). Also, given that memory cells are increased among CD8 T cells when
371 *TCF-7* is lost, we hypothesized that activation and/or exhaustion of these cells may also be
372 affected. Ki-67 (Blessin et al., 2021) is a marker of T cell activation and proliferation, and TOX
373 (Khan et al., 2019) and PD-1 are markers of exhaustion (Ahn et al., 2018). Therefore, we wanted
374 to determine the Ki-67, TOX, and PD-1 expression levels on WT and *TCF-7* cKO CD8 T cells *in*
375 *vitro*. We cultured splenocytes from either WT mice or *TCF-7* cKO mice *in vitro* with anti-CD3
376 and anti-CD28 antibodies for 24, 48, and 72 hours. We did not observe any difference in Ki-67
377 expression in cells that were not stimulated, but the CD8 T cells from *TCF-7* cKO mice that were
378 stimulated for 72 hours *in vitro* showed significant upregulation of Ki-67 expression (**Fig. 4 C-**
379 **D**), suggesting that CD8 T cells from *TCF-7* cKO mice could potentially proliferate more than
380 CD8 T cells from WT mice when restimulated**.** We also observed the same trend of increased
381 expression for PD-1 at 72 hours post-stimulation **(Fig.4E-F)**. There were no differences in
382 expression of TOX at any time points *in vitro* when CD8 T cells from *TCF-7* cKO mice were
383 compared to WT **(Supp.Fig.3C).**
384 Next, we checked the expression of these markers *in vivo* from donor cells that were allo-
385 transplanted in recipient Balb/c mice as described earlier. At day 7 post-transplant, splenocytes

386 were isolated and Ki-67, TOX, and PD-1 expression were detected by flow cytometry. We
387 observed that donor CD8+T cells from *TCF-7* cKO mice expressed more TOX compared to WT,
388 suggesting that donor T cells *TCF-7* cKO mice were more exhausted following
389 allotransplantation **(Fig.5G-H)**. We did not observe any statistically significant differences in Ki-
390 67 or PD-1 expression at day 7 post-transplant **(Supp.Fig.3D-E).** Taken together these data
391 suggest that CD8 T cells from *TCF-7* cKO mice could be more exhausted than WT CD8 T cells
392 both *in vivo* and *in vitro*.
393 One of the major functions of alloactivated T cells is migration from spleen to
394 GVHD target organs, including liver and small intestine(Beilhack *et al.*, 2005; Ferrara, 2014).
395 Expression of chemokines and chemokine receptors is a critical aspect of T cell migration to
396 target organs. To determine whether expression of these molecules was affected by loss of *TCF-*
397 *7* in CD8 T cells, we FACS sorted pre- and post-transplanted donor CD8 T cells from WT or
398 *TCF-7* cKO mice (spleen only for pre-transplant, spleen, or liver for post-transplant). We then
399 extracted RNA from the cells, converted it to cDNA, and performed qPCR using a 96-well
400 mouse chemokine/chemokine receptor plate (Thermo Fisher). As expected, expression of these
401 markers was generally upregulated in alloactivated cells. Expression of these markers was
402 generally higher in *TCF-7* cKO CD8 T cells from pre-transplant spleen compared to WT pre-
403 transplant spleen **(Supp. Fig. 4A)**, but these markers were generally downregulated in *TCF-7*
404 cKO CD8 T cells from post-transplant liver and spleen compared to WT cells **(Supp. Fig. 4B-**
405 **C)**. Therefore, *TCF-7* controls expression of CD8 T cell chemokine/chemokine receptors.
406
407 **Loss of *TCF-7* in donor CD8 T cells led to decreased damage to the GVHD target organs.**
408 During GVHD, host tissues are damaged by the activity of alloactivated T cells. To determine

409 whether damage to target organs of GVHD (skin, liver, and small intestine) was altered by loss
410 of *TCF-7* in donor T cells, we collected organs from mice allotransplanted as described above
411 (Beilhack *et al.*, 2005; Mammadli *et al.*, 2021a; Mammadli *et al.*, 2021d; Weeks *et al.*, 2021). At
412 day 7 and day 21 post-transplant, we collected pieces of skin, small intestine, and liver from
413 recipient BALB/c mice. These organs were fixed, sectioned, stained with hematoxylin and eosin
414 (H&E), and analyzed by a pathologist (L.S.) **(Fig. 5)**. At day 7, *TCF-7* cKO mice showed
415 significantly less inflammatory infiltrates in all the organs. We observed much less inflammatory
416 infiltrates in the bile duct epithelium of the portal triad (black arrows showing the interlobular
417 bile ducts) in the liver of the *TCF-7* cKO-transplanted recipients compared with WT-transplanted
418 recipients **(Fig. 5A)**. In the small intestines, no apoptotic bodies were seen in the crypts of the
419 small intestine in the *TCF-7* cKO CD8 T cell-transplanted mice, while frequent apoptotic bodies
420 were present in the WT CD8 T cell-transplanted mice at day 7 post-transplantation (black
421 arrows) **(Fig. 5B)**. In the skin, a mild increase in inflammatory cells was observed in the dermis
422 of the WT CD8 T transplanted mice, while the dermis of the *TCF-7* cKO CD8 T transplanted
423 mice appears normal at day 7 post-transplantation **(Fig. 5C)**.
424 Again, at day 21 post-transplant, *TCF-7* cKO CD8 T cell transplanted mice showed
425 significant less inflammatory infiltrates in all the sectioned GVHD target organs. We observed
426 much less inflammatory infiltrates involving the bile duct epithelium of the portal triad (black
427 arrows showing the interlobular bile ducts) in the liver of the *TCF-7* cKO CD8 T cell-
428 transplanted mice compared with WT CD8 T cell-transplanted mice **(Fig. 5D)**. At day 21 post-
429 transplant, no apoptotic bodies were seen in the crypts of the small intestines of the *TCF-7* cKO
430 CD8 T cell transplanted mice, while few apoptotic bodies are present in the small intestines of
431 the WT CD8 T cell transplanted mice (black arrows) **(Fig. 5E)**. A marked increase in

432 inflammatory cells (red circle) and destruction of the adnexal glands was observed in the dermis
433 of the WT CD8 T cell-transplanted recipients, while the dermis of the *TCF-7* cKO CD8 T cell
434 transplanted recipients showed only a mild increase in dermal inflammatory cells, with
435 preservation of adnexal glands **(Fig. 5F)**. Altogether, these data suggest that *TCF-7* normally
436 promotes GVHD damage to healthy tissues and is indispensable for T cell-driven damage. Thus,
437 loss of *TCF-7* in donor T cells leads to reduced severity and persistence of GVHD over time.
438
439 ***TCF-7* alters the transcriptomic signature of alloactivated T cells.** Given that the phenotype
440 and functions of donor T cells, as well as disease outcomes, were significantly altered by loss of
441 *TCF-7* on donor cells, we sought to determine what specific gene changes occurred to support
442 this. We allotransplanted recipient BALB/c mice with $1X10^6$ donor CD3 T cells as above, and
443 FACS-sorted pre- and post-transplant WT or *TCF-7* cKO donor CD8 T cells, which were stored
444 in Trizol and transcriptionally profiled. When we analyzed the genetic profile of the pre-
445 transplanted CD8 T cells from *TCF-7* cKO and WT mice, we were not able to determine any
446 differentially expressed genes (DEGs, FDR<0.1). However, when we performed Gene Set
447 Enrichment analysis (GSEA) using the Hallmark pathways collection from Molecular Signatures
448 Database (MSigDB), we identified that cytokine signaling pathways like TNF-a Signaling via
449 NF-κβ and Interferon gamma response were enriched in pre-transplanted CD8 T cells from WT
450 mice compared with cells from *TCF-7* cKO mice **(Supp.Fig.5A-C)**. Meanwhile, a number of
451 pathways involved in cell cycle also were enriched in WT cells versus *TCF-7* cKO pre-
452 transplanted CD8 T cells, like the P53 pathway, G2M checkpoint, DNA repair, and Myc targets
453 pathways **(Supp.Fig.5A).** MTOR signaling, Allograft rejection, and Oxidative phosphorylation
454 pathways were also enriched in pre-transplant CD8 T cells from WT mice **(Supp.Fig.5A,6D-F),**

455 suggesting that loss of *TCF-7* alters the transcriptional profile of CD8 T cell towards decreased
456 cytokine release while also altering the cell cycle, leading to a lessening of the alloactivation
457 responses.

458 When we analyzed the post-transplanted CD8 T cells which were alloactivated *in vivo*, we
459 identified 2548 differentially expressed genes (DEGs; FDR<0.1) when comparing *TCF-7* cKO
460 cells to WT cells **(Fig. 6A-B).** A majority of the DEGs (2000 genes) were downregulated
461 (module 2 in heatmap) and only 548 genes (module 1 in heatmap) were upregulated in post-
462 transplant CD8 T cells from *TCF-7* cKO mice compared to WT mice **(Fig. 6A-B).** We analyzed
463 both up- and downregulated DEGs for the Gene Ontology (GO) enrichment analysis using
464 Functional Annotation Chart tools, selecting only the top 20 GO BP (Biological Process) terms
465 in the Database for Visualization and Integrative Discovery (DAVID)(Huang da et al., 2009;
466 Sherman et al., 2022). The analysis showed that the differentially expressed genes in post-
467 transplant CD8 T cells from *TCF-7* cKO mice compared to WT were involved in Cell Cycle,
468 Cell-cell adhesion, Cell division, Apoptotic process, Antigen processing and presentation via
469 MHC class I, TCR signaling, Regulation of NF-κB signaling, Metabolic process, and others
470 **(Supp.Fig.6).** Once we knew which processes these DEGs played a role in, we pulled out the top
471 genes that were altered for each GO BP term that we were interested in. When we looked at the
472 top 35 DEGs based on P-value that were altered in Cell cycle, we observed that a majority of
473 them were downregulated in *TCF-7* cKO compared to WT **(Fig.6C).** We also looked at the top
474 30 genes based on P-value that were altered in Apoptotic processes **(Fig.6D**), which also showed
475 that most of the genes were downregulated in CD8 T cells in *TCF-7* cKO mice. When we looked
476 at the top 30 genes that play a role in metabolic processes, we observed that only 1 gene was
477 upregulated, and the rest were downregulated in *in vivo* alloactivated CD8 T cells from *TCF-7*

478 cKO mice **(Fig. 6E).** While the upregulated genes in the NF-κB pathway were Fasl, Ubd, Chuk
479 and others, the downregulated genes were Rela, Irf3, Traf2, Mavs, Tradd, Nod1, Tnfrsf1a, and
480 Trim25 **(Fig.6F)**.
481 Gene Set Enrichment analysis (GSEA) using the Hallmark pathways identified that
482 signaling pathways like PI3K-AKT-MTOR Signaling and TNFA Signaling via NF-κβ were
483 enriched in post-transplanted CD8 T cell from WT mice compared to cells from TCF-7 cKO
484 mice **(Supp.Fig.7A-B)**. GSEA analysis using the C2 canonical pathways showed that a number
485 of cytokines signaling pathways involving IL-1, IL-2, IL-4, and IL-7 were enriched in post-
486 transplanted CD8 T cells from WT mice compared to cells from *TCF-7* cKO mice **(Fig.6G)**.
487 While Cell cycle pathways were enriched in CD8 T cells from *TCF-7* cKO mice compared to
488 cells from WT mice, Apoptosis and Cell adhesion pathways were enriched in post-transplanted
489 CD8 T cells from WT mice **(Fig.6H).** Meanwhile, a number of cells signaling pathways were
490 also enriched in WT CD8 T cells compared to *TCF-7* cKO cells, such as TCR signaling, Toll
491 like receptor signaling, Jak-Stat signaling, ERK-MAPK signaling, and NF-kB pathways **(Fig.6I).**
492 We also analyzed the genes that were altered in KEGG pathways, which revealed that
493 DEGs that were altered in *in vivo* alloactivated CD8 T cells from *TCF-7* cKO mice (compared to
494 WT) were involved in pathways like Cell cycle, DNA replication, Metabolic pathways, Natural
495 killer mediated cytotoxicity, TCR signaling, JAK-STAT signaling, Chemokine receptor
496 signaling, and others **(Fig.7A).** Specifically, Klrk1 gene for NKG2D on Natural killer mediated
497 cytotoxicity pathway were enriched in allo-activated *TCF-7* deficient CD8+ T cells compared to
498 WT CD8+ T cells. Clustering of genes that were affected in TCR signaling showed that while
499 AKT1, AKT2, Pik3r5, Zap70, LCK, Lat, PLCγ1, Pdcd1, Vav1, Rela, Mapk3, Nfkbia, and Nfatc1
500 were downregulated, Ifng and Ptprc were upregulated in post-transplanted CD8 T cells from

501 *TCF-7* cKO mice **(Fig.7B).** The JAK/STAT signaling pathway is important for cytokine
502 production and for the response of T cells to cytokines. Analysis revealed that IL2RB, JAK3,
503 STAT5B, STAT3, STAT1, Cish, Il2rb, Socs3, and Socs1 genes were downregulated in the JAK-
504 STAT pathway for *TCF-7* cKO CD8 T cells compared to WT **(Fig.7C)**.
505 In order to confirm these changes in genes, we isolated CD8 T cells from WT and *TCF-7*
506 *cKO* mice and determined the baseline level protein expression of LCK, ZAP70, LAT, ITK,
507 PLCγ1, ERK1-2, Jak2, Jak3, Stat3, p65-rela, AKT, and actin in unstimulated and 10 minute-anti-
508 CD3/CD28-stimulated samples. Data from non-stimulated samples revealed that protein
509 expression of most of the markers was downregulated in CD8 T cells from *TCF-7* cKO mice
510 compared to WT mice; only ZAP70, JAK3 and AKT were not affected by loss of *TCF-7*
511 **(Fig.7D, Supp.Fig.8A).** We observed even more robust differences in samples that were
512 stimulated with anti-CD3/CD28 for 10 minutes, and again only ZAP70 and AKT were
513 unaffected by loss of *TCF-7* **(Fig.7E, Supp.Fig.8B).** Altogether, the data from RNA sequencing
514 analysis and Western blots of stimulated and unstimulated samples showed attenuation of TCR
515 signaling and many other pathways in CD8 T cells from *TCF-7* cKO mice. These results help to
516 explain why CD8 T cells from *TCF-7* cKO mice cannot induce GVHD as severely as CD8 T
517 cells from WT mice.
518
519
520
521

522 **Discussion**

523 T Cell Factor-1 (*TCF-7*) is a critical regulatory transcription factor in T cell development and
524 functions (Zuniga-Pflucker, 2004). *TCF-7* is known to be important for T cell development, as
525 well as activation in some contexts (Yu et al., 2010). *TCF-7* has been extensively studied in viral
526 infection(Escobar *et al.*, 2020; He *et al.*, 2016; Im *et al.*, 2016; Kurtulus *et al.*, 2019; Miller *et al.*,
527 2019; Siddiqui *et al.*, 2019; Utzschneider *et al.*, 2016; Weber *et al.*, 2011; Wu *et al.*, 2016).
528 However, the role of (*TCF-7*) in a mouse model of allogeneic transplant has not been
529 investigated. Using a murine allogeneic transplant model, we have shown that CD8 T cells from
530 *TCF-7* cKO effectively clear tumor cells without inducing GVHD by producing significantly less
531 inflammatory cytokines (Ju *et al.*, 2005; Seif *et al.*, 2017). Our data also uncovered that CD8 T
532 cells from *TCF-7* cKO mice cause significantly less tissue damage in GVHD target organs
533 (Bleakley *et al.*, 2012; Breems and Lowenberg, 2005). Here, we show that loss of *TCF-7* alters a
534 number of CD8 T cell functions, and while it is dispensable for anti-tumor responses, it is
535 essential for host tissue damage, cytokine production and signaling, and gene expression, playing
536 a role in a number of immunological and biological pathways during alloactivation. (Yu *et al.*,
537 2010). This murine model allows us to study T cell function, clinical outcomes, and gene
538 expression all in one model. Here, we showed that *TCF-7*-deficiency alters the phenotype of
539 CD8 T cells by upregulating CD44 and CD122. We and other have shown that innate memory-
540 like CD8 T cells expressing CD12hi and CD44 hi, Eomes and T-bet ameliorate GVHD
541 development (Huang et al., 2019; Karimi *et al.*, 2014; Mammadli *et al.*, 2020; Mammadli *et al.*,
542 2021d; Zheng et al., 2009). The role of central ($CD44^{hi}$, $CD62L^{hi}$) and effector ($CD44^{hi}$,
543 $CD62L^{low}$) memory phenotypes has been investigated previously (Huang *et al.*, 2019; Zheng *et*
544 *al.*, 2009). Our data demonstrated that *TCF-7* significantly impacts CD8 T cell central memory
545 phenotypes, suggesting that *TCF-7* might be a regulator for T cell activation. While effector and

546 naive cells are known to cause severe GVHD, central memory cells are often associated with less
547 severe disease (Dutt *et al.*, 2011; Tugues et al., 2018; Zheng *et al.*, 2009). Our findings
548 suggesting that this phenotypic change in *TCF-7 cKO* cells may be beneficial for reducing
549 disease severity. Our experiments in mixed bone marrow chimeras showed that bone marrow-
550 derived CD8 T cells from WT and or *TCF-7* cKO mice developed in the same thymus have a
551 similar phenotype to each other, and a different phenotype than CD8 T cells from naïve WT or
552 *TCF-7* cKO mice. We found that the upregulation of activation marker expression like Eomes,
553 CD122, and the effector memory phenotype is primarily cell-intrinsic, with changes to other
554 markers being either cell-extrinsic or primarily cell-intrinsic with other extrinsic effects.
555 Donor T cells are crucial for target organ injury in graft-versus-host disease (GVHD).
556 These alloactivated T cells proliferate, migrate to target organs (liver, skin, and small intestine),
557 and produce cytokines during GVHD(Bastien et al., 2012; Reddy and Ferrara, 2008; Villarroel et
558 al., 2014). Our data showed that tissue damage in liver, skin, and small intestine (all target
559 organs) was reduced by loss of *TCF-7* in donor CD8 T cells at all timepoints. This shows that
560 *TCF-7* in donor T cells is required for GVHD damage and persistence over time.
561 Donor T cells eliminate tumor cells (GVL) but also cause graft-versus-host disease
562 (GVHD) (Bleakley *et al.*, 2012; Tugues *et al.*, 2018). Our data showed that CD8 T cells from
563 *TCF-7* cKO mice were able to clear tumor without causing GVHD, suggesting that *TCF-7* is
564 dispensable for anti-tumor responses. Our data revealed that CD8 T cells from *TCF-7* cKO mice
565 mediate cytolytic function via NKG2D. We also confirmed this hypothesis by blocking the
566 surface NKG2D by anti-NKG2D antibody on CD8 T cells from *TCF-7* cKO and WT mice and
567 performing an *in vitro* cytotoxicity assay. While the anti-tumor response of TCF1-deficient CD8
568 T cell against A20 cells (which express the NKG2D ligands like Rae1, H60, and MULT1)

569 (Nishimura *et al.*, 2008) was diminished, cytotoxicity of WT CD8 T cells was not affected.
570 Upregulation of the *KLRK1* gene (also known as NKG2D) in alloactivated *TCF-7* deficient
571 CD8+ donor T cells further confirmed our hypothesis. Furthermore, the increase in Granzyme B
572 expression in *TCF-7* cKO CD8 T cells by flow cytometry and Western blot also provides
573 evidence as to why the anti-tumor response is preserved despite weakened TCR signaling in
574 TCF-7 cKO CD8 T cells (Presotto et al., 2017).
575 Once we had a clear mechanism for the GVL effect, we looked at functions that were
576 altered in CD8 T cells from *TCF-7* cKO mice that could produce the attenuated GVHD effect.
577 We discovered that the serum levels of cytokines like TNFα and IFNγ were decreased in *TCF-7*
578 deficient CD8 T cell-transplanted mice. Published data has shown the CD8 T cell lacking *TCF-7*
579 develop exhaustion while clearing viral infection(Gautam et al., 2019; Seo et al., 2019) While the
580 expression of TOX, an exhaustion marker, was not affected in freshly isolated or *in vitro*-
581 stimulated *TCF-7* deficient CD8 T cells, alloactivated *TCF-7*-deficient CD8 donor T cells
582 upregulated TOX at day 7 post-transplant (Scott et al., 2019). Another exhaustion marker, PD-1,
583 was upregulated after 72 hours in *in vitro*-stimulated CD8 T cells from TCF-7 cKO mice, but *in*
584 *vivo* expression of PD-1 in donor T cells was not increased (Wang et al., 2019a; Xu et al., 2019).
585 This could be explained by differences between alloactivation *in vivo* and TCR-mediated
586 activation *in vitro.* Ki-67, a proliferation marker, was also altered by loss of *TCF-7*, suggesting
587 that CD8 T cells from *TCF-7* cKO mice may proliferate more compared to WT CD8 T cells
588 (Sobecki et al., 2016). We also confirmed that CD8 T cells from *TCF-7* cKO mice cause less
589 tissue damage to the target organs, and loss of *TCF-7* alters chemokine receptor expression both
590 pre- and post-transplant, which could explain why these cells cause less severe GVHD with
591 increased survival of recipient mice (Ferrara, 2014).

592 These studies provide evidence for how *TCF-7* regulates the functions of peripheral T
593 cells. The phenotype caused by loss of *TCF-7* is clinically optimal, because it allows for
594 clearance of residual malignant cells while limiting the risk of life-threatening GVHD damage
595 (Guinan et al., 1999). This observation, coupled with the increase in exhaustion of *TCF-7* cKO
596 donor CD8 T cells, suggests that donor cells lacking *TCF-7* are highly activated and cytotoxic to
597 malignant cells early on following transplant, but quickly become exhausted, limiting GVHD
598 progression.

599 Finally, to identify the changes to the genetic program of donor T cells that occurred in the
600 absence of *TCF-7*, we performed RNA sequencing analysis on pre- and post-transplant donor T
601 cells. Even though we could not identify the Differentially Expressed Genes (DEGs) in pre-
602 transplanted T cells (which we attribute to technical problems), gene set enrichment analysis
603 revealed that loss of *TCF-7* alters the genetic signature of pre-transplanted CD8 T cells. A
604 number of signaling pathways involved in cytokine production and cell cycle were enriched in
605 pre-transplanted CD8 T cell from WT mice compared to cells from *TCF-7* cKO mice, suggesting
606 that loss of *TCF-7* alters the transcriptional profile of the CD8 T cell towards decreased cytokine
607 release, while altering the cell cycle in baseline and leading to the lessening of the allo-activation
608 response. Meanwhile, 2548 DEGs (FDR<0.1) were identified when comparing post-transplanted
609 CD8 T cells from *TCF-7* cKO mice and WT mice. Both GO Annotation analysis of DEGs and
610 Gene Set Enrichment analysis revealed that a number of pathways such as Cell cycle, DNA
611 replication, Metabolic pathways, TCR signaling, JAK-STAT signaling, and Chemokine receptor
612 signaling were enriched in post-transplanted CD8 T cells from WT mice compared with cells
613 from *TCF-7* cKO mice. Transcriptomic analysis also revealed that KLRK-1 gene for NKG2D
614 were upregulated in allo-activated *TCF-7* cKO CD8+ T cells compared to the WT CD8+T cells,

615 which confirming our findings in in-vitro cytotoxicity assay and flow cytometry data. These
616 findings suggest that loss of *TCF-7* leads to changes in the transcriptomic profile of the CD8 T
617 cells towards producing less cytokines and attenuating the T cell response, while increasing
618 cytotoxicity. Chemokine receptor pathways were also enriched in alloactivated WT CD8 T cells
619 which confirmed the qPCR analysis of chemokine receptors. The decrease in chemokine
620 receptors helps to explain why we observed less tissue damage in GVHD target organs after allo-
621 transplantation, and attenuated GVHD persistence, in mice given *TCF-7* cKO CD8 T cells. By
622 using Western blotting, we also confirmed changes in TCR and JAK/STAT signaling before and
623 after stimulation with anti-CD3/CD28, which helps to explain why we saw less serum cytokines
624 at day 7 and day 14 post-transplant in mice given *TCF-7* cKO CD8 T cells. This also helps to
625 explain why GVHD didn't persist in recipients given CD8 T cells which lack *TCF-7*.
626 Altogether, these data suggest that *TCF-7* is a major transcription factor that plays a role
627 in T cell development. Our work shows that *TCF-7* is dispensable for cytotoxic function of
628 mature alloactivated CD8 T cells but is indispensable for GVHD. TCR, JAK-STAT, and NF-
629 κB signaling as well as cytokine production, these findings will help to establish an
630 understanding of *TCF-7* as a critical factor in the GVHD/GVL regulatory network of CD8 T
631 cells.
632
633
634
635
636
637
638
639
640

641 **Materials and Methods**
642
643 **Mouse Models.** For transplant, the following female donor mice were used: B6-Ly5.1
644 (CD45.1+, "WT" or B6.SJL-Ptprca Pepcb/BoyCrl, 494 from Charles River), C57Bl/6J
645 (CD45.2+, "WT", 000664 from Jackson Laboratories), or Tcf7 flox x CD4cre (referred to here as
646 " *TCF-7 cKO*" (Ma *et al.*, 2012) , obtained from Dr. Jyoti Misra Sen at NIH by permission of Dr.
647 Howard Xue, and bred in-house),. These donor mice were age-matched to each other and to
648 recipients as closely as possible. BALB/c female mice (CR:028 from Charles River, age 6-8
649 weeks or older) were used as recipient mice for transplant experiments, and Thy1.1 mice
650 (B6.PL-Thy1a/CyJ, 000406 from Jackson Labs) were used as recipient mice for chimera
651 experiments.
652
653 **Allotransplant and Tumor Models.** BALB/c recipient mice were irradiated with two doses of
654 400 cGy of x-rays (total dose 800 cGy) and rested for at least 12 hours between doses. Mice
655 were also rested for 4 hours prior to transplantation. T cells (total CD3+ or CD8+) were
656 separated from WT and *TCF-7 cKO* spleens using CD90.2 or CD8 microbeads and LS columns
657 (Miltenyi, CD8: 130-117-044, CD90.2: 130-121-278, LS: 130-042-401). $1X10^6$ donor cells
658 (unless otherwise mentioned) were injected IV into the tail vein in PBS, along with $10X10^6$ WT
659 bone marrow cells. Bone marrow was T-cell depleted with CD90.2 MACS beads (130-121-278
660 from Miltenyi) and LD columns (130-042-901 from Miltenyi). For short-term experiments, at
661 day 7 post-transplant, recipient mice were euthanized and serum, spleen, lymph nodes, small
662 intestine, or liver were collected, depending on the experiment. For GVHD and GVL
663 experiments, recipient mice were also given $2X10^6$ luciferase expressing B-cell lymphoma (A-
664 20) (Edinger *et al.*, 2003a). Recipient mice were weighed, given a clinical score, and imaged

665 using the IVIS 50 imaging system three times per week until day 70 or longer. Clinical scores
666 were composed of scores for skin integrity, fur texture, posture, activity, diarrhea, and weight
667 loss. Imaging was done by injecting recipients I.P. with D-luciferin to detect tumor cell
668 bioluminescence. To produce mixed bone marrow chimeras, Thy1.1 mice were lethally
669 irradiated and reconstituted with a 1:4 (WT: *TCF-7 cKO*) mixture of bone marrow cells (total
670 $50x10^6$ cells), then rested for 9 weeks. At 9 weeks, tail vein blood was collected and checked by
671 flow cytometry for CD45.1 and CD45.2 to ensure reconstitution with both donor cell types. At
672 10 weeks, mice were used for phenotyping experiments.
673
674 **Flow Cytometry, Sorting, and Phenotyping.** Splenocytes (or cells from other organs) were
675 obtained from WT or *TCF-7* cKO mice or recipient allotransplanted mice. Lymphocytes were
676 obtained and lysed with RBC Lysis Buffer (00-4333-57 from eBioscience) to remove red blood
677 cells if needed. Cells were then stained with extracellular markers for 30 min on ice in MACS
678 buffer (1X PBS with EDTA and 4g/L BSA). If intracellular markers were used, the cells were
679 then fixed and permeabilized using the Fix/Perm Concentrate and Fixation Diluent from FOXP3
680 Transcription Factor Staining Buffer Set (eBioscience cat. No. 00-5523-00). The cells were then
681 run on a BD LSR Fortessa cytometer and data were analyzed using FlowJo software v9
682 (Treestar). All antibodies were used at a 1:100 dilution. For FACS sorting, the same methods
683 were applied, and cells were run on a BD FACS Aria IIIu with cold-sorting blocks. Cells were
684 sorted into sorting media (10% FBS in RPMI) or Trizol, depending on the experiment.
685 Depending on the experiment, antibodies used were: anti-CD4 (FITC, PE, BV785, BV21), anti-
686 CD8 (FITC, PE, APC, PerCP, Pacific Blue, PE/Cy7), anti-CD3 (BV605 or APC/Cy7), anti-
687 H2Kb-Pacific Blue, anti-H2Kd-PE/Cy7, anti-CD122 (FITC or APC), anti-CD44 (APC or Pacific

688 Blue), anti-CD62L (APC/Cy7), anti-TNF-α-FITC, anti-IFN-γ-APC, anti-Eomes (AF488 or
689 PE/Cy7), anti-T-bet-BV421, anti-CD45.2-PE/Dazzle594, anti-CD45.1-APC, anti-Ki67 (PE or
690 BV421), anti-PD1-BV785, anti-CTLA4-PE, NKG2D-BV711, Granzyme B-PE/Cy7.
691
692 **Histology.** Recipient mice were allotransplanted as described, and organs were removed for
693 histology at day 7, and day 21 post-transplant. Spleen, liver, small intestine, and skin (from ear
694 and back) were fixed, sectioned, and stained with H&E at Cornell University (
695 https://www.vet.cornell.edu/animal-health-diagnostic-center/laboratories/anatomic-
696 pathology/services). A pathologist (L.S) analyzed the sections for T cell-induced damage.
697
698 **Cytokine Restimulation.** Recipient BALB/c mice were allotransplanted with $1.5X10^6$ CD3
699 donor T cells and euthanized at day 7. Splenocytes were taken and cultured for 6 hours with
700 GolgiPlug (1:1000) and PBS (control) or anti-CD3 (1ug/mL)/anti-CD28 (2ug/mL) (TCR
701 stimulation) at 37 C and 7% CO2. After 6 hours of culture, the cells were stained for CD3, CD4,
702 CD8, $H2K^b$, TNF-α, and IFN-γ using the BD Cytokine Staining kit (BD Biosciences, 555028),
703 and run on a flow cytometer.
704
705 **LegendPLEX Serum ELISA Assay.** Serum from cardiac blood was collected from recipient
706 mice in the cytokine restimulation experiment. Serum was analyzed using the Biolegend
707 LEGENDPlex Assay Mouse Th Cytokine Panel kit (741043). This kit quantifies serum
708 concentrations of: IL-2 (T cell proliferation), IFN-γ and TNF-α (Th1 cells, inflammatory), IL-4,
709 IL-5, and IL-13 (Th2 cells), IL-10 (Treg cells, suppressive), IL-17A/F (Th17 cells), IL-21 (Tfh

710 cells), IL-22 (Th22 cells), IL-6 (acute/chronic inflammation/T cell survival factor), and IL-9
711 (Th2, Th17, iTreg, Th9 – skin/allergic/intestinal inflammation).
712
713 **Western blot.** Splenocytes from WT or *TCF-7* cKO donor mice were collected. CD8 T cells
714 were separated using CD8 MACS beads. CD8 T cells were either stimulated with 2.5ug/ml anti-
715 CD3 (Biolegend #100202) and anti-CD28 antibodies (Biolegend #102115) for 10 minutes or left
716 unstimulated. These cells were counted and lysed with RIPA Buffer (89900 from Thermo Fisher)
717 plus protease inhibitors (11697498001 from Millipore Sigma) and phosphatase inhibitors
718 (P5726-1ML and P0044-1ML from Millipore Sigma). The lysates were run on a Western blot
719 and probed for Perforin (Cell Signaling Technology #3693), Granzyme B (Cell Signaling
720 Technology #4275), LCK (Thermo Fisher PA5-34653), ZAP70(Cell Signaling Technology
721 #3165), LAT(Cell Signaling Technology # 45533), ITK (Thermo Fisher PA5-49363), PLCγ1
722 (Cell Signaling Technology #2822), ERK1-2 (Cell Signaling Technology #9107), JAK 2(Cell
723 Signaling Technology # 3230), JAK3 (Cell Signaling Technology #8863), STAT3 (Cell
724 Signaling Technology #9139), p65-Rela (Cell Signaling Technology #4764), AKT (Cell
725 Signaling Technology #9272), , and β-actin (Cell Signaling Technology #4970). All the western
726 blots repeated at least three times and one representative of each protein and quantification is
727 shown.
728
729 **qPCR Analysis.** To perform qPCR, BALB/c mice were allotransplanted as described ($1X10^6$
730 CD3 donor T cells). Pre-transplant donor cells and post-transplant (day 7) spleen and liver cells
731 from recipients were FACS-sorted to obtain CD8 donor cells. The cells were sorted into Trizol,
732 RNA was extracted using chloroform (https://www.nationwidechildrens.org/

733 Document/Get/93327), and eluted using the Qiagen RNEasy Mini kit (74104 from Qiagen).
734 Concentration was checked with a spectrophotometer, then RNA was converted to cDNA with
735 an Invitrogen Super Script IV First Strand synthesis System kit (18091050 from Invitrogen).
736 Final cDNA concentration was checked with a spectrophotometer, then cDNA was mixed with
737 Taqman Fast Advanced Master Mix (4444557 from Invitrogen) at a 10ng/µL cDNA
738 concentration. This master mix was added to premade 96 well TaqMan Array plates with
739 chemokine/chemokine receptor primers (Thermo Fisher, Mouse Chemokines & Receptors Array
740 plate, 4391524). qPCR was performed in a Quant Studio 3 thermocycler, and data were analyzed
741 using the Design and Analysis software v2.4 (provided by Thermo Fisher). Five separate
742 recipient mice were sorted, and cells were combined to make one sample for qPCR testing per
743 condition/organ.
744
745 **NKG2D expression and NKG2D mediated cytotoxicity in CD8 T cells.** To determine the
746 NKG2D expression in CD8 T cells, we obtained splenocytes from WT and *TCF-7* cKO mice and
747 stimulated T cells with 2.5ug/ml anti-CD3 (Biolegend #100202) and anti-CD28 antibodies
748 (Biolegend #102115) for 24, 48, or 72 hours in culture, or left them unstimulated. GolgiPlug
749 (1:1000) was added to stimulated samples for each time point, and samples were incubated at 37
750 C and 7% CO2. After 6 hours of culture, the cells were stained with LIVE/DEAD Aqua and for
751 CD3, CD8, NKG2D, and Granzyme B using the BD Cytokine Staining kit (BD Biosciences,
752 555028), and run on a flow cytometer. To assess the NKG2D mediated cytotoxicity, we used
753 luciferase-expressing A20 cells as target cells as described earlier. Effector cells (MACS-sorted
754 CD8 T cells from *TCF-7* cKO or WT mice) were incubated in 2.5µg/ml anti-CD3 and anti-CD28
755 coated plates for 48 hours to induce optimal NKG2D expression. Then effector cells were added

756 at 40:1 effector-to-target ratios and incubated at 37°C for 4 hours with the A20 cells. Anti-
757 NKG2D antibody (10 µg/mL, Bio X Cell #BE0334) or rat IgG1 isotype control antibody (10
758 µg/mL, Bio X Cell #BE0334) was added and incubated for 30 minutes before washing and
759 plating. Triplicate wells were averaged and percent lysis was calculated from the data using the
760 following equation: % specific lysis = 100 × (spontaneous death bioluminescence – test
761 bioluminescence)/(spontaneous death bioluminescence – maximal killing bioluminescence).
762
763 **Exhaustion/Activation Assay.** To determine the *in vitro* exhaustion and activation of CD8 T
764 cells, we obtained splenocytes from WT and *TCF-7* cKO mice and either activated them with
765 2.5ug/ml anti-CD3 (Biolegend #100202) and anti-CD28 antibodies (Biolegend #102115) for 24,
766 48, or 72 hours in culture, or left them unstimulated, and stained for CD3, CD8, Ki-67, Tox, and
767 PD-1 markers. To assess exhaustion and activation of *in vivo* donor CD8 T cells, recipient mice
768 were allotransplanted as before ($1X10^6$ CD3 donor T cells) and euthanized at day 7.
769 Lymphocytes were obtained from spleen, and stained for CD3, CD4, CD8, $H2K^b$, TOX, Ki-67
770 and PD-1 markers.
771
772 **DNA Extraction and PCR.** Donor mice were genotyped using PCR on DNA extracted from ear
773 punches. At 4 weeks of age mice were ear punched, and DNA was extracted using the Accustart
774 II Mouse Genotyping kit (95135-500 from Quanta Biosciences). Standard PCR reaction
775 conditions and primer sequences from Jackson Laboratories were used for CD4cre. For Tcf7,
776 primer sequences and reaction conditions were obtained from Dr. Jyoti Misra Sen of NIH.
777

778 **RNA Sequencing.** Recipient mice were allotransplanted as before ($1X10^6$ CD3 donor T cells),
779 except that donor CD8 T cells were also FACS-sorted prior to transplant. A sample of sorted
780 donor cells was also saved for pre-transplanted RNA sequencing in Trizol. At day 7 post-
781 transplant, donor CD8 T cells were FACS-sorted back from recipient spleen of *TCF-7* cKO and
782 WT transplanted mice. The cells were all sorted into Trizol, then RNA was extracted and
783 prepped by the Molecular Analysis Core (SUNY Upstate,
784 https://www.upstate.edu/research/facilities/molecular-analysis.php). Paired end sequencing was
785 done with an Illumina NovaSeq 6000 system at the University at Buffalo Genomics Core
786 (http://ubnextgencore.buffalo.edu). For data analysis we used the statistical computing
787 environment R (v4.0.4), the Bioconductor suite of packages for R, and R studio (v1.4.1106). We
788 calculated the transcript abundance by performing pseudoalignment using the Kallisto (Bray et
789 al., 2016) (version 0.46.2). Calculated Transcript per million (TPM) values were normalized and
790 fitted to a linear model by empirical Bayes method with the Voom (Law et al., 2014) and Limma
791 (Ritchie et al., 2015) R packages to determine Differentially expressed genes – DEGs (FDR<0.1,
792 after controlling for multiple testing using the Benjamini-Hochberg method). DEG's were used
793 for hierarchical clustering and heatmap generation in R. Gene Ontology enrichment analysis was
794 conducted using either the Function Annotation Chart tools using only GO BP and KEGG terms
795 in the Database for Visualization and Integrative Discovery (Huang da et al., 2009a; b) (Huang
796 da *et al.*, 2009a) DAVID enrichment scores >1.3 are equivalent to a P value<0.05. For Gene set
797 enrichment analysis (GSEA) we used Hallmark and C2 gene set collections of Molecular
798 Signatures Database (MsigDB) and cluster Profiler package in R. Data will be deposited on the
799 Gene Expression Omnibus (GEO) database for public access
800 https://www.ncbi.nlm.nih.gov/geo/

801 The RNAseq experiment described here was performed as part of the experiment described in
802 other recent publications from our laboratory (Mammadli et al., 2021a; Mammadli et al., 2021b;
803 Mammadli et al., 2020; Mammadli et al., 2021c). Therefore, the data generated for WT pre- and
804 post-transplanted samples (CD4 and CD8) are the same as that shown in the papers mentioned,
805 but here, these data are compared to data for *Cat-Tg* mice(Mammadli *et al.*, 2021a).
806
807 **Statistical Analysis.** Unless otherwise noted in the figure legends, all numerical data are
808 presented as means and standard deviations with or without individual points. Analysis was done
809 in GraphPad Prism v7 or v9. Most data were analyzed with Student's t-test, one-way ANOVA,
810 or two-way ANOVA, with Tukey's multiple comparisons test for ANOVA methods, depending
811 on the number of groups. Kaplan-Meier survival analyses were done for survival experiments.
812 All tests were two-sided, and p-values less than or equal to (≤) 0.05 were considered significant.
813 Transplant experiments used 3-5 mice per group, with at least two repeats. *Ex vivo* experiments
814 were done two to three times unless otherwise noted with at least three replicates per condition
815 each time. RNA seq was done once with three replicates per group and condition. qPCR was
816 done once with one sample per condition, and 5 mice were combined to make the one sample.
817 Western blots were done 3 times for unstimulated and 10 min anti-CD3/CD28 stimulated
818 samples, one experiment each is shown.
819
820 **Study Approval.** All animal studies were reviewed and approved by the IACUC at SUNY
821 Upstate Medical University. All procedures and experiments were performed according to these
822 approved protocols.
823

824 **Author Contributions**

825 RH, MM, and MK designed and conducted experiments, analyzed data, and wrote the
826 manuscript. MK assisted with scientific/technical research design. MK, and JMS edited the
827 manuscript. MK, SH assisted with data collection. LS performed histology analyses. QY
828 provided technical and scientific advice and assisted with data analysis.

829

830 **Acknowledgments**

831 We thank all members of the Karimi lab for helpful discussions. We also thank Joel Wilmore for
832 help in flow cytometry analysis. This research was funded in part by a grant from the National
833 Blood Foundation Scholar Award to MK, the National Institutes of Health (NIH LRP #L6
834 MD0010106 and K22 (AI130182) to MK), and an Upstate Medical University Cancer Center
835 grant (1146249-1-75632) to MK.

836 JMS was supported by the Intramural Research Program of the National Institute of
837 Aging. We thank Dr. Howard Xue for permission to use *TCF-7* cKO mice. *TCF-7* flox/flox
838 mice were provided by Dr. Jyoti Misra Sen from NIH. RH was a PH. D student at SUNY
839 Upstate Medical University at the time the study was conducted from 2017-2021. A version of
840 this manuscript was previously included as a chapter in RH's dissertation.

841
842
843
844
845
846
847
848
849
850
851
852

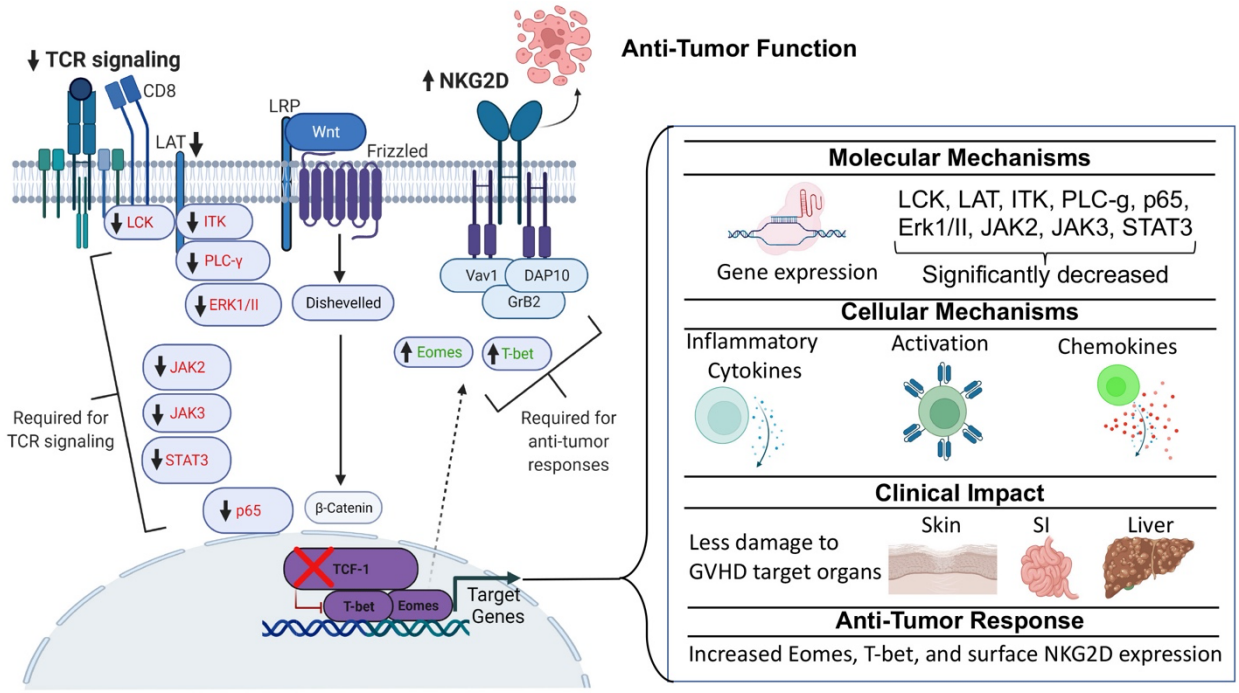

Summary Figure: *TCF-7* is required for persistent function of CD8 T cells but dispensable for anti-tumor response. Here we have utilized a novel mouse model that lacks *TCF-7* specifically on CD8 T cells for an allogeneic transplant model. We uncovered a molecular mechanism of how *TCF-7* regulates key signaling pathways at both transcriptomic and protein levels. These key molecules included LCK, LAT, ITK, PLC-γ1, p65, ERK I/II, and JAK/STAT signaling. Next, we showed that the lack of *TCF-7* impacted phenotype, proinflammatory cytokine production, chemokine expression, T cell activation. We provided clinical evidence for how these changes impact GVHD target organs (skin, small intestine, and liver). Finally, we provided evidence that *TCF-7* regulates NKG2D expression on mouse naïve and activated CD8 T cells. We have shown that CD8 T cells from *TCF-7* cKO mice mediate cytolytic functions via NKG2D.

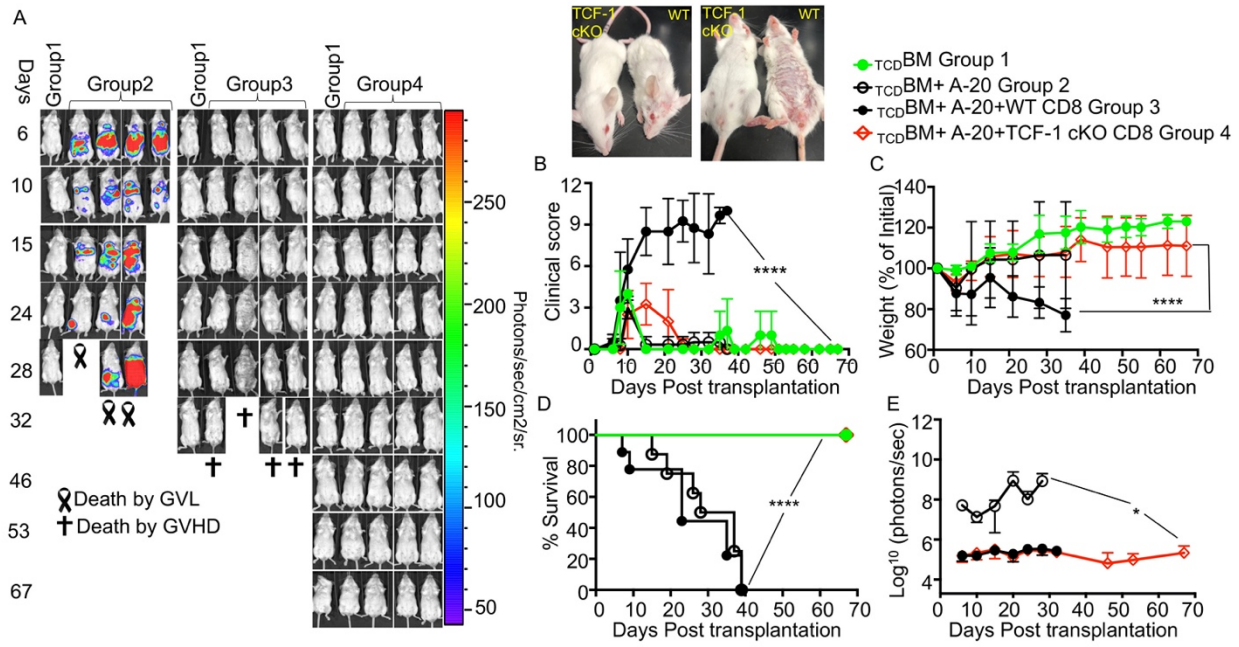

Figure 1: Loss of *TCF-7* in donor CD8 T cells reduces severity and persistence of GVHD symptoms. BALB/c recipient mice (MHC haplotype d) were lethally irradiated and allotransplanted with $1X10^6$ CD8 T cells from WT or *TCF-7* cKO donor mice (MHC haplotype b), as well as $10X10^6$ T cell-depleted bone marrow cells (BM) from WT mice (MHC haplotype b). Recipient mice were also given $2X10^5$ luciferase-expressing A20 tumor cells **(A)** The recipient mice were imaged 1 time a week using IVIS50 for 70 days. Gross pictures of representatives of recipients transplanted with CD8 T cells from *TCF-7* cKO and WT mice at day 25 post-transplant are shown. **(B)** Recipient mice were also given a GVHD clinical score three times per week until day 70, based on combined scores of fur texture, activity level, weight loss, posture, skin integrity, and diarrhea. Mean and SD are plotted, analyzed by one-way ANOVA. **(C)** Weight changes of the recipient mice also were tracked over the time course of disease. **(D)** Survival for each group of recipient mice up to 70 days post-transplant, analyzed by Kaplan-Meier survival analysis. **(E)** Quantification of bioluminescence of tumor growth. For all graphs, * means p-value ≤ 0.05, ** means p-value ≤ 0.01, *** means p-value ≤ 0.001, and ****

880 means p-value ≤ 0.0001 (n = 3 mice/group for BM alone: n = 4 experimental mice/group for all

881 other groups). Survival is a combination of two experiments. Note: Control mouse is one of the

882 mice from bone marrow only transplanted group used as a negative control for BLI.

883

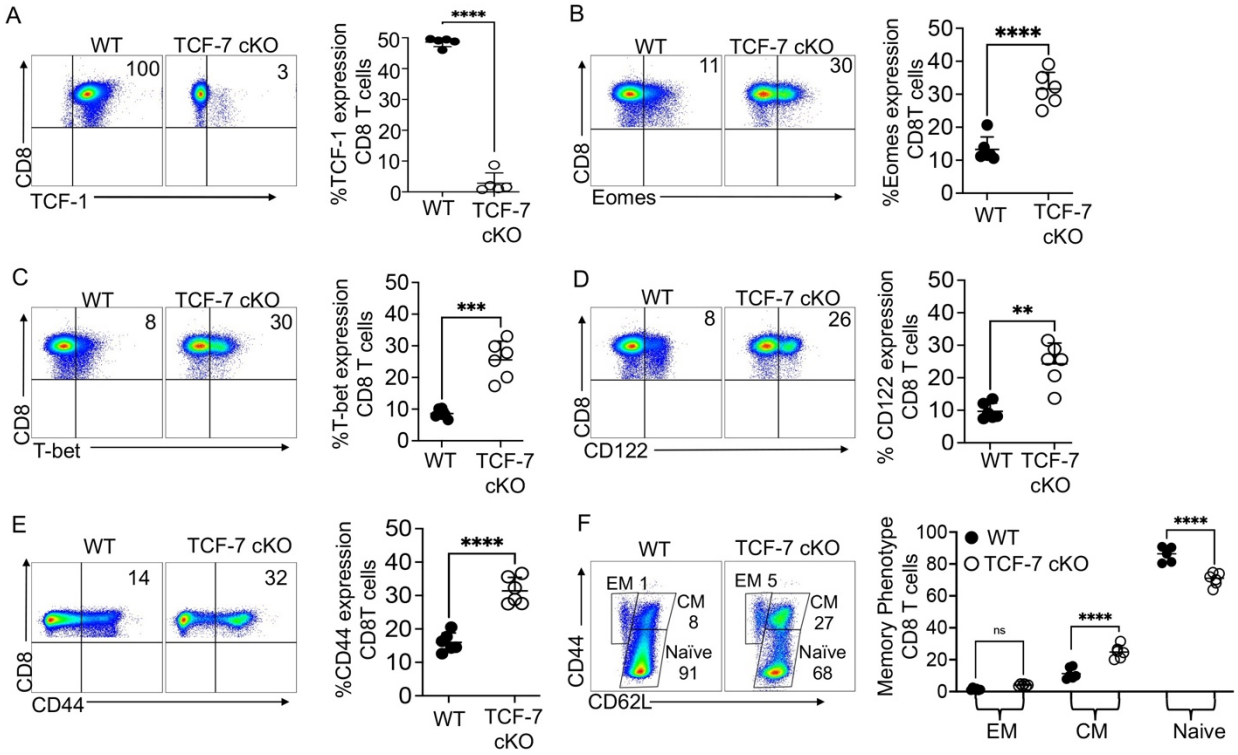

884

885 **Figure 2. Loss of *TCF-7* changes the mature CD8 T cell phenotype.** Naive WT or *TCF-7*

886 cKO donor mice were euthanized and splenocytes were stained for flow cytometry phenotyping**.**

887 **(A)** Percent of CD8 T cells expressing *TCF-7* and quantified statistical analysis **(B)** Percent of

888 CD8 T cells expressing Eomes and quantified statistical analysis. **(C)** Percent of CD8 T cells

889 expressing T-bet and quantified statistical analysis. **(D)** Percent of CD8 T cells expressing

890 CD122 and quantified statistical analysis. **(E)** Percent of CD8 T cells expressing CD44 and

891 quantified statistical analysis. **(F)** Percent of CD8 T cells expressing central memory, effector

892 memory, or naive phenotypes and quantified statistical analysis. All data are plotted as individual

893 points with mean and SD, all were analyzed with one-way ANOVA, or Student's t-test

894 (depending on groups). For all graphs, * means p-value ≤ 0.05, ** means p-value ≤ 0.01, ***

895 means p-value ≤ 0.001, and **** means p-value ≤ 0.0001. N=2-3 per group per experiment, with

896 combined data from 3 experiments shown.

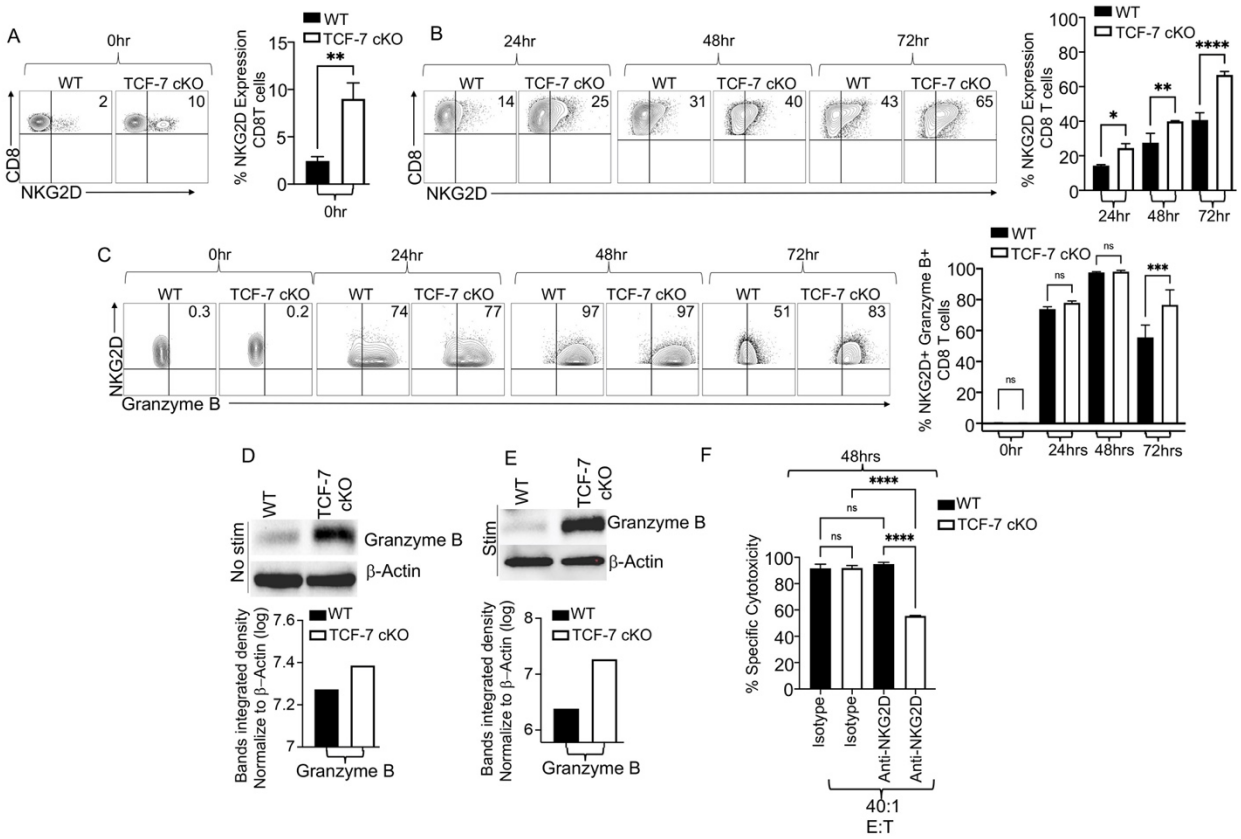

897

898 **Figure 3: Loss of *TCF-7* alters cytotoxic mediator production by mature alloactivated CD8**

899 **T cells.** Total splenocytes were isolated from *TCF-7* cKO or WT mice and either left

900 unstimulated or stimulated with anti-CD3/CD28 for 24, 48, or 72 hours in culture. GolgiPlug

901 (1:1000) was added to stimulated samples in each time point except 0-hour samples, and samples

902 were incubated at 37 C with 7% CO2. After 6 hours of culture, the cells were stained with

903 LIVE/DEAD Aqua, and for CD3, CD8, NKG2D, and Granzyme B expression, as determined by

904 flow cytometry. **(A)** Percent of NKG2D expression in freshly isolated CD8 T cells from WT or

905 *TCF-7* cKO mice and quantified statistical analysis. **(B)** Percent of NKG2D expression in 24, 48,
906 or 72 hour-stimulated CD8 T cells from WT and *TCF-7* cKO mice and quantified statistical
907 analysis. **(C)** Percent of Granzyme B expression in unstimulated or 24, 48, or 72 hour-stimulated
908 CD3+ CD8+ NKG2D+ T cells from WT and *TCF-7* cKO mice, and quantified statistical
909 analysis. **(D)** Granzyme B expression in unstimulated CD8 T cells from WT and *TCF-7* cKO
910 mice by Western blot, and bands' integrated density normalized to β-actin (quantified). **(E)**
911 Granzyme B expression in 10 minute-anti-CD3/CD28-stimulated CD8 T cells from WT and
912 *TCF-7* cKO mice by Western blot, and bands' integrated density normalized to β-actin
913 (quantified) **(F)** To assess the NKG2D-mediated cytotoxicity, we used luciferase-expressing A20
914 cells as target cells. Effector cells (MACS-sorted CD8 T cells from *TCF-7* cKO or WT mice)
915 were incubated in 2.5μg/ml anti-CD3 and anti-CD28 coated plates for 48 hours to induce optimal
916 NKG2D expression. Then effector cells were added at 40:1 effector-to-target ratios and
917 incubated at 37°C for 4 hours with A20 cells. Anti-NKG2D antibody (10 μg/mL) or rat IgG1
918 isotype control antibody (10 μg/mL) was added and incubated for 30 minutes before washing
919 and plating. Triplicate wells were averaged and percent lysis was calculated from the data using
920 the following equation: % specific lysis = 100 × (spontaneous death bioluminescence – test
921 bioluminescence)/ (spontaneous death bioluminescence – maximal killing
922 bioluminescence)(Karimi et al., 2014a; Karimi et al., 2015; Karimi et al., 2014b). N=4 per group
923 with one rappresentative of 2 experiments shown. Western blot were repeated twice and
924 representative examples are shown. All data are shown as individual points with mean and SD,
925 and were analyzed with Student's t-test or one-way ANOVA (depending on groups). * means p-
926 value ≤ 0.05, ** means p-value ≤ 0.01, and *** means p-value ≤ 0.001.

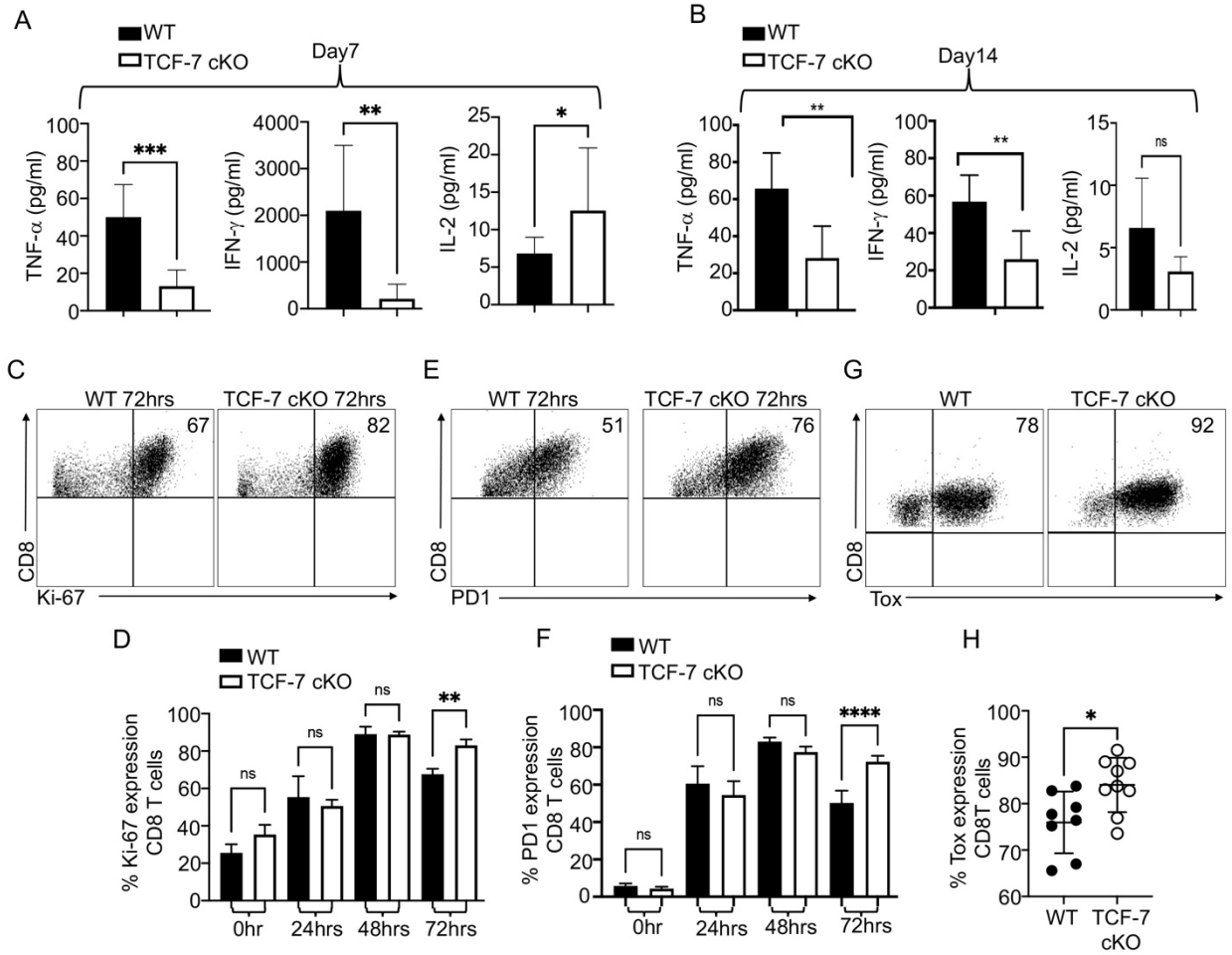

927

928 **Fig.4. *TCF-7* controls cytokine production and exhaustion of mature alloactivated CD8 T**

929 **cells. (A-B)** Recipient mice were allotransplanted with 1.5X10^6 WT or *TCF-7* cKO donor CD3 T

930 cells as before**.** At day 7 and day 14 post-transplant, serum was obtained from cardiac blood of

931 allotransplanted recipient mice and tested for various cytokines using a LEGENDplex ELISA

932 assay. **(A)** Serum levels (pg/mL) of TNF-α, IFN-γ, and IL-2 for WT and *TCF-7* cKO-

933 transplanted mice at day 7 post-transplant. **(B)** Serum levels (pg/mL) of TNF-α, IFN-γ, and IL-2

934 for WT and *TCF-7* cKO-transplanted mice at day 14 post-transplant. **(C-F)** Splenocytes from

935 *TCF-7* cKO and WT mice were obtained and stimulated with anti-CD3/CD28 antibodies for

936 24hrs, 48hrs, or 72hrs in culture and stained for Ki-67 and PD-1 or were stained immediately

937 after isolation without stimulation. **(C)** Percent expression of Ki-67 in CD8 T cells after 72

938 hours of anti-CD3/CD28 stimulation in culture determined by flow cytometry. **(D)**
939 Quantification of the *in vitro* Ki-67 expression of CD8 T cells at different time points. **(E)**
940 Percent expression of PD-1 in CD8 T cells after 72 hours of anti-CD3/CD28 stimulation in
941 culture determined by flow cytometry. **(F)** Quantification of the *in vitro* PD-1 expression of CD8
942 T cells are different time points**. (G-H)** Balb/c mice were allotransplanted as before, with WT or
943 *TCF-7* cKO CD8 donor T cells. On day 7, spleens were removed from recipients, processed to
944 isolate lymphocytes, and spleen-derived lymphocytes from allotransplanted recipient mice were
945 stained for CD3, CD8, $H2K^b$, and TOX to identify exhausted T cells. **(G)** Percent expression of
946 TOX in CD8 T cells after allotransplantation (day 7 post-transplant) as determined by flow
947 cytometry. **(H)** Quantification of the TOX expression in *in vivo* donor CD8 T cells. N=3-5 per
948 group for **A-B** with two experiments shown. N=4 per group for **C-F,** one representative of two
949 experiments shown. N=3-5 per group with one representative experiment shown for **G-H**. All
950 data are shown as individual points with mean and SD, and were analyzed with Student's t-test
951 or two-way ANOVA (depending on groups). * means p-value ≤ 0.05, ** means p-value ≤ 0.01,
952 and *** means p-value ≤ 0.001.

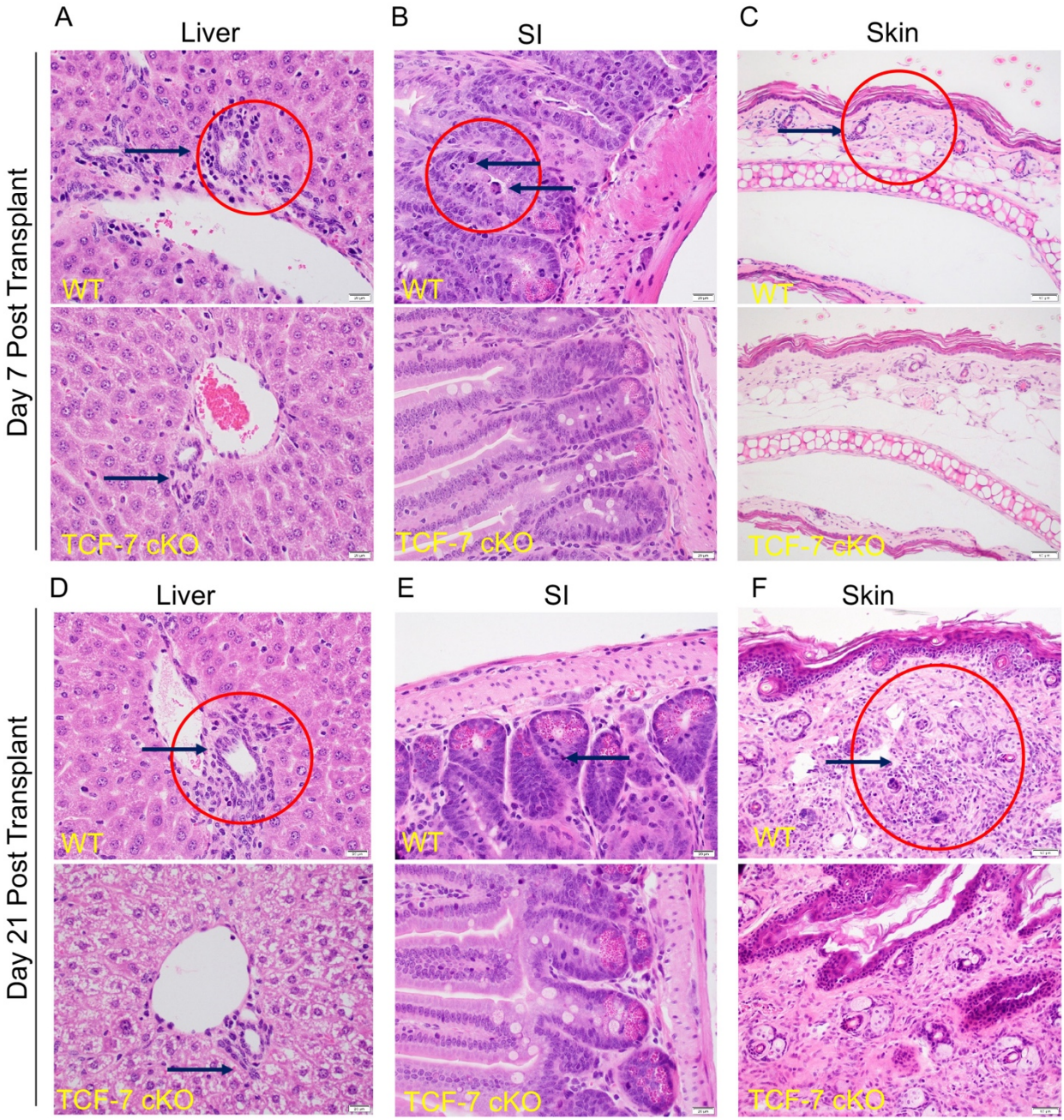

953

954 **Fig.5. Loss of *TCF-7* in donor CD8 T cells decrease the damage to the GVHD target organs.**

955 We collected organs from mice allotransplanted as described above. At day 7 and day 21 post-

956 transplant, organs were taken from recipient mice for histology analyses. Skin, liver, spleen, and

957 small intestine were sectioned, stained with H&E and analyzed by pathologist. Representative

958 sections for each organ per group and timepoint are shown. **(A)** H&E staining of the liver of the

recipient mice at day 7 post-transplant (black arrows showing the interlobular bile ducts and red circle showing inflammatory infiltrates). **(B)** H&E staining of the small intestines of the recipient mice at day 7 post-transplant (black arrows showing the crypts of the small intestine and red circle showing apoptotic bodies). **(C)** H&E staining of the skin of the recipient mice at day 7 post-transplant (black arrows showing the dermis of the skin and red circle showing increase of inflammatory cells) **(D)** H&E staining of the liver of the recipient mice at day 21 post-transplant (black arrows showing the interlobular bile ducts and red circle showing inflammatory infiltrates). **(E)** H&E staining of the small intestines of the recipient mice at day 21 post-transplant (blacks arrows showing apoptotic bodies). **(F)** H&E staining of the skin of the recipient mice at day 21 (black arrows showing dermis of skin and red circle showing increased inflammatory cells with destructed adnexal glands).

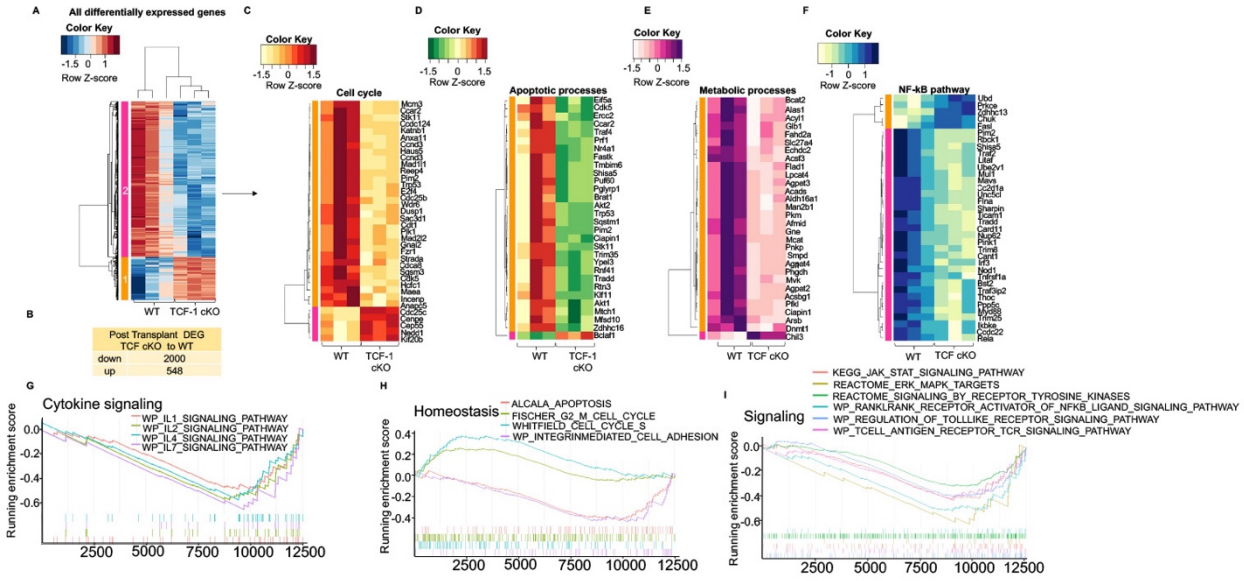

Fig.6. Loss of *TCF-7* changes the genetic signature of alloactivated donor CD8 T cells. CD8 T cells from WT and *TCF-7* cKO mice were FACS sorted either into Trizol as pre-transplanted samples, or into 10% FBS-containing media for transplantation into recipient mice as described previously. At day 7 post-transplant, donor CD8 T cells were FACS-sorted back

975 from recipient spleens of *TCF-7* cKO- and WT-transplanted mice. RNA was extracted and
976 prepped by the Molecular Analysis Core (SUNY Upstate). Paired end sequencing was done with
977 an Illumina NovaSeq 6000 system at the University at Buffalo Genomics Core. For data analysis,
978 we used the statistical computing environment R (v4.0.4), the Bioconductor suite of packages for
979 R, and RStudio (v1.4.1106). We calculated the transcript abundance by performing
980 pseudoalignment using Kallisto. **(A)** Hierarchical clustering of genes and samples, heatmap
981 illustrating the expression of the differentially expressing genes (DEG's; FDR<0.1) of post-
982 transplanted CD8 T cells *TCF-7* cKO compared to WT. **(B)** Table showing the number of up- or
983 downregulated DEGs in post-transplanted CD8 T cells (*TCF-7* cKO compared to WT). **(C)**
984 Heatmap showing top significant 35 differentially expressed genes that play a role in the Cell
985 Cycle pathway, identified using DAVID Functional Annotation Analysis and GO-BP terms in
986 post-transplanted CD8 T cells (*TCF-7* cKO compared to WT)**.** **(D)** Heatmap showing top
987 significant 30 differentially expressed genes that play a role in the Apoptotic Processes pathway,
988 identified using DAVID Functional Annotation Analysis and GO-BP terms in post-transplanted
989 CD8 T cells (*TCF-7* cKO compared to WT). **(E)** Heatmap showing top significant 30
990 differentially expressed genes that play a role in the Metabolic Processes pathway, identified
991 using DAVID Functional Annotation Analysis and GO-BP terms in post-transplanted CD8 T
992 cells (*TCF-7* cKO compared to WT). **(F)** Heatmap showing top significant 35 differentially
993 expressed genes that play a role in the NF-κB pathway, identified using DAVID Functional
994 Annotation Analysis and GO-BP terms in post-transplanted CD8 T cells (*TCF-7* cKO compared
995 to WT). **(G)** Gene set enrichment analysis (GSEA) enrichment plots of Cytokine signaling
996 pathways, including IL-1, IL-2, IL-4, and IL-7 signaling pathways from WP terms that are
997 enriched in post-transplanted CD8 T cells from WT mice (versus *TCF-7* cKO). Negative

998 Enrichment Score is an indicator of downregulation, and positive Enrichment Score is an
999 indicator of upregulation of the genes in the post-transplanted CD8 T cells from *TCF-7* cKo
1000 mice. DAVID enrichment scores >1.3 are equivalent to a P value<0.05 (**H)** GSEA enrichment
1001 plots of G2 to M Cell Cycle and Cell Cycle S pathways that are enriched in *TCF-7* cKO mice,
1002 and Integrin Mediated Cell Adhesion and Apoptosis pathways that are enriched in post-
1003 transplanted CD8 T cells from WT mice. **(I)** GSEA enrichment plots of JAK-STAT signaling,
1004 Toll like receptor signaling, T cell receptor signaling, ERK MAPK signaling, signaling by
1005 Tyrosine kinases, Rankl - Rank mediated NF-kB signaling pathways that are enriched in post-
1006 transplanted CD8 T cells from WT mice. Again, Negative Enrichment Score is an indicator of
1007 downregulation, and positive Enrichment Score is an indicator of upregulation of the genes in the
1008 post-transplanted CD8+ T cells from *TCF-7* cKo mice. DAVID enrichment scores >1.3 are
1009 equivalent to a P value<0.05.

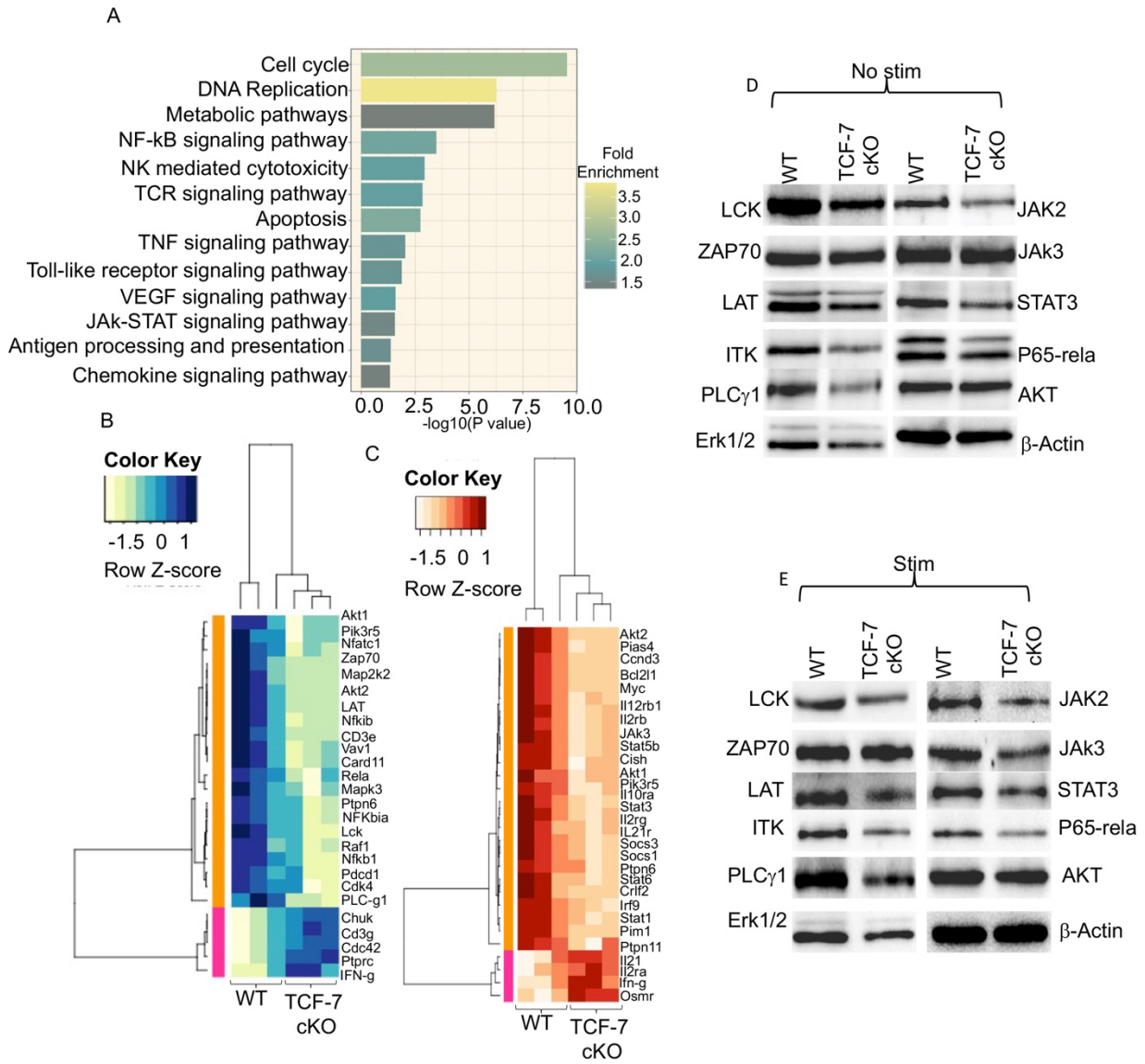

1010

1011 **Fig.7. Loss of *TCF-7* decrease TCR, JAK-STAT, and NF-kB signaling downstream. (A)** A

1012 bar plot showing KEGG (Kyoto Encyclopedia of Genes and Genomes) pathways identified by

1013 David functional annotation analysis. **(B)** Heatmap showing the altered genes in TCR signaling

1014 pathway from KEGG pathways**. (C)** Heatmap showing the altered genes in JAK-STAT signaling

1015 pathway from KEGG pathways. **(D)** Western blot showing the protein expression levels of LCK,

1016 ZAP70, LAT, ITK, PLCγ1, ERK1/2, JAK2, JAK3, STAT3, P65-RelA, AKT, and β-actin of

1017 freshly isolated CD8 T cell lysates from *TCF-7* cKO and WT mice**. (E)** Western blot showing

1018 the protein expression levels of LCK, ZAP70, LAT, ITK, PLCγ1, ERK1/2, JAK2, JAK3,

1019 STAT3, P65-RelA, AKT, and β-actin in 10 minute-CD3/CD28-stimulated CD8 T cell lysates

1020 from *TCF-7* cKO and WT mice**.** All the western blots repeated at least three and one

1021 representative of each protein and quantification is shown.

1022

1023

1024 **Supplemental Figure Legends:**

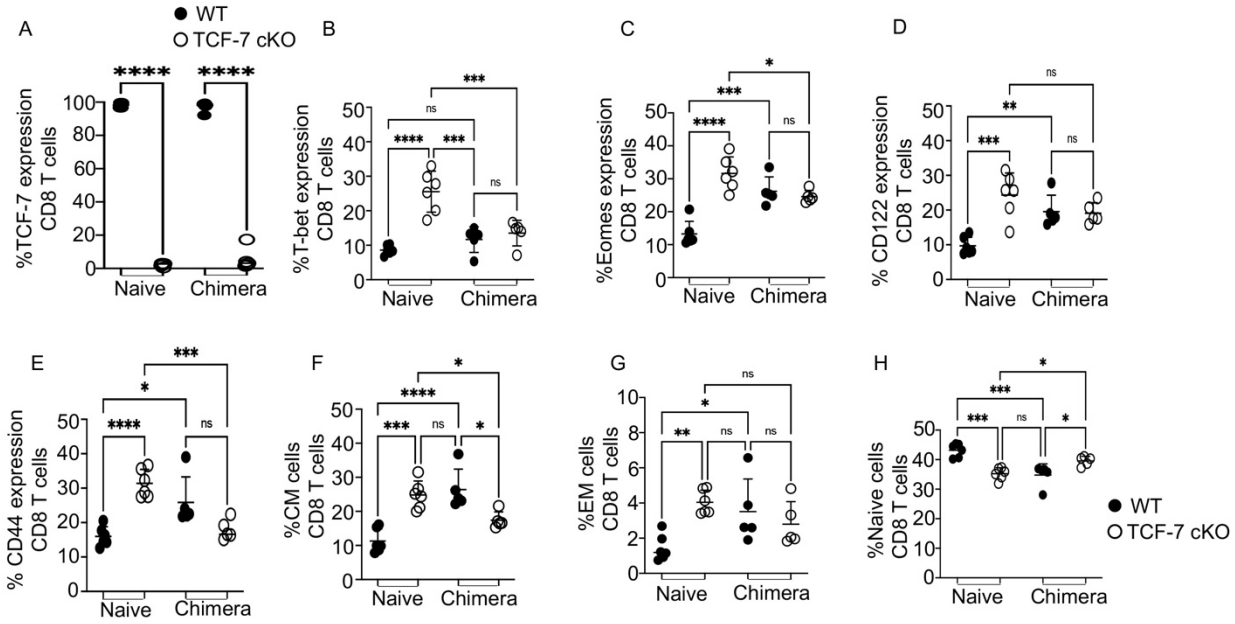

1025

1026 **Supp.Fig.1. Related to Fig2. Loss of *TCF-7* drives changes to mature CD8 T cell phenotype**
1027 **that are cell-intrinsic, with the possibility of extrinsic effects.** Bone marrow chimeras were
1028 developed by lethally irradiating Thy1.1 mice and reconstituting with a 1:4 (WT:*TCF-7* cKO)
1029 mixture of bone marrow cells. Blood was tested at 9 weeks to ensure reconstitution with both
1030 donor cell types, and splenocytes were used at 10 weeks for phenotyping by flow cytometry. **(A)**
1031 Percentage of CD8 T cells from chimeric and naive mice expressing *TCF-7*. **(B)** Percentage of
1032 CD8 T cells from chimeric and naive mice expressing T-bet. **(C)** Percentage of CD8 T cells from
1033 chimeric and naive mice expressing Eomes. **(D)** Percentage of CD8 T cells from chimeric and
1034 naive mice expressing CD122. **(E)** Percentage of CD8 T cells from chimeric and naive mice
1035 expressing CD44. **(F)** Percentage of CD8 T cells from chimeric and naive mice expressing
1036 central memory (CM) phenotype. **(G)** Percentage of CD8 T cells from chimeric and naive mice
1037 expressing effector memory (EM) phenotype. **(H)** Percentage of CD8 T cells from chimeric and
1038 naive mice expressing naïve phenotype. All data are plotted as individual points with mean and

1039 SD, all were analyzed with one-way ANOVA, or Student's t-test (depending on groups). For all
1040 graphs, * means p-value ≤ 0.05, *** means p-value ≤ 0.001, and **** means p-value ≤ 0.0001.
1041 For naïve cells 3 different experiments combined (N=2-3 per group of mice) and for chimera cell
1042 (N=5) with one experiment shown (done once).

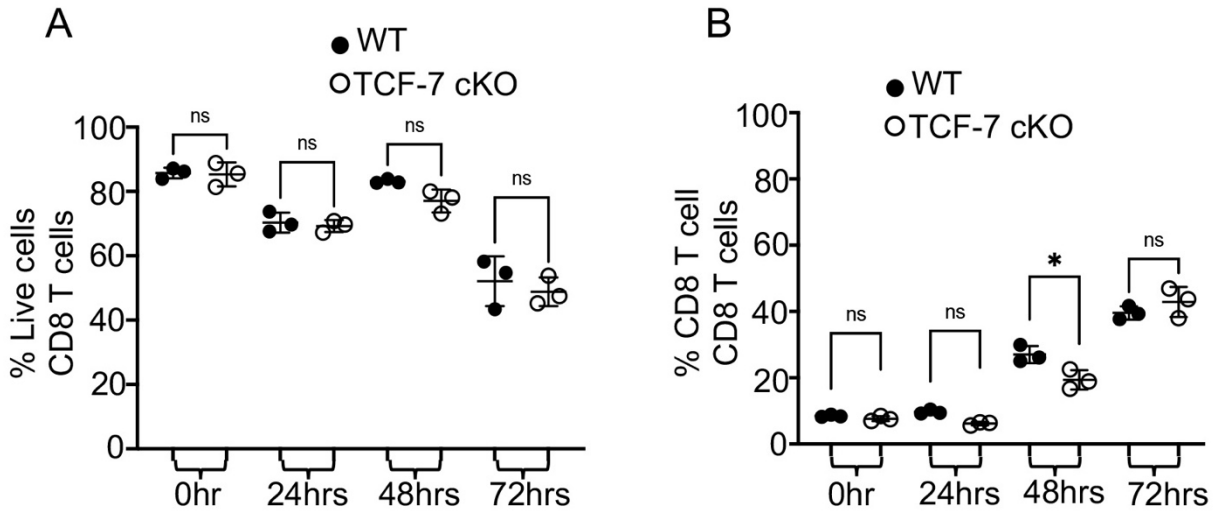

1043

1044 **Supp.Fig.2 Related to Fig.3. Cell viability and CD8 + T cell percent in NKG2D induction *in***
1045 ***vitro*.** Total splenocytes were isolated from *TCF-7* cKO or WT mice and either left unstimulated
1046 or stimulated with anti-CD3/CD28 for 24, 48, or 72 hrs in culture. GolgiPlug (1:1000) was added
1047 to stimulated samples for each time point except 0 hr samples, and samples were incubated at 37
1048 C with 7% CO2. After 6 hours of culture, the cells were stained for CD3, CD8, NKG2D, and
1049 Granzyme B expression, as determined by flow cytometry**. (A)** Quantification of percent of live
1050 cells (dead cells that were positive for LIVE/DEAD Aqua excluded) for different time points of
1051 stimulation. **(B)** Quantification of CD8 T cell percentages for different time points of
1052 stimulation. N=4 per group with one representative of 2 experiments shown. All data are shown
1053 as individual points with mean and SD, and were analyzed with two-way ANOVA (depending
1054 on groups). * means p-value ≤ 0.05, ** means p-value ≤ 0.01, and *** means p-value ≤ 0.001.

1055

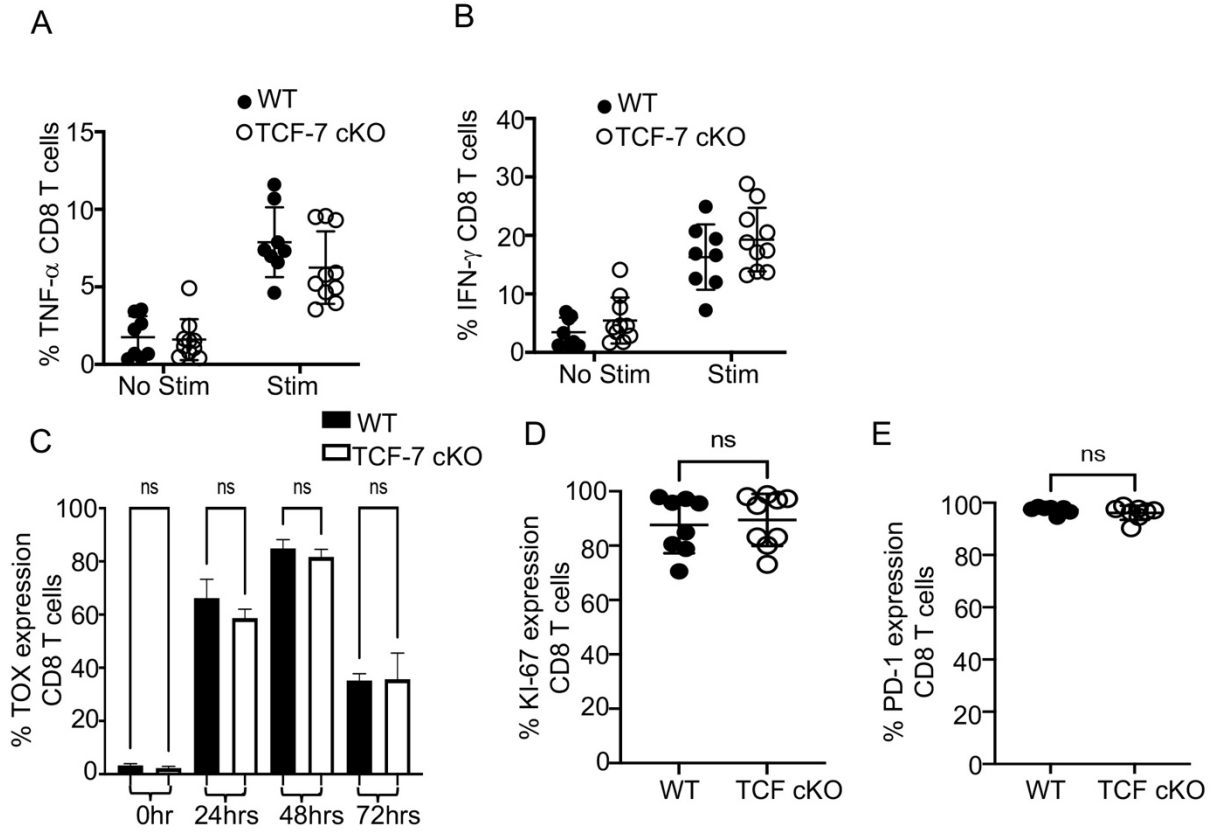

1056

1057 **Supp.Fig3. Related to Fig.5. *TCF-7* controls cytokine production and exhaustion of mature**

1058 **alloactivated CD8 T cells. (A-B)** Recipient mice were allotransplanted with $1.5X10^6$ WT or

1059 *TCF-7* cKO donor CD3 T cells as before. Splenocytes were taken at day 7 post-transplant,

1060 restimulated by 6-hour culture with Golgi Plug and PBS (control) or anti-CD3/anti-CD28 (TCR

1061 restim.), then stained for $H2K^b$, CD3, CD4, CD8, TNF-α, and IFN-γ. **(A)** TNF-α production and

1062 **(B)** IFN-γ production by donor CD8 T cells, as measured by percent cytokine-positive donor

1063 cells. **(C)** Splenocytes from *TCF-7* cKO and WT mice were obtained and either stimulated with

1064 anti-CD3/CD28 antibodies for 24hrs, 48hrs, or 72hrs in culture and stained for TOX, or were

1065 immediately stained after isolation without stimulation. Percent expression of TOX in CD8 T

1066 cells after 72 hours of CD3/CD28 stimulation in culture, as determined by flow cytometry. **(D-E)**

Balb/c mice were allo-transplanted as before, with WT BM and WT or *TCF-7* cKO CD8 donor T cells. On day 7, spleens were removed from recipients, processed to isolate lymphocytes, and lymphocytes were stained for CD3, CD8, H2K^b, Ki-67, and PD-1 to identify proliferating and exhausted T cells, respectively. **(D)** Quantification of the Ki-67 expression in *in vivo* donor CD8 T cells. (**E)** Quantification of the PD-1 expression in *in vivo* donor CD8 T cells. N=3-5 per group for **A-B and D-E** with two experiments shown. N=4 per group for **C,** one representative of two experiments shown. All data are shown as individual points with mean and SD, and were analyzed with Student's t-test or two-way ANOVA (depending on groups). * means p-value ≤ 0.05, ** means p-value ≤ 0.01, and *** means p-value ≤ 0.001.

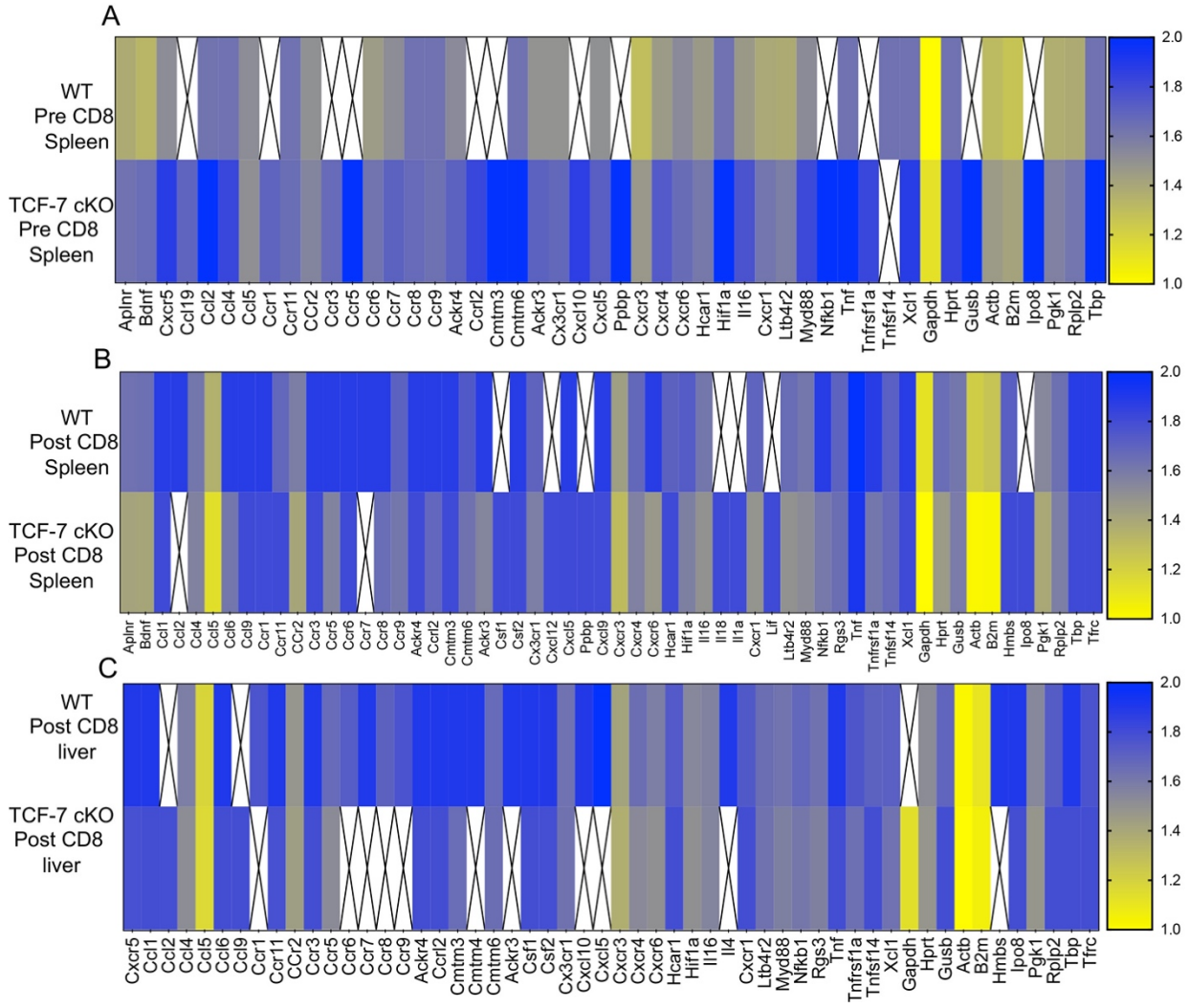

1077 **Supp.Fig.4. *TCF-7* controls chemokine and chemokine receptor expression of donor CD8 T**
1078 **cells during alloactivation.** As before, BALB/c mice were allotransplanted with BM and $1X10^6$
1079 donor CD3 T cells from WT or *TCF-7* cKO mice (not mixed). Donor CD8 T cells were FACS-
1080 sorted from spleen of donor's pre-transplant, and from spleen and liver of recipients at day 7
1081 post-transplant. Cells were sorted into Trizol, then RNA was extracted using chloroform and
1082 converted to cDNA for qPCR analysis. cDNA was run on premade mouse chemokine/chemokine
1083 receptor assay plates, and results are displayed as heatmaps. Scales are shown at right, with fold
1084 change per gene compared to an 18S reference gene on each plate. White boxes with an "X"
1085 represent signals too low to detect or otherwise unreadable due to technical limitation/error. **(A)**
1086 Pre-transplant spleen donor CD8 T cells, **(B)** post-transplant spleen donor CD8 T cells, and **(C)**
1087 post-transplant liver donor CD8 T cells for WT versus *TCF-7* cKO donors. N=5 mice into one
1088 sample per condition**,** summary data shown.

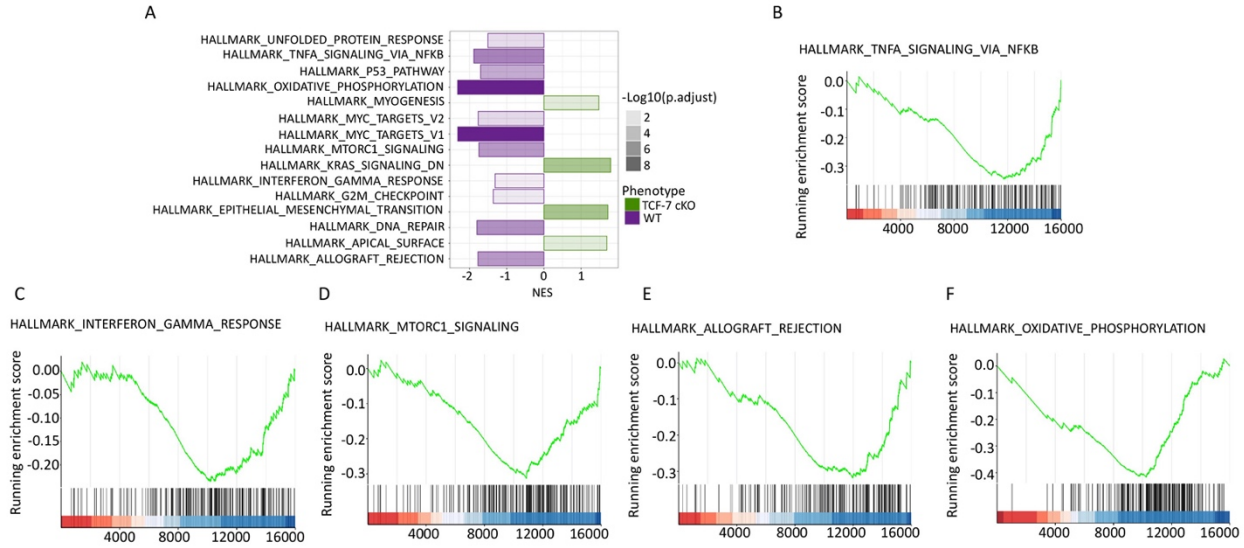

1089

1090 **Supp.Fig.5: Loss of *TCF-7* alters the enrichment of gene sets in pre-transplanted CD8+T**
1091 **cells. (A)** Bar plot of the altered pathways indentified in Gene set enrichment analysis (GSEA)
1092 by using Hallmark gene set collections of the Molecular Signatures Database (MSigDB) in pre-

1093 transplanted CD8 T cells (*TCF-7* cKO compared to WT). The normalized enrichment score
1094 (NES) for the pathway is defined as the peak score furthest from zero, with a negative NES
1095 meaning enrichment in the WT group. **(B)** GSEA plot for the
1096 "HALLMARK_TNFA_SIGNALING_VIA_NFKB" pathway comparing pre-transplanted CD8 T
1097 cells from *TCF-7* cKO to WT cells. The running enrichment score (ES) for the pathway is
1098 defined as the peak score furthest from zero, with a negative ES meaning enrichment in the WT
1099 group. **(C)** GSEA plot for the "HALLMARK_INTERFERON_GAMMA_RESPONSE" pathway
1100 comparing pre-transplanted CD8 T cells from *TCF*-7 cKO to WT cells. **(D)** GSEA plot for the
1101 "HALLMARK_MTORC1_SIGNALING" pathway comparing pre-transplanted CD8 T cells
1102 from *TCF-7* cKO to WT cells. **(E)** GSEA plot for the
1103 "HALLMARK_ALLOGRAFT_REJECTION" pathway comparing pre-transplanted CD8 T cells
1104 from *TCF-7* cKO to WT cells. **(F)** GSEA plot for the
1105 "HALLMARK_OXIDATIVE_PHOSPHORYLATION" pathway comparing pre-transplanted
1106 CD8 T cells from *TCF-7* cKO to WT cells.

Top 20 pathways in GO-BP

Term ID	Term	Count	%	P Value	Fold Enrichment	FDR
GO:0007049	Cell cycle	141	5.73870574	2.34E-14	1.906511069	1.19E-10
GO:0015031	Protein transport	134	5.45380545	3.42E-13	1.879194277	8.74E-10
GO:0098609	Cell-cell adhesion	55	2.23850224	6.46E-10	2.415958527	9.33E-07
GO:0051301	Cell division	88	3.58160358	7.31E-10	1.953438125	9.33E-07
GO:0007067	Mitotic nuclear division	69	2.80830281	5.24E-09	2.068035126	5.35E-06
GO:0006915	Apoptotic process	114	4.63980464	4.40E-08	1.660422406	3.75E-05
GO:0006810	Transport	291	11.8437118	1.39E-07	1.325968496	1.01E-04
GO:0006974	Cellular response to DNA damage stimulus	86	3.5002035	8.53E-07	1.699956273	5.31E-04
GO:0016192	Vesicle-mediated transport	52	2.11640212	9.36E-07	2.026806693	5.31E-04
GO:0006783	Heme biosynthetic process	12	0.48840049	2.25E-06	5.243439176	0.0011491
GO:0002479	Antigen processing and presentation of exogenous peptide antigen via MHC class I, TAP-dependent	15	0.61050061	2.85E-06	4.151056015	0.00132461
GO:0050852	T cell receptor signaling pathway	20	0.81400081	3.32E-06	3.255730208	0.00141253
GO:0006260	DNA replication	34	1.38380138	5.93E-06	2.294892756	0.00232917
GO:0002376	Immune system process	76	3.09320309	1.26E-05	1.647416486	0.00460664
GO:0043123	Positive regulation of I-kappaB kinase/NF-kappaB signaling	36	1.46520147	6.87E-05	2.005879416	0.02338981
GO:0008152	Metabolic process	84	3.41880342	1.21E-04	1.506214709	0.03848315
GO:0031663	Lipopolysaccharide-mediated signaling pathway	13	0.52910053	1.40E-04	3.481530851	0.04077673
GO:0006281	DNA repair	62	2.52340252	1.44E-04	1.618650773	0.04077673
GO:0008643	Carbohydrate transport	14	0.56980057	2.33E-04	3.141339687	0.06257663

Supp.Fig.6. Related to Fig.7. Top 20 GO-BP terms identified in DAVID functional annotation analysis of differentially expressed genes in post-transplanted samples. Count mean – number of genes involved in the Term, % - percentage of involved genes/ total genes in the Term.

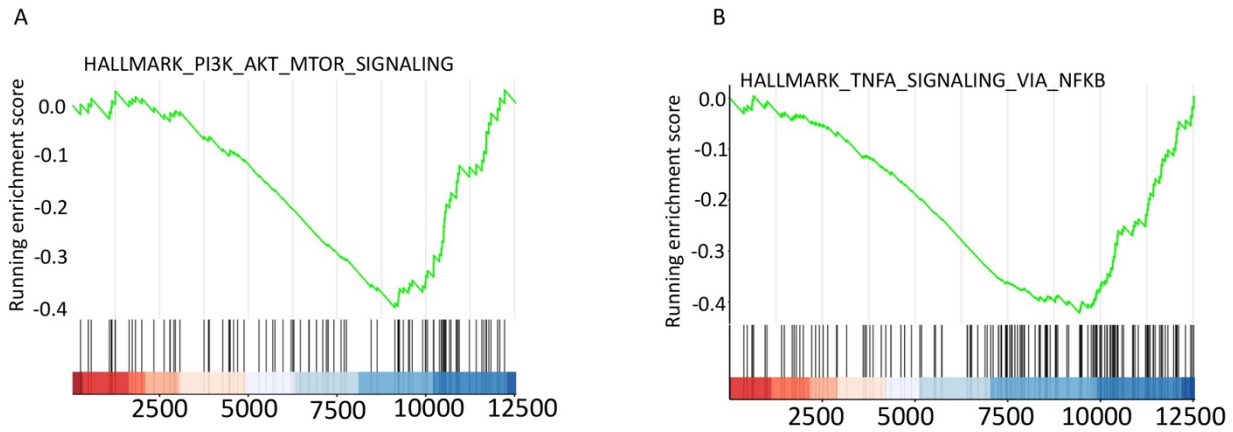

Supp.Fig.7. Loss of *TCF-7* alters the Gene Set Enrichment Analysis (GSEA) of post-transplanted CD8+T cells. (A) GSEA plot for the "HALLMARK_PI3K_AKT_MTOR_SIGNALING" pathway comparing post-transplanted CD8 T cells from *TCF-7* cKO to WT mice. The running enrichment score (ES) for the pathway is defined as the peak score furthest from zero, with a negative ES meaning enrichment in the WT group. **(B)** GSEA plot for the "HALLMARK_TNFA_SIGNALING_VIA_NFKB" pathway comparing post-transplanted CD8 T cells from *TCF-7* cKO to WT mice. Again, the running enrichment score (ES) for the pathway is defined as the peak score furthest from zero, with a negative ES meaning enrichment in the WT group.

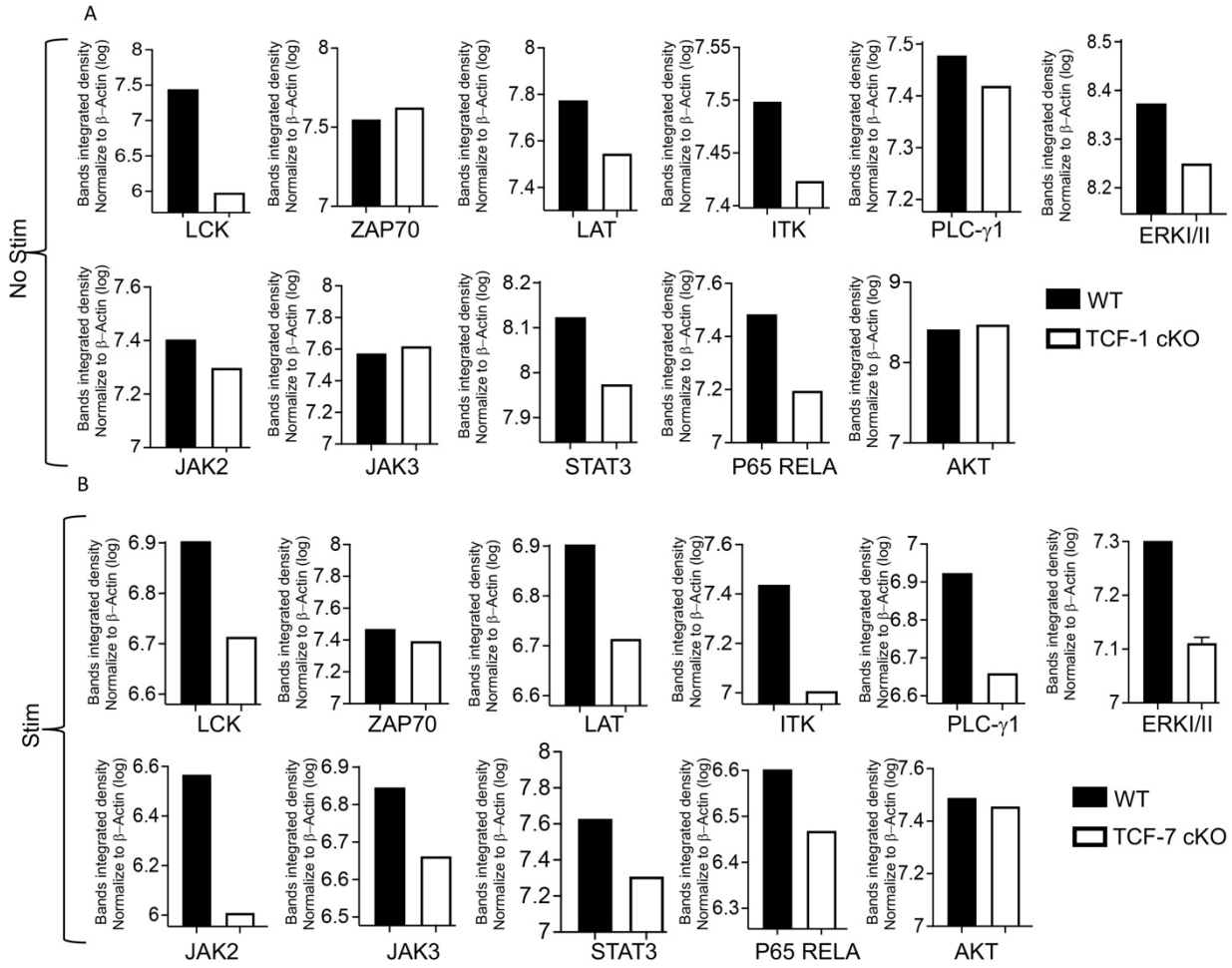

1122 **Supp.Fig.8. Related to Fig.8**. **Quantification of Western blot of TCR and JAK-STAT**
1123 **signaling.** (**A)** Comparison of the quantified bands integrated density normalized to β-actin for
1124 unstimulated CD8 T cells from *TCF-7* cKO and WT mice**. (B)** Comparison of the quantified
1125 bands integrated density normalized to β-actin for 10-minute-anti-CD3/CD28-stimulated CD8 T
1126 cells from *TCF-7* cKO and WT mice. All the western blots repeated at least three times and one
1127 representative of each protein and quantification is shown.

1128

1129

1130

1131

1132

1133

1134

1135

1136 References

1137 Abel, A.M., Yang, C., Thakar, M.S., and Malarkannan, S. (2018). Natural Killer Cells:
1138 Development, Maturation, and Clinical Utilization. Front Immunol *9*, 1869.
1139 10.3389/fimmu.2018.01869.
1140 Ahn, E., Araki, K., Hashimoto, M., Li, W., Riley, J.L., Cheung, J., Sharpe, A.H., Freeman, G.J.,
1141 Irving, B.A., and Ahmed, R. (2018). Role of PD-1 during effector CD8 T cell differentiation. Proc
1142 Natl Acad Sci U S A *115*, 4749-4754. 10.1073/pnas.1718217115.
1143 Al Dulaimi, D., Klibi, J., Olivo Pimentel, V., Parietti, V., Allez, M., Toubert, A., and Benlagha, K.
1144 (2018). Critical Contribution of NK Group 2 Member D Expressed on Invariant Natural Killer T
1145 Cells in Concanavalin A-Induced Liver Hepatitis in Mice. Front Immunol *9*, 1052.
1146 10.3389/fimmu.2018.01052.
1147 Balassa, K., Danby, R., and Rocha, V. (2019). Haematopoietic stem cell transplants: principles
1148 and indications. Br J Hosp Med (Lond) *80*, 33-39. 10.12968/hmed.2019.80.1.33.
1149 Bastien, J.P., Roy, J., and Roy, D.C. (2012). Selective T-cell depletion for haplotype-mismatched
1150 allogeneic stem cell transplantation. Seminars in oncology *39*, 674-682.
1151 10.1053/j.seminoncol.2012.09.004.
1152 Beilhack, A., Schulz, S., Baker, J., Beilhack, G.F., Wieland, C.B., Herman, E.I., Baker, E.M., Cao,
1153 Y.A., Contag, C.H., and Negrin, R.S. (2005). In vivo analyses of early events in acute graft-versus-
1154 host disease reveal sequential infiltration of T-cell subsets. Blood *106*, 1113-1122.
1155 10.1182/blood-2005-02-0509.
1156 Beltra, J.C., Manne, S., Abdel-Hakeem, M.S., Kurachi, M., Giles, J.R., Chen, Z., Casella, V., Ngiow,
1157 S.F., Khan, O., Huang, Y.J., et al. (2020). Developmental Relationships of Four Exhausted CD8(+)
1158 T Cell Subsets Reveals Underlying Transcriptional and Epigenetic Landscape Control
1159 Mechanisms. Immunity *52*, 825-841 e828. 10.1016/j.immuni.2020.04.014.
1160 Berga-Bolanos, R., Zhu, W.S., Steinke, F.C., Xue, H.H., and Sen, J.M. (2015). Cell-autonomous
1161 requirement for TCF1 and LEF1 in the development of Natural Killer T cells. Mol Immunol *68*,
1162 484-489. 10.1016/j.molimm.2015.09.017.
1163 Bleakley, M., Turtle, C.J., and Riddell, S.R. (2012). Augmentation of anti-tumor immunity by
1164 adoptive T-cell transfer after allogeneic hematopoietic stem cell transplantation. Expert Rev
1165 Hematol *5*, 409-425. 10.1586/ehm.12.28.
1166 Blessin, N.C., Li, W., Mandelkow, T., Jansen, H.L., Yang, C., Raedler, J.B., Simon, R., Buscheck, F.,
1167 Dum, D., Luebke, A.M., et al. (2021). Prognostic role of proliferating CD8(+) cytotoxic Tcells in
1168 human cancers. Cell Oncol (Dordr) *44*, 793-803. 10.1007/s13402-021-00601-4.
1169 Bray, N.L., Pimentel, H., Melsted, P., and Pachter, L. (2016). Near-optimal probabilistic RNA-seq
1170 quantification. Nat Biotechnol *34*, 525-527. 10.1038/nbt.3519.
1171 Breems, D.A., and Lowenberg, B. (2005). Autologous stem cell transplantation in the treatment
1172 of adults with acute myeloid leukaemia. Br J Haematol *130*, 825-833. BJH5628 [pii]
1173 10.1111/j.1365-2141.2005.05628.x.
1174 Chen, Z., Ji, Z., Ngiow, S.F., Manne, S., Cai, Z., Huang, A.C., Johnson, J., Staupe, R.P., Bengsch, B.,
1175 Xu, C., et al. (2019). *TCF-1*-Centered Transcriptional Network Drives an Effector versus
1176 Exhausted CD8 T Cell-Fate Decision. Immunity *51*, 840-855 e845.
1177 10.1016/j.immuni.2019.09.013.
1178 Chu, T., Tyznik, A.J., Roepke, S., Berkley, A.M., Woodward-Davis, A., Pattacini, L., Bevan, M.J.,

1179 Zehn, D., and Prlic, M. (2013). Bystander-activated memory CD8 T cells control early pathogen
1180 load in an innate-like, NKG2D-dependent manner. Cell Rep *3*, 701-708.
1181 10.1016/j.celrep.2013.02.020.
1182 Cieri, N., Camisa, B., Cocchiarella, F., Forcato, M., Oliveira, G., Provasi, E., Bondanza, A.,
1183 Bordignon, C., Peccatori, J., Ciceri, F., et al. (2013). IL-7 and IL-15 instruct the generation of
1184 human memory stem T cells from naive precursors. Blood *121*, 573-584. 10.1182/blood-2012-
1185 05-431718.
1186 Cooke, K.R., Kobzik, L., Martin, T.R., Brewer, J., Delmonte, J., Jr., Crawford, J.M., and Ferrara, J.L.
1187 (1996). An experimental model of idiopathic pneumonia syndrome after bone marrow
1188 transplantation: I. The roles of minor H antigens and endotoxin. Blood *88*, 3230-3239.
1189 Cui, W., Liu, Y., Weinstein, J.S., Craft, J., and Kaech, S.M. (2011). An interleukin-21-interleukin-
1190 10-STAT3 pathway is critical for functional maturation of memory CD8+ T cells. Immunity *35*,
1191 792-805. 10.1016/j.immuni.2011.09.017.
1192 Decman, V., Laidlaw, B.J., Dimenna, L.J., Abdulla, S., Mozdzanowska, K., Erikson, J., Ertl, H.C.,
1193 and Wherry, E.J. (2010). Cell-intrinsic defects in the proliferative response of antiviral memory
1194 CD8 T cells in aged mice upon secondary infection. J Immunol *184*, 5151-5159.
1195 10.4049/jimmunol.0902063.
1196 Dutt, S., Baker, J., Kohrt, H.E., Kambham, N., Sanyal, M., Negrin, R.S., and Strober, S. (2011).
1197 CD8+CD44(hi) but not CD4+CD44(hi) memory T cells mediate potent graft antilymphoma
1198 activity without GVHD. Blood *117*, 3230-3239. 10.1182/blood-2010-10-312751.
1199 Edinger, M., Hoffmann, P., Contag, C.H., and Negrin, R.S. (2003a). Evaluation of effector cell fate
1200 and function by in vivo bioluminescence imaging. Methods *31*, 172-179. 10.1016/s1046-
1201 2023(03)00127-0.
1202 Edinger, M., Hoffmann, P., Ermann, J., Drago, K., Fathman, C.G., Strober, S., and Negrin, R.S.
1203 (2003b). CD4+CD25+ regulatory T cells preserve graft-versus-tumor activity while inhibiting
1204 graft-versus-host disease after bone marrow transplantation. Nat Med *9*, 1144-1150.
1205 10.1038/nm915.
1206 Escobar, G., Mangani, D., and Anderson, A.C. (2020). T cell factor 1: A master regulator of the T
1207 cell response in disease. Sci Immunol *5*. 10.1126/sciimmunol.abb9726.
1208 Ferrara, J.L. (2014). Blood and Marrow Transplant Clinical Trials Network: Progress since the
1209 State of the Science Symposium 2007. Biology of blood and marrow transplantation : journal of
1210 the American Society for Blood and Marrow Transplantation *20*, 149-153.
1211 10.1016/j.bbmt.2013.11.006.
1212 Gattinoni, L., Lugli, E., Ji, Y., Pos, Z., Paulos, C.M., Quigley, M.F., Almeida, J.R., Gostick, E., Yu, Z.,
1213 Carpenito, C., et al. (2011). A human memory T cell subset with stem cell-like properties. Nat
1214 Med *17*, 1290-1297. 10.1038/nm.2446.
1215 Gautam, S., Fioravanti, J., Zhu, W., Le Gall, J.B., Brohawn, P., Lacey, N.E., Hu, J., Hocker, J.D.,
1216 Hawk, N.V., Kapoor, V., et al. (2019). The transcription factor c-Myb regulates CD8(+) T cell
1217 stemness and antitumor immunity. Nat Immunol *20*, 337-349. 10.1038/s41590-018-0311-z.
1218 Germar, K., Dose, M., Konstantinou, T., Zhang, J., Wang, H., Lobry, C., Arnett, K.L., Blacklow,
1219 S.C., Aifantis, I., Aster, J.C., and Gounari, F. (2011). T-cell factor 1 is a gatekeeper for T-cell
1220 specification in response to Notch signaling. Proc Natl Acad Sci U S A *108*, 20060-20065.
1221 10.1073/pnas.1110230108.
1222 Giralt, S., and Bishop, M.R. (2009). Principles and overview of allogeneic hematopoietic stem

1223 cell transplantation. Cancer Treat Res *144*, 1-21. 10.1007/978-0-387-78580-6_1.
1224 Gounari, F., and Khazaie, K. (2022). TCF-1: a maverick in T cell development and function. Nat
1225 Immunol. 10.1038/s41590-022-01194-2.
1226 Guinan, E.C., Boussiotis, V.A., Neuberg, D., Brennan, L.L., Hirano, N., Nadler, L.M., and Gribben,
1227 J.G. (1999). Transplantation of anergic histoincompatible bone marrow allografts. N Engl J Med
1228 *340*, 1704-1714. 10.1056/NEJM199906033402202.
1229 Hall, E., and Shenoy, S. (2019). Hematopoietic Stem Cell Transplantation: A Neonatal
1230 Perspective. Neoreviews *20*, e336-e345. 10.1542/neo.20-6-e336.
1231 He, R., Hou, S., Liu, C., Zhang, A., Bai, Q., Han, M., Yang, Y., Wei, G., Shen, T., Yang, X., et al.
1232 (2016). Follicular CXCR5- expressing CD8(+) T cells curtail chronic viral infection. Nature *537*,
1233 412-428. 10.1038/nature19317.
1234 Hoffmann, P., Ermann, J., Edinger, M., Fathman, C.G., and Strober, S. (2002). Donor-type
1235 CD4(+)CD25(+) regulatory T cells suppress lethal acute graft-versus-host disease after allogeneic
1236 bone marrow transplantation. J Exp Med *196*, 389-399. 10.1084/jem.20020399.
1237 Hu, J., Batth, I.S., Xia, X., and Li, S. (2016). Regulation of NKG2D(+)CD8(+) T-cell-mediated
1238 antitumor immune surveillance: Identification of a novel CD28 activation-mediated, STAT3
1239 phosphorylation-dependent mechanism. Oncoimmunology *5*, e1252012.
1240 10.1080/2162402X.2016.1252012.
1241 Huang da, W., Sherman, B.T., and Lempicki, R.A. (2009a). Bioinformatics enrichment tools:
1242 paths toward the comprehensive functional analysis of large gene lists. Nucleic Acids Res *37*, 1-
1243 13. 10.1093/nar/gkn923.
1244 Huang da, W., Sherman, B.T., and Lempicki, R.A. (2009b). Systematic and integrative analysis of
1245 large gene lists using DAVID bioinformatics resources. Nat Protoc *4*, 44-57.
1246 10.1038/nprot.2008.211.
1247 Huang, W., Hu, J., and August, A. (2013). Cutting edge: innate memory CD8+ T cells are distinct
1248 from homeostatic expanded CD8+ T cells and rapidly respond to primary antigenic stimuli. J
1249 Immunol *190*, 2490-2494. 10.4049/jimmunol.1202988.
1250 Huang, W., Mo, W., Jiang, J., Chao, N.J., and Chen, B.J. (2019). Donor Allospecific CD44(high)
1251 Central Memory T Cells Have Decreased Ability to Mediate Graft-vs.-Host Disease. Front
1252 Immunol *10*, 624. 10.3389/fimmu.2019.00624.
1253 Im, S.J., Hashimoto, M., Gerner, M.Y., Lee, J., Kissick, H.T., Burger, M.C., Shan, Q., Hale, J.S., Lee,
1254 J., Nasti, T.H., et al. (2016). Defining CD8+ T cells that provide the proliferative burst after PD-1
1255 therapy. Nature *537*, 417-421. 10.1038/nature19330.
1256 Jiang, H., Fu, D., Bidgoli, A., and Paczesny, S. (2021). T Cell Subsets in Graft Versus Host Disease
1257 and Graft Versus Tumor. Front Immunol *12*, 761448. 10.3389/fimmu.2021.761448.
1258 Jiang, T., Piao, D., Zhu, A., and Jiang, H. (2014). Changes in T lymphocyte subsets in mice with
1259 CT26 colon tumors after treatment with donor lymphocyte infusion. Tumour Biol *35*, 5599-
1260 5605. 10.1007/s13277-014-1740-4.
1261 Johnson, J.L., Georgakilas, G., Petrovic, J., Kurachi, M., Cai, S., Harly, C., Pear, W.S., Bhandoola,
1262 A., Wherry, E.J., and Vahedi, G. (2018). Lineage-Determining Transcription Factor TCF-1 Initiates
1263 the Epigenetic Identity of T Cells. Immunity *48*, 243-257 e210. 10.1016/j.immuni.2018.01.012.
1264 Ju, X.P., Xu, B., Xiao, Z.P., Li, J.Y., Chen, L., Lu, S.Q., and Huang, Z.X. (2005). Cytokine expression
1265 during acute graft-versus-host disease after allogeneic peripheral stem cell transplantation.
1266 Bone Marrow Transplant *35*, 1179-1186. 10.1038/sj.bmt.1704972.

1267 Karimi, M.A., Bryson, J.L., Richman, L.P., Fesnak, A.D., Leichner, T.M., Satake, A., Vonderheide,
1268 R.H., Raulet, D.H., Reshef, R., and Kambayashi, T. (2015). NKG2D expression by CD8+ T cells
1269 contributes to GVHD and GVT effects in a murine model of allogeneic HSCT. Blood *125*, 3655-
1270 3663. 10.1182/blood-2015-02-629006.
1271 Karimi, M.A., Lee, E., Bachmann, M.H., Salicioni, A.M., Behrens, E.M., Kambayashi, T., and
1272 Baldwin, C.L. (2014). Measuring cytotoxicity by bioluminescence imaging outperforms the
1273 standard chromium-51 release assay. PLoS One *9*, e89357. 10.1371/journal.pone.0089357.
1274 Khan, O., Giles, J.R., McDonald, S., Manne, S., Ngiow, S.F., Patel, K.P., Werner, M.T., Huang, A.C.,
1275 Alexander, K.A., Wu, J.E., et al. (2019). TOX transcriptionally and epigenetically programs CD8(+)
1276 T cell exhaustion. Nature *571*, 211-218. 10.1038/s41586-019-1325-x.
1277 Kiekens, L., Van Loocke, W., Taveirne, S., Wahlen, S., Persyn, E., Van Ammel, E., De Vos, Z.,
1278 Matthys, P., Van Nieuwerburgh, F., Taghon, T., et al. (2021). T-BET and EOMES Accelerate and
1279 Enhance Functional Differentiation of Human Natural Killer Cells. Front Immunol *12*, 732511.
1280 10.3389/fimmu.2021.732511.
1281 Kim, C., Jin, J., Weyand, C.M., and Goronzy, J.J. (2020). The Transcription Factor TCF1 in T Cell
1282 Differentiation and Aging. Int J Mol Sci *21*. 10.3390/ijms21186497.
1283 Kurtulus, S., Madi, A., Escobar, G., Klapholz, M., Nyman, J., Christian, E., Pawlak, M., Dionne, D.,
1284 Xia, J., Rozenblatt-Rosen, O., et al. (2019). Checkpoint Blockade Immunotherapy Induces
1285 Dynamic Changes in PD-1(-)CD8(+) Tumor-Infiltrating T Cells. Immunity *50*, 181-194 e186.
1286 10.1016/j.immuni.2018.11.014.
1287 LaFleur, M.W., Nguyen, T.H., Coxe, M.A., Miller, B.C., Yates, K.B., Gillis, J.E., Sen, D.R., Gaudiano,
1288 E.F., Al Abosy, R., Freeman, G.J., et al. (2019). PTPN2 regulates the generation of exhausted
1289 CD8(+) T cell subpopulations and restrains tumor immunity. Nat Immunol *20*, 1335-1347.
1290 10.1038/s41590-019-0480-4.
1291 Larson, J.H., Marron, B.M., Beever, J.E., Roe, B.A., and Lewin, H.A. (2006). Genomic organization
1292 and evolution of the ULBP genes in cattle. BMC Genomics *7*, 227. 10.1186/1471-2164-7-227.
1293 Law, C.W., Chen, Y., Shi, W., and Smyth, G.K. (2014). voom: Precision weights unlock linear
1294 model analysis tools for RNA-seq read counts. Genome Biol *15*, R29. 10.1186/gb-2014-15-2-r29.
1295 Liu, L., Chen, X., Jin, H.M., Zhao, S.S., Zhu, Y., Qian, S.X., and Wu, Y.J. (2022). [The Expression and
1296 Function of NK Cells in Patients with Acute Myeloid Leukemia]. Zhongguo Shi Yan Xue Ye Xue Za
1297 Zhi *30*, 49-55. 10.19746/j.cnki.issn.1009-2137.2022.01.009.
1298 Lugli, E., Dominguez, M.H., Gattinoni, L., Chattopadhyay, P.K., Bolton, D.L., Song, K., Klatt, N.R.,
1299 Brenchley, J.M., Vaccari, M., Gostick, E., et al. (2013). Superior T memory stem cell persistence
1300 supports long-lived T cell memory. J Clin Invest *123*, 594-599. 10.1172/JCI66327.
1301 Lynch Kelly, D., Lyon, D.E., Ameringer, S.A., and Elswick, R.K. (2015). Symptoms, Cytokines, and
1302 Quality of Life in Patients Diagnosed with Chronic Graft-Versus-Host Disease Following
1303 Allogeneic Hematopoietic Stem Cell Transplantation. Oncol Nurs Forum *42*, 265-275.
1304 10.1188/15.ONF.265-275.
1305 Ma, J., Wang, R., Fang, X., and Sun, Z. (2012). beta-catenin/TCF-1 pathway in T cell development
1306 and differentiation. J Neuroimmune Pharmacol *7*, 750-762. 10.1007/s11481-012-9367-y.
1307 Maasho, K., Opoku-Anane, J., Marusina, A.I., Coligan, J.E., and Borrego, F. (2005). NKG2D is a
1308 costimulatory receptor for human naive CD8+ T cells. J Immunol *174*, 4480-4484.
1309 10.4049/jimmunol.174.8.4480.
1310 Mammadli, M., Harris, R., Mahmudlu, S., Verma, A., May, A., Dhawan, R., Waickman, A.T., Sen,

1311 J.M., August, A., and Karimi, M. (2021a). Human Wnt/beta-Catenin Regulates Alloimmune
1312 Signaling during Allogeneic Transplantation. Cancers (Basel) *13*. 10.3390/cancers13153798.
1313 Mammadli, M., Harris, R., Mahmudlu, S., Verma, A., May, A., Dhawan, R., Waickman, A.T., Sen,
1314 J.M., and Karimi, M. (2021b). Wnt/β-catenin regulates alloreactive T cells for the treatment of
1315 hematological malignancies. bioRxiv, 2021.2004.2012.439538. 10.1101/2021.04.12.439538.
1316 Mammadli, M., Harris, R., Suo, L., May, A., Gentile, T., Waickman, A.T., Bah, A., August, A.,
1317 Nurmemmedov, E., and Karimi, M. (2021c). Interleukin-2-inducible T-cell kinase (Itk) signaling
1318 regulates potent noncanonical regulatory T cells. Clin Transl Med *11*, e625. 10.1002/ctm2.625.
1319 Mammadli, M., Huang, W., Harris, R., Sultana, A., Cheng, Y., Tong, W., Pu, J., Gentile, T., Dsouza,
1320 S., Yang, Q., et al. (2020). Targeting Interleukin-2-Inducible T-Cell Kinase (ITK) Differentiates GVL
1321 and GVHD in Allo-HSCT. Front Immunol *11*, 593863. 10.3389/fimmu.2020.593863.
1322 Mammadli, M., Huang, W., Harris, R., Xiong, H., Weeks, S., May, A., Gentile, T., Henty-Ridilla, J.,
1323 Waickman, A.T., August, A., et al. (2021d). Targeting SLP76:ITK interaction separates GVHD
1324 from GVL in allo-HSCT. iScience *24*, 102286. https://doi.org/10.1016/j.isci.2021.102286.
1325 Mavers, M., and Bertaina, A. (2018). High-Risk Leukemia: Past, Present, and Future Role of NK
1326 Cells. J Immunol Res *2018*, 1586905. 10.1155/2018/1586905.
1327 Miller, B.C., Sen, D.R., Al Abosy, R., Bi, K., Virkud, Y.V., LaFleur, M.W., Yates, K.B., Lako, A., Felt,
1328 K., Naik, G.S., et al. (2019). Author Correction: Subsets of exhausted CD8(+) T cells differentially
1329 mediate tumor control and respond to checkpoint blockade. Nat Immunol *20*, 1556.
1330 10.1038/s41590-019-0528-5.
1331 Mohty, M., Blaise, D., Faucher, C., Vey, N., Bouabdallah, R., Stoppa, A.M., Viret, F., Gravis, G.,
1332 Olive, D., and Gaugler, B. (2005). Inflammatory cytokines and acute graft-versus-host disease
1333 after reduced-intensity conditioning allogeneic stem cell transplantation. Blood *106*, 4407-
1334 4411. 10.1182/blood-2005-07-2919.
1335 Nakajima, Y., Chamoto, K., Oura, T., and Honjo, T. (2021). Critical role of the
1336 CD44(low)CD62L(low) CD8(+) T cell subset in restoring antitumor immunity in aged mice. Proc
1337 Natl Acad Sci U S A *118*. 10.1073/pnas.2103730118.
1338 Nishimura, R., Baker, J., Beilhack, A., Zeiser, R., Olson, J.A., Sega, E.I., Karimi, M., and Negrin,
1339 R.S. (2008). In vivo trafficking and survival of cytokine-induced killer cells resulting in minimal
1340 GVHD with retention of antitumor activity. Blood *112*, 2563-2574. 10.1182/blood-2007-06-
1341 092817.
1342 Paley, M.A., and Wherry, E.J. (2010). TCF-1 flips the switch on Eomes. Immunity *33*, 145-147.
1343 10.1016/j.immuni.2010.08.008.
1344 Philip, M., Fairchild, L., Sun, L., Horste, E.L., Camara, S., Shakiba, M., Scott, A.C., Viale, A., Lauer,
1345 P., Merghoub, T., et al. (2017). Chromatin states define tumour-specific T cell dysfunction and
1346 reprogramming. Nature *545*, 452-456. 10.1038/nature22367.
1347 Prajapati, K., Perez, C., Rojas, L.B.P., Burke, B., and Guevara-Patino, J.A. (2018). Functions of
1348 NKG2D in CD8(+) T cells: an opportunity for immunotherapy. Cell Mol Immunol *15*, 470-479.
1349 10.1038/cmi.2017.161.
1350 Presotto, D., Erdes, E., Duong, M.N., Allard, M., Regamey, P.O., Quadroni, M., Doucey, M.A.,
1351 Rufer, N., and Hebeisen, M. (2017). Fine-Tuning of Optimal TCR Signaling in Tumor-Redirected
1352 CD8 T Cells by Distinct TCR Affinity-Mediated Mechanisms. Front Immunol *8*, 1564.
1353 10.3389/fimmu.2017.01564.
1354 Raulet, D.H. (2003). Roles of the NKG2D immunoreceptor and its ligands. Nat Rev Immunol *3*,

1355 781-790. 10.1038/nri1199.
1356 Raulet, D.H., Gasser, S., Gowen, B.G., Deng, W., and Jung, H. (2013). Regulation of ligands for
1357 the NKG2D activating receptor. Annu Rev Immunol *31*, 413-441. 10.1146/annurev-immunol-
1358 032712-095951.
1359 Reddy, P., and Ferrara, J.L.M. (2008). Mouse models of graft-versus-host disease. In StemBook.
1360 10.3824/stembook.1.36.1.
1361 Ritchie, M.E., Phipson, B., Wu, D., Hu, Y., Law, C.W., Shi, W., and Smyth, G.K. (2015). limma
1362 powers differential expression analyses for RNA-sequencing and microarray studies. Nucleic
1363 Acids Res *43*, e47. 10.1093/nar/gkv007.
1364 Schietinger, A., Philip, M., Krisnawan, V.E., Chiu, E.Y., Delrow, J.J., Basom, R.S., Lauer, P.,
1365 Brockstedt, D.G., Knoblaugh, S.E., Hammerling, G.J., et al. (2016). Tumor-Specific T Cell
1366 Dysfunction Is a Dynamic Antigen-Driven Differentiation Program Initiated Early during
1367 Tumorigenesis. Immunity *45*, 389-401. 10.1016/j.immuni.2016.07.011.
1368 Scott, A.C., Dundar, F., Zumbo, P., Chandran, S.S., Klebanoff, C.A., Shakiba, M., Trivedi, P.,
1369 Menocal, L., Appleby, H., Camara, S., et al. (2019). TOX is a critical regulator of tumour-specific T
1370 cell differentiation. Nature *571*, 270-274. 10.1038/s41586-019-1324-y.
1371 Seif, F., Khoshmirsafa, M., Aazami, H., Mohsenzadegan, M., Sedighi, G., and Bahar, M. (2017).
1372 The role of JAK-STAT signaling pathway and its regulators in the fate of T helper cells. Cell
1373 Commun Signal *15*, 23. 10.1186/s12964-017-0177-y.
1374 Seo, H., Chen, J., Gonzalez-Avalos, E., Samaniego-Castruita, D., Das, A., Wang, Y.H., Lopez-
1375 Moyado, I.F., Georges, R.O., Zhang, W., Onodera, A., et al. (2019). TOX and TOX2 transcription
1376 factors cooperate with NR4A transcription factors to impose CD8(+) T cell exhaustion. Proc Natl
1377 Acad Sci U S A *116*, 12410-12415. 10.1073/pnas.1905675116.
1378 Shi, J., Chi, S., Xue, J., Yang, J., Li, F., and Liu, X. (2016). Emerging Role and Therapeutic
1379 Implication of Wnt Signaling Pathways in Autoimmune Diseases. J Immunol Res *2016*, 9392132.
1380 10.1155/2016/9392132.
1381 Siddiqui, I., Schaeuble, K., Chennupati, V., Fuertes Marraco, S.A., Calderon-Copete, S., Pais
1382 Ferreira, D., Carmona, S.J., Scarpellino, L., Gfeller, D., Pradervand, S., et al. (2019). Intratumoral
1383 Tcf1(+)PD-1(+)CD8(+) T Cells with Stem-like Properties Promote Tumor Control in Response to
1384 Vaccination and Checkpoint Blockade Immunotherapy. Immunity *50*, 195-211 e110.
1385 10.1016/j.immuni.2018.12.021.
1386 Sobecki, M., Mrouj, K., Camasses, A., Parisis, N., Nicolas, E., Lleres, D., Gerbe, F., Prieto, S.,
1387 Krasinska, L., David, A., et al. (2016). The cell proliferation antigen Ki-67 organises
1388 heterochromatin. Elife *5*, e13722. 10.7554/eLife.13722.
1389 Steinke, F.C., Yu, S., Zhou, X., He, B., Yang, W., Zhou, B., Kawamoto, H., Zhu, J., Tan, K., and Xue,
1390 H.H. (2014). TCF-1 and LEF-1 act upstream of Th-POK to promote the CD4(+) T cell fate and
1391 interact with Runx3 to silence Cd4 in CD8(+) T cells. Nat Immunol *15*, 646-656. 10.1038/ni.2897.
1392 Stojanovic, A., Correia, M.P., and Cerwenka, A. (2018). The NKG2D/NKG2DL Axis in the Crosstalk
1393 Between Lymphoid and Myeloid Cells in Health and Disease. Front Immunol *9*, 827.
1394 10.3389/fimmu.2018.00827.
1395 Tugues, S., Amorim, A., Spath, S., Martin-Blondel, G., Schreiner, B., De Feo, D., Lutz, M.,
1396 Guscetti, F., Apostolova, P., Haftmann, C., et al. (2018). Graft-versus-host disease, but not graft-
1397 versus-leukemia immunity, is mediated by GM-CSF-licensed myeloid cells. Sci Transl Med *10*.
1398 10.1126/scitranslmed.aat8410.

1399 Utzschneider, D.T., Charmoy, M., Chennupati, V., Pousse, L., Ferreira, D.P., Calderon-Copete, S.,
1400 Danilo, M., Alfei, F., Hofmann, M., Wieland, D., et al. (2016). T Cell Factor 1-Expressing Memory-
1401 like CD8(+) T Cells Sustain the Immune Response to Chronic Viral Infections. Immunity *45*, 415-
1402 427. 10.1016/j.immuni.2016.07.021.
1403 Utzschneider, D.T., Legat, A., Fuertes Marraco, S.A., Carrie, L., Luescher, I., Speiser, D.E., and
1404 Zehn, D. (2013). T cells maintain an exhausted phenotype after antigen withdrawal and
1405 population reexpansion. Nat Immunol *14*, 603-610. 10.1038/ni.2606.
1406 Villarroel, V.A., Okiyama, N., Tsuji, G., Linton, J.T., and Katz, S.I. (2014). CXCR3-mediated skin
1407 homing of autoreactive CD8 T cells is a key determinant in murine graft-versus-host disease. J
1408 Invest Dermatol *134*, 1552-1560. 10.1038/jid.2014.2.
1409 Wang, S., Wu, Q., Chen, T., Su, R., Pan, C., Qian, J., Huang, H., Yin, S., Xie, H., Zhou, L., and
1410 Zheng, S. (2022). Blocking CD47 promotes anti-tumor immunity through CD103+ dendritic cell-
1411 NK cell axis in murine hepatocellular carcinoma model. J Hepatol. 10.1016/j.jhep.2022.03.011.
1412 Wang, X., He, Q., Shen, H., Xia, A., Tian, W., Yu, W., and Sun, B. (2019a). TOX promotes the
1413 exhaustion of antitumor CD8(+) T cells by preventing PD1 degradation in hepatocellular
1414 carcinoma. J Hepatol *71*, 731-741. 10.1016/j.jhep.2019.05.015.
1415 Wang, Y., Hu, J., Li, Y., Xiao, M., Wang, H., Tian, Q., Li, Z., Tang, J., Hu, L., Tan, Y., et al. (2019b).
1416 The Transcription Factor TCF1 Preserves the Effector Function of Exhausted CD8 T Cells During
1417 Chronic Viral Infection. Front Immunol *10*, 169. 10.3389/fimmu.2019.00169.
1418 Weber, B.N., Chi, A.W., Chavez, A., Yashiro-Ohtani, Y., Yang, Q., Shestova, O., and Bhandoola, A.
1419 (2011). A critical role for TCF-1 in T-lineage specification and differentiation. Nature *476*, 63-68.
1420 10.1038/nature10279.
1421 Weeks, S., Harris, R., and Karimi, M. (2021). Targeting ITK signaling for T cell-mediated diseases.
1422 iScience *24*, 102842. 10.1016/j.isci.2021.102842.
1423 Wensveen, F.M., Jelencic, V., and Polic, B. (2018). NKG2D: A Master Regulator of Immune Cell
1424 Responsiveness. Front Immunol *9*, 441. 10.3389/fimmu.2018.00441.
1425 Wu, T., Ji, Y., Moseman, E.A., Xu, H.C., Manglani, M., Kirby, M., Anderson, S.M., Handon, R.,
1426 Kenyon, E., Elkahloun, A., et al. (2016). The TCF1-Bcl6 axis counteracts type I interferon to
1427 repress exhaustion and maintain T cell stemness. Sci Immunol *1*. 10.1126/sciimmunol.aai8593.
1428 Xing, S., Li, F., Zeng, Z., Zhao, Y., Yu, S., Shan, Q., Li, Y., Phillips, F.C., Maina, P.K., Qi, H.H., et al.
1429 (2016). Tcf1 and Lef1 transcription factors establish CD8(+) T cell identity through intrinsic
1430 HDAC activity. Nat Immunol *17*, 695-703. 10.1038/ni.3456.
1431 Xu, W., Zhao, X., Wang, X., Feng, H., Gou, M., Jin, W., Wang, X., Liu, X., and Dong, C. (2019). The
1432 Transcription Factor Tox2 Drives T Follicular Helper Cell Development via Regulating Chromatin
1433 Accessibility. Immunity *51*, 826-839 e825. 10.1016/j.immuni.2019.10.006.
1434 Yang, B.H., Wang, K., Wan, S., Liang, Y., Yuan, X., Dong, Y., Cho, S., Xu, W., Jepsen, K., Feng, G.S.,
1435 et al. (2019). TCF1 and LEF1 Control Treg Competitive Survival and Tfr Development to Prevent
1436 Autoimmune Diseases. Cell Rep *27*, 3629-3645 e3626. 10.1016/j.celrep.2019.05.061.
1437 Yu, Q., Sharma, A., and Sen, J.M. (2010). TCF1 and beta-catenin regulate T cell development and
1438 function. Immunol Res *47*, 45-55. 10.1007/s12026-009-8137-2.
1439 Zander, R., Schauder, D., Xin, G., Nguyen, C., Wu, X., Zajac, A., and Cui, W. (2019). CD4(+) T Cell
1440 Help Is Required for the Formation of a Cytolytic CD8(+) T Cell Subset that Protects against
1441 Chronic Infection and Cancer. Immunity *51*, 1028-1042 e1024. 10.1016/j.immuni.2019.10.009.
1442 Zheng, H., Matte-Martone, C., Jain, D., McNiff, J., and Shlomchik, W.D. (2009). Central memory

1443 CD8+ T cells induce graft-versus-host disease and mediate graft-versus-leukemia. J Immunol
1444 *182*, 5938-5948. 10.4049/jimmunol.0802212.
1445 Zhou, X., Yu, S., Zhao, D.M., Harty, J.T., Badovinac, V.P., and Xue, H.H. (2010). Differentiation
1446 and persistence of memory CD8(+) T cells depend on T cell factor 1. Immunity *33*, 229-240.
1447 10.1016/j.immuni.2010.08.002.
1448 Zhu, Y., Ju, S., Chen, E., Dai, S., Li, C., Morel, P., Liu, L., Zhang, X., and Lu, B. (2010). T-bet and
1449 eomesodermin are required for T cell-mediated antitumor immune responses. J Immunol *185*,
1450 3174-3183. 10.4049/jimmunol.1000749.
1451 Zuniga-Pflucker, J.C. (2004). T-cell development made simple. Nat Rev Immunol *4*, 67-72.
1452 10.1038/nri1257.

1453

1454

1455 Huang da, W., Sherman, B.T., and Lempicki, R.A. (2009). Systematic and integrative analysis of
1456 large gene lists using DAVID bioinformatics resources. Nat Protoc *4*, 44-57.
1457 10.1038/nprot.2008.211.
1458 Karimi, M.A., Aguilar, O., Zou, B., Bachmann, M.H., Carlyle, J.R., Baldwin, C.L., and Kambayashi,
1459 T. (2014a). A truncated human NKG2D splice isoform negatively regulates NKG2D-mediated
1460 function. J Immunol *193*, 2764-2771. 10.4049/jimmunol.1400920.
1461 Karimi, M.A., Bryson, J.L., Richman, L.P., Fesnak, A.D., Leichner, T.M., Satake, A., Vonderheide,
1462 R.H., Raulet, D.H., Reshef, R., and Kambayashi, T. (2015). NKG2D expression by CD8+ T cells
1463 contributes to GVHD and GVT effects in a murine model of allogeneic HSCT. Blood *125*, 3655-
1464 3663. 10.1182/blood-2015-02-629006.
1465 Karimi, M.A., Lee, E., Bachmann, M.H., Salicioni, A.M., Behrens, E.M., Kambayashi, T., and
1466 Baldwin, C.L. (2014b). Measuring cytotoxicity by bioluminescence imaging outperforms the
1467 standard chromium-51 release assay. PLoS One *9*, e89357. 10.1371/journal.pone.0089357.
1468 Mammadli, M., Harris, R., Mahmudlu, S., Verma, A., May, A., Dhawan, R., Waickman, A.T., Sen,
1469 J.M., August, A., and Karimi, M. (2021a). Human Wnt/beta-Catenin Regulates Alloimmune
1470 Signaling during Allogeneic Transplantation. Cancers (Basel) *13*. 10.3390/cancers13153798.
1471 Mammadli, M., Harris, R., Suo, L., May, A., Gentile, T., Waickman, A.T., Bah, A., August, A.,
1472 Nurmemmedov, E., and Karimi, M. (2021b). Interleukin-2-inducible T-cell kinase (Itk) signaling
1473 regulates potent noncanonical regulatory T cells. Clin Transl Med *11*, e625. 10.1002/ctm2.625.
1474 Mammadli, M., Huang, W., Harris, R., Sultana, A., Cheng, Y., Tong, W., Pu, J., Gentile, T., Dsouza,
1475 S., Yang, Q., et al. (2020). Targeting Interleukin-2-Inducible T-Cell Kinase (ITK) Differentiates GVL
1476 and GVHD in Allo-HSCT. Front Immunol *11*, 593863. 10.3389/fimmu.2020.593863.
1477 Mammadli, M., Huang, W., Harris, R., Xiong, H., Weeks, S., May, A., Gentile, T., Henty-Ridilla, J.,
1478 Waickman, A.T., August, A., et al. (2021c). Targeting SLP76:ITK interaction separates GVHD from
1479 GVL in allo-HSCT. iScience *24*, 102286. https://doi.org/10.1016/j.isci.2021.102286.
1480 Sherman, B.T., Hao, M., Qiu, J., Jiao, X., Baseler, M.W., Lane, H.C., Imamichi, T., and Chang, W.
1481 (2022). DAVID: a web server for functional enrichment analysis and functional annotation of
1482 gene lists (2021 update). Nucleic Acids Res. 10.1093/nar/gkac194.

1483

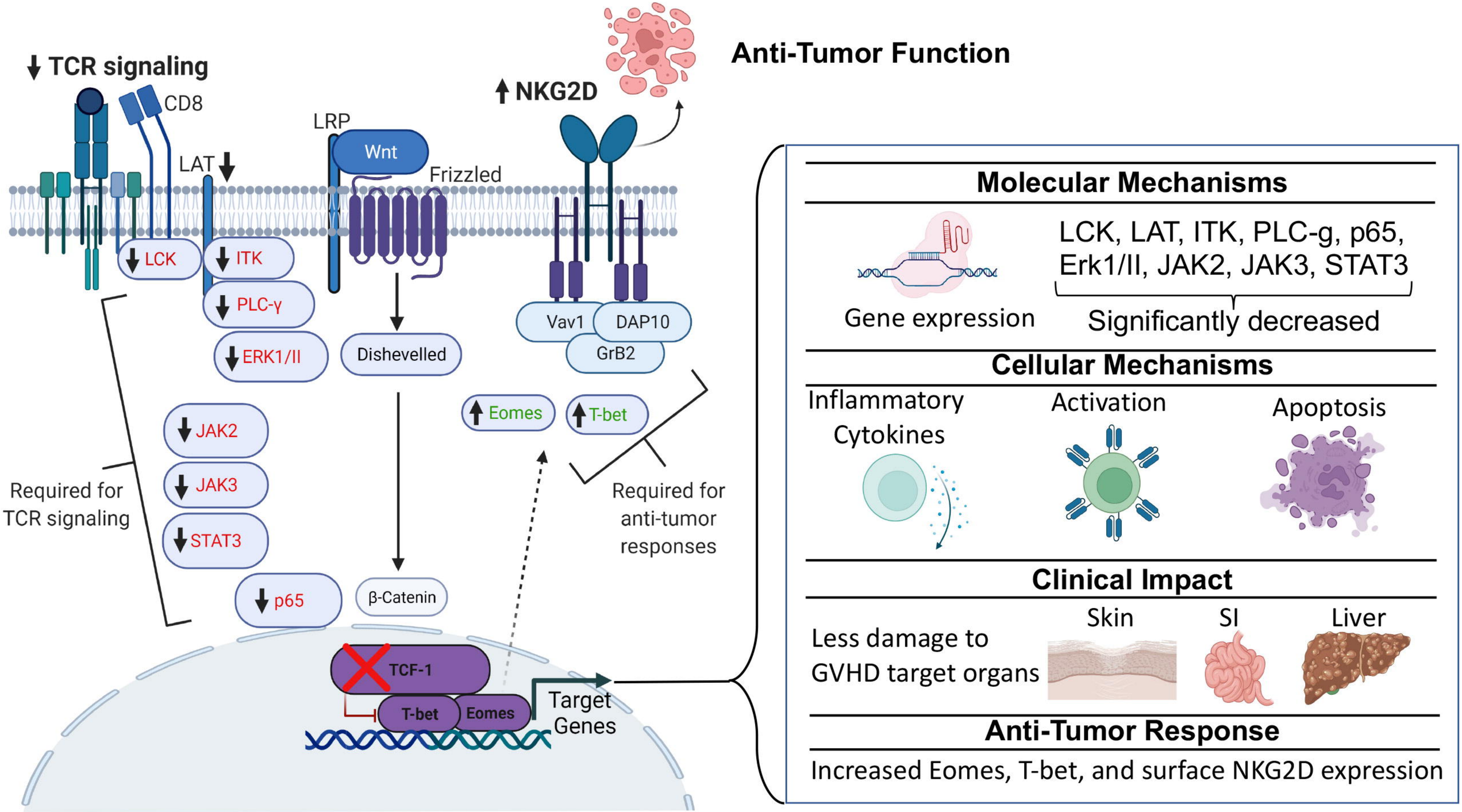
Anti-Tumor Function
TCR signaling
CD8
LAT
LCK
ITK
PLC-γ
ERK1/II
JAK2
JAK3
STAT3
p65
Required for TCR signaling
LRP
Wnt
Frizzled
Dishevelled
β-Catenin
NKG2D
Vav1
DAP10
GrB2
Eomes
T-bet
Required for anti-tumor responses
TCF-1
T-bet
Eomes
Target Genes
Molecular Mechanisms
Gene expression
LCK, LAT, ITK, PLC-g, p65, Erk1/II, JAK2, JAK3, STAT3
Significantly decreased
Cellular Mechanisms
Inflammatory Cytokines
Activation
Apoptosis
Clinical Impact
Less damage to GVHD target organs
Skin
SI
Liver
Anti-Tumor Response
Increased Eomes, T-bet, and surface NKG2D expression

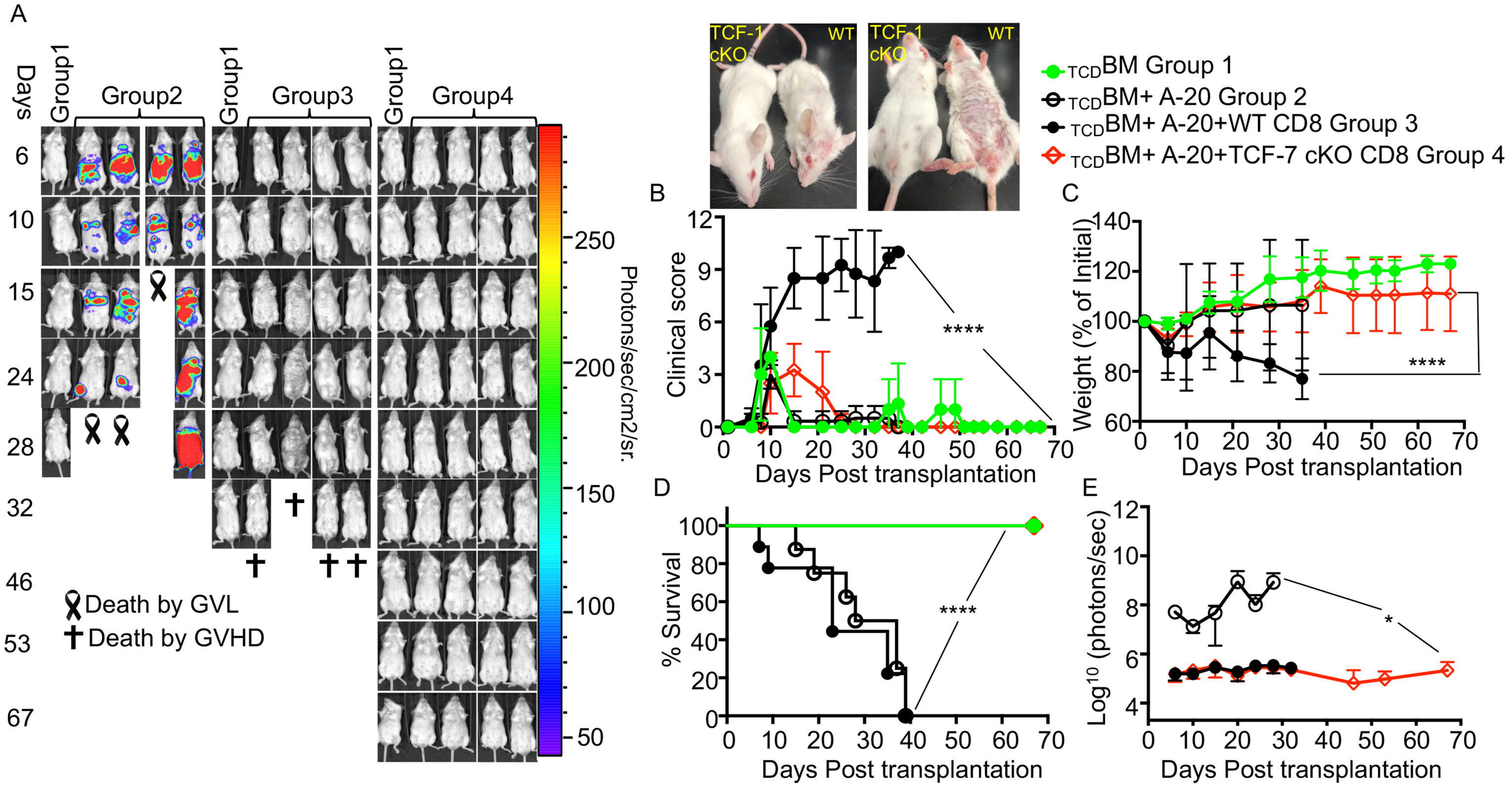
A
Days
Group1
Group2
Group3
Group4
6
10
15
24
28
32
46
53
67
Death by GVL
Death by GVHD
Photons/sec/cm2/sr.
250
200
150
100
50
TCF-1 cKO
WT
TCD BM Group 1
TCD BM+ A-20 Group 2
TCD BM+ A-20+WT CD8 Group 3
TCD BM+ A-20+TCF-7 cKO CD8 Group 4
B
Clinical score
Days Post transplantation
****
C
Weight (% of Initial)
Days Post transplantation
****
D
% Survival
Days Post transplantation
****
E
Log10 (photons/sec)
Days Post transplantation
*

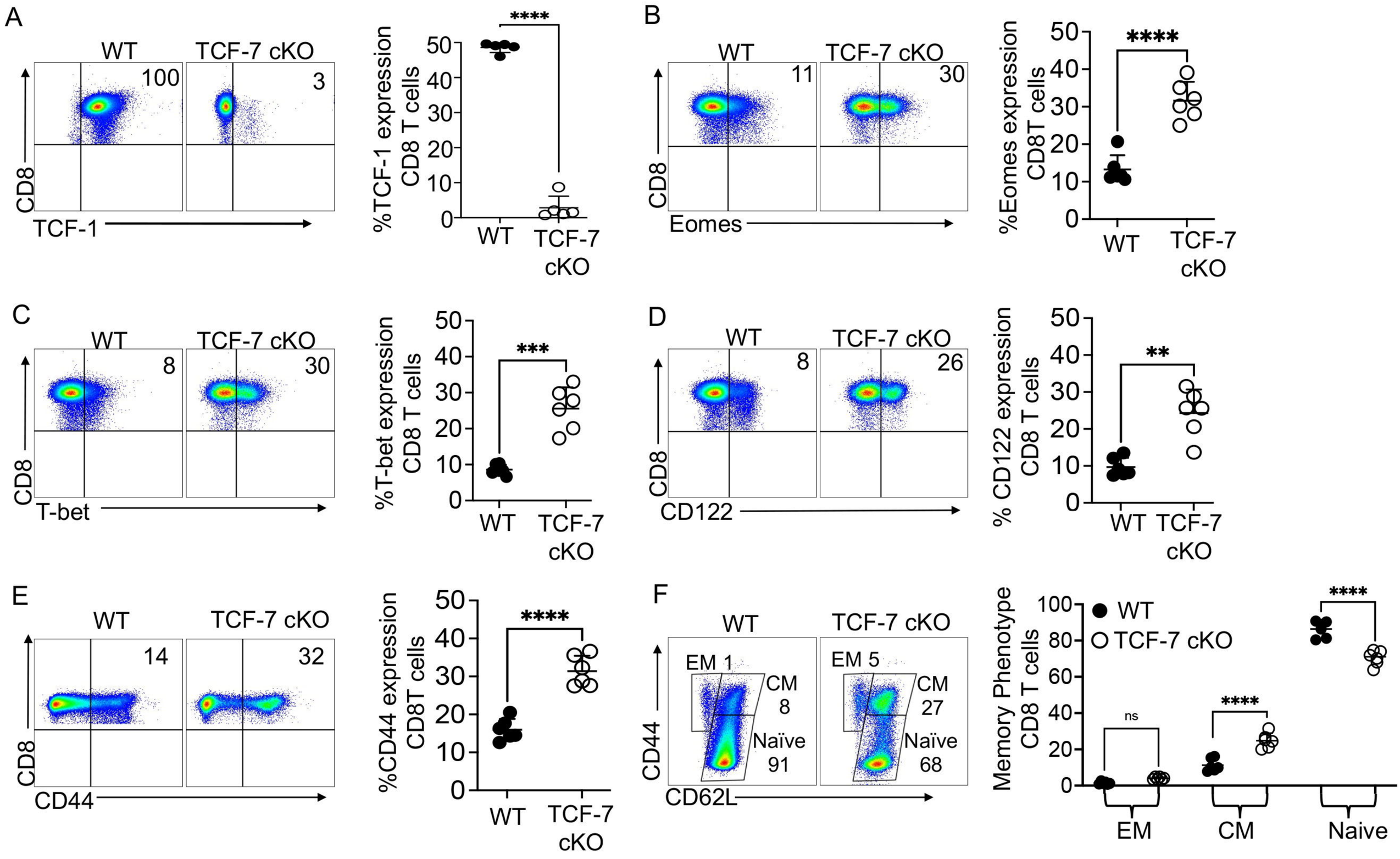
A
WT
TCF-7 cKO
100
3
CD8
TCF-1
%TCF-1 expression CD8 T cells
****
WT
TCF-7 cKO
B
WT
TCF-7 cKO
11
30
CD8
Eomes
%Eomes expression CD8T cells
****
WT
TCF-7 cKO
C
WT
TCF-7 cKO
8
30
CD8
T-bet
%T-bet expression CD8 T cells
***
WT
TCF-7 cKO
D
WT
TCF-7 cKO
8
26
CD8
CD122
% CD122 expression CD8 T cells
**
WT
TCF-7 cKO
E
WT
TCF-7 cKO
14
32
CD8
CD44
%CD44 expression CD8T cells
****
WT
TCF-7 cKO
F
WT
TCF-7 cKO
EM 1
CM 8
Naïve 91
EM 5
CM 27
Naïve 68
CD44
CD62L
Memory Phenotype CD8 T cells
WT
TCF-7 cKO
ns
****
****
EM
CM
Naive

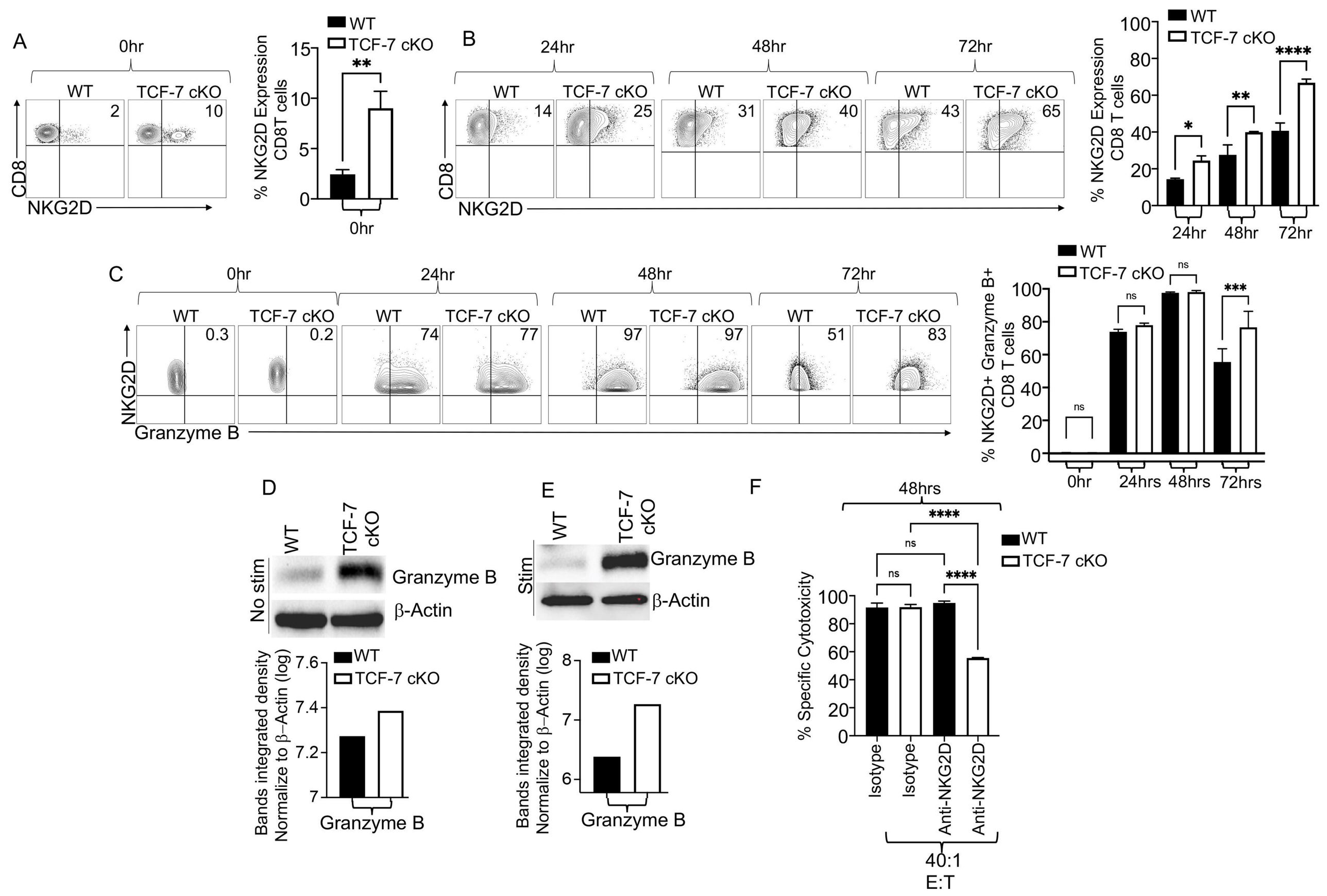
A
0hr
WT
TCF-7 cKO
2
10
CD8
NKG2D
% NKG2D Expression CD8T cells
WT
TCF-7 cKO
**
0hr
B
24hr
48hr
72hr
14
25
31
40
43
65
% NKG2D Expression CD8 T cells
*
**
****
24hr
48hr
72hr
C
0.3
0.2
74
77
97
97
51
83
NKG2D
Granzyme B
% NKG2D+ Granzyme B+ CD8 T cells
ns
***
0hr
24hrs
48hrs
72hrs
D
No stim
Granzyme B
β-Actin
Bands integrated density Normalize to β–Actin (log)
E
Stim
F
48hrs
% Specific Cytotoxicity
Isotype
Anti-NKG2D
40:1
E:T

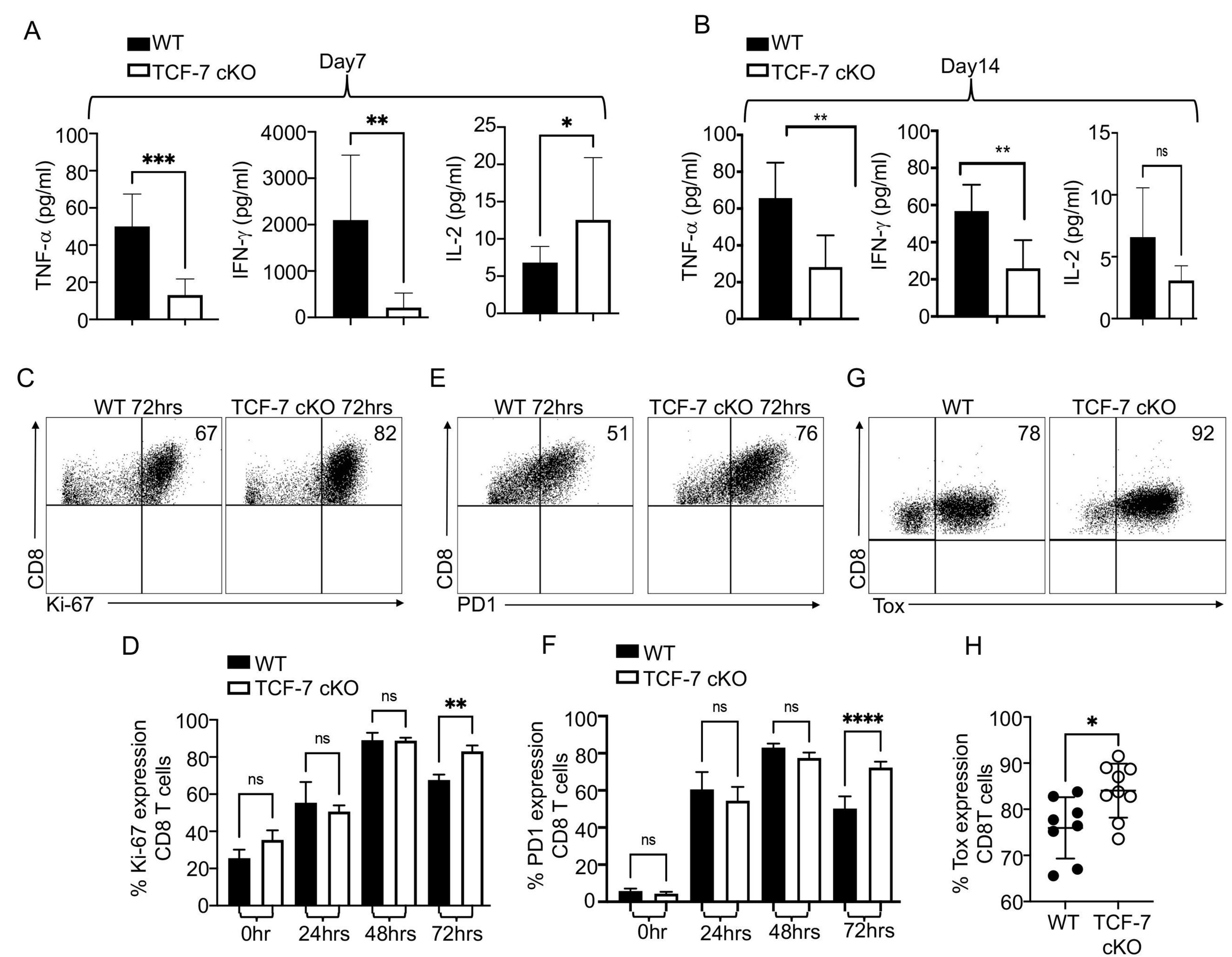
A
WT
TCF-7 cKO
Day7
TNF-α (pg/ml)
IFN-γ (pg/ml)
IL-2 (pg/ml)
***
**
*
B
WT
TCF-7 cKO
Day14
TNF-α (pg/ml)
IFN-γ (pg/ml)
IL-2 (pg/ml)
**
**
ns
C
WT 72hrs
TCF-7 cKO 72hrs
67
82
CD8
Ki-67
E
WT 72hrs
TCF-7 cKO 72hrs
51
76
CD8
PD1
G
WT
TCF-7 cKO
78
92
CD8
Tox
D
WT
TCF-7 cKO
% Ki-67 expression CD8 T cells
ns
ns
ns
**
0hr
24hrs
48hrs
72hrs
F
WT
TCF-7 cKO
% PD1 expression CD8 T cells
ns
ns
ns
****
0hr
24hrs
48hrs
72hrs
H
% Tox expression CD8T cells
*
WT
TCF-7 cKO

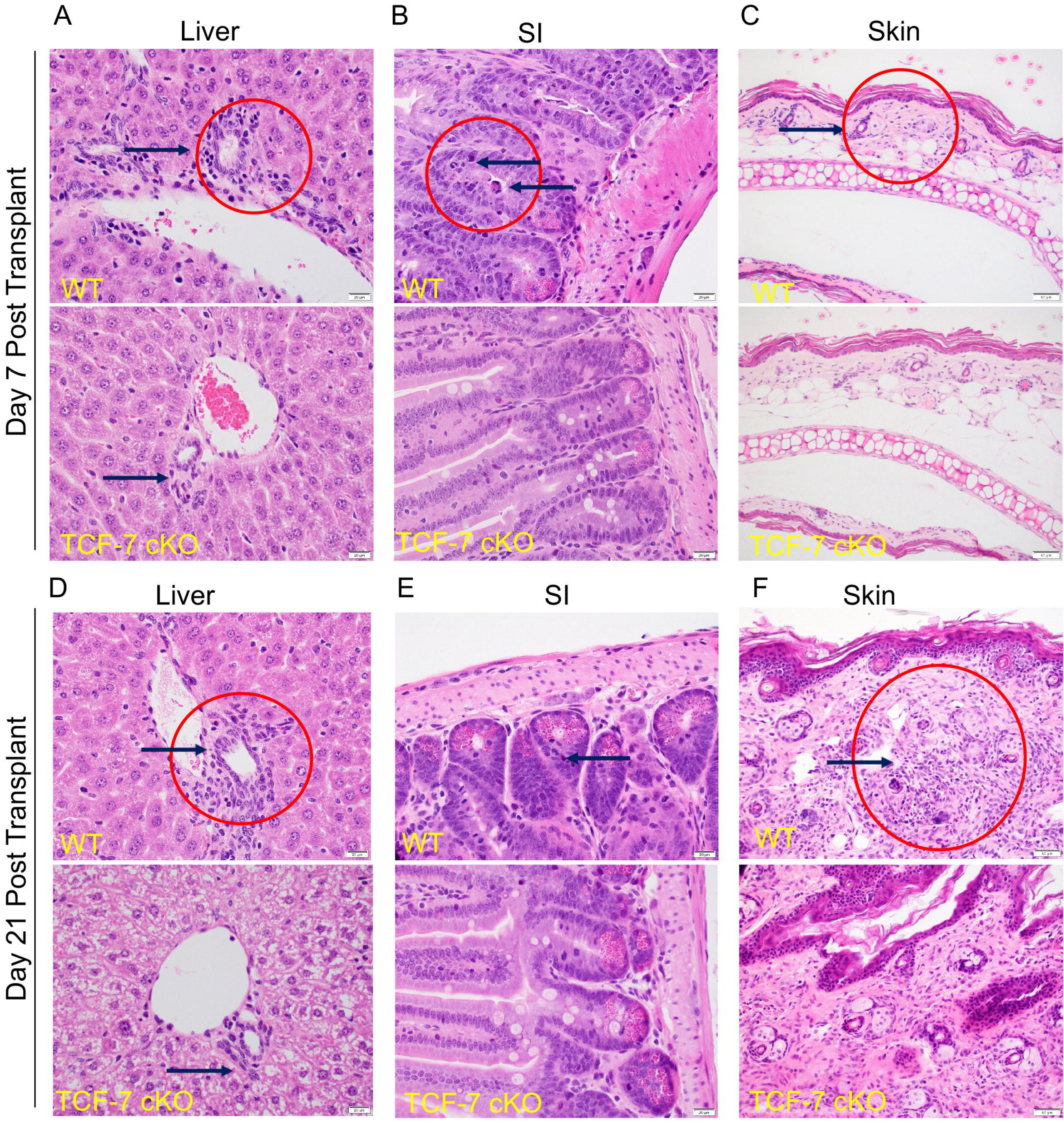
A
Liver
B
SI
C
Skin
Day 7 Post Transplant
WT
WT
WT
TCF-7 cKO
TCF-7 cKO
TCF-7 cKO
D
Liver
E
SI
F
Skin
Day 21 Post Transplant
WT
WT
WT
TCF-7 cKO
TCF-7 cKO
TCF-7 cKO

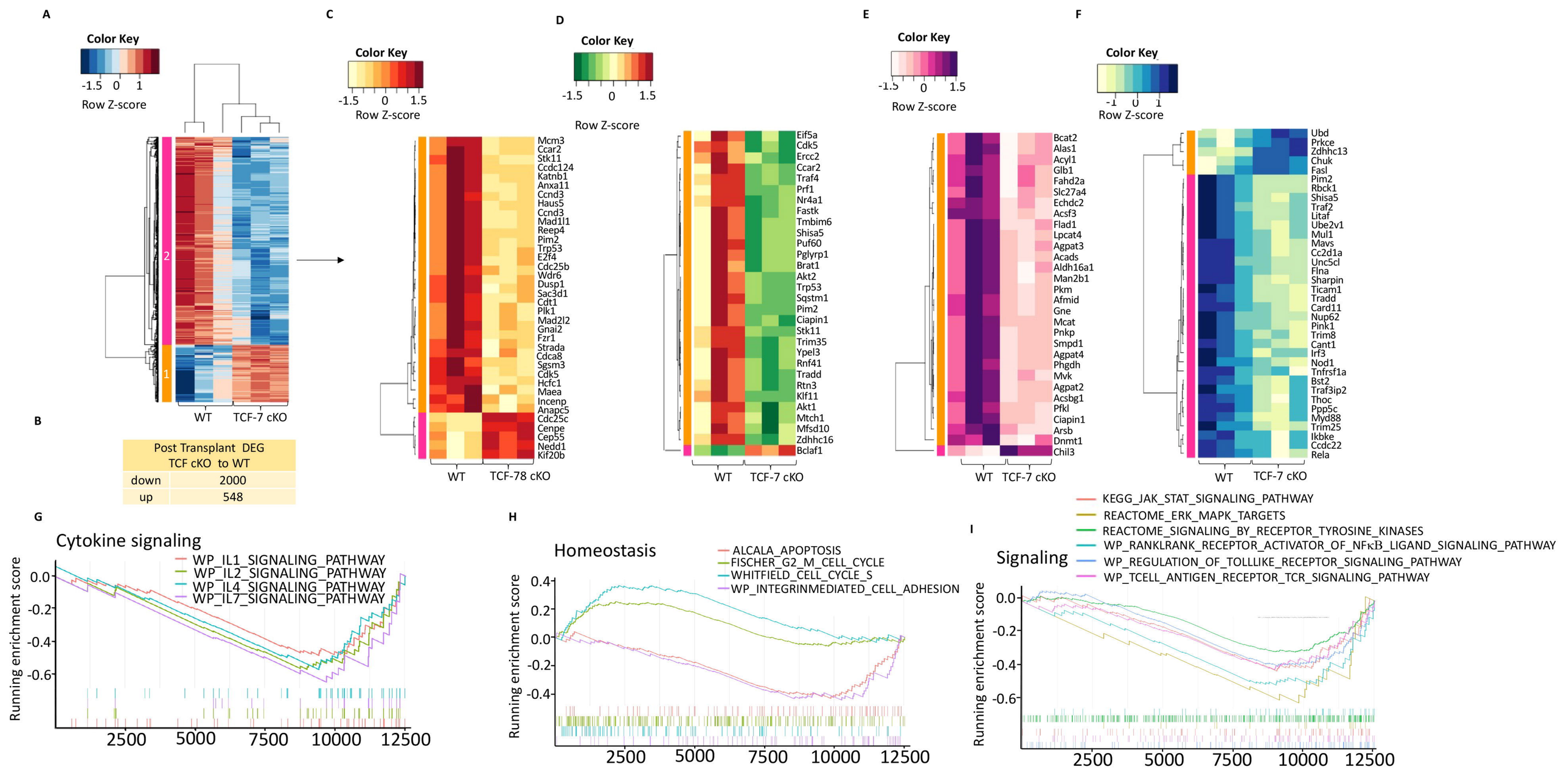
A
Color Key
-1.5 0 1
Row Z-score
2
1
WT
TCF-7 cKO
B
Post Transplant DEG
TCF cKO to WT
down 2000
up 548
C
Color Key
-1.5 0 1.5
Row Z-score
Mcm3
Ccar2
Stk11
Ccdc124
Katnb1
Anxa11
Ccnd3
Haus5
Ccnd3
Mad1l1
Reep4
Pim2
Trp53
E2f4
Cdc25b
Wdr6
Dusp1
Sac3d1
Cdt1
Plk1
Mad2l2
Gnai2
Fzr1
Strada
Cdca8
Sgsm3
Cdk5
Hcfc1
Maea
Incenp
Anapc5
Cdc25c
Cenpe
Cep55
Nedd1
Kif20b
WT
TCF-78 cKO
D
Color Key
-1.5 0 1.5
Row Z-score
Eif5a
Cdk5
Ercc2
Ccar2
Traf4
Prf1
Nr4a1
Fastk
Tmbim6
Shisa5
Puf60
Pglyrp1
Brat1
Akt2
Trp53
Sqstm1
Pim2
Ciapin1
Stk11
Trim35
Ypel3
Rnf41
Tradd
Rtn3
Klf11
Akt1
Mtch1
Mfsd10
Zdhhc16
Bclaf1
WT
TCF-7 cKO
E
Color Key
-1.5 0 1.5
Row Z-score
Bcat2
Alas1
Acyl1
Glb1
Fahd2a
Slc27a4
Echdc2
Acsf3
Flad1
Lpcat4
Agpat3
Acads
Aldh16a1
Man2b1
Pkm
Afmid
Gne
Mcat
Pnkp
Smpd1
Agpat4
Phgdh
Mvk
Agpat2
Acsbg1
Pfkl
Ciapin1
Arsb
Dnmt1
Chil3
WT
TCF-7 cKO
F
Color Key
-1 0 1
Row Z-score
Ubd
Prkce
Zdhhc13
Chuk
Fasl
Pim2
Rbck1
Shisa5
Traf2
Litaf
Ube2v1
Mul1
Mavs
Cc2d1a
Unc5cl
Flna
Sharpin
Ticam1
Tradd
Card11
Nup62
Pink1
Trim8
Cant1
Irf3
Nod1
Tnfrsf1a
Bst2
Traf3ip2
Thoc
Ppp5c
Myd88
Trim25
Ikbke
Ccdc22
Rela
WT
TCF-7 cKO
G
Cytokine signaling
WP_IL1_SIGNALING_PATHWAY
WP_IL2_SIGNALING_PATHWAY
WP_IL4_SIGNALING_PATHWAY
WP_IL7_SIGNALING_PATHWAY
Running enrichment score
0.0
-0.2
-0.4
-0.6
2500
5000
7500
10000
12500
H
Homeostasis
ALCALA_APOPTOSIS
FISCHER_G2_M_CELL_CYCLE
WHITFIELD_CELL_CYCLE_S
WP_INTEGRINMEDIATED_CELL_ADHESION
Running enrichment score
0.4
0.2
0.0
-0.2
-0.4
2500
5000
7500
10000
12500
I
Signaling
KEGG_JAK_STAT_SIGNALING_PATHWAY
REACTOME_ERK_MAPK_TARGETS
REACTOME_SIGNALING_BY_RECEPTOR_TYROSINE_KINASES
WP_RANKLRANK_RECEPTOR_ACTIVATOR_OF_NFκB_LIGAND_SIGNALING_PATHWAY
WP_REGULATION_OF_TOLLLIKE_RECEPTOR_SIGNALING_PATHWAY
WP_TCELL_ANTIGEN_RECEPTOR_TCR_SIGNALING_PATHWAY
Running enrichment score
0.0
-0.2
-0.4
-0.6
2500
5000
7500
10000
12500

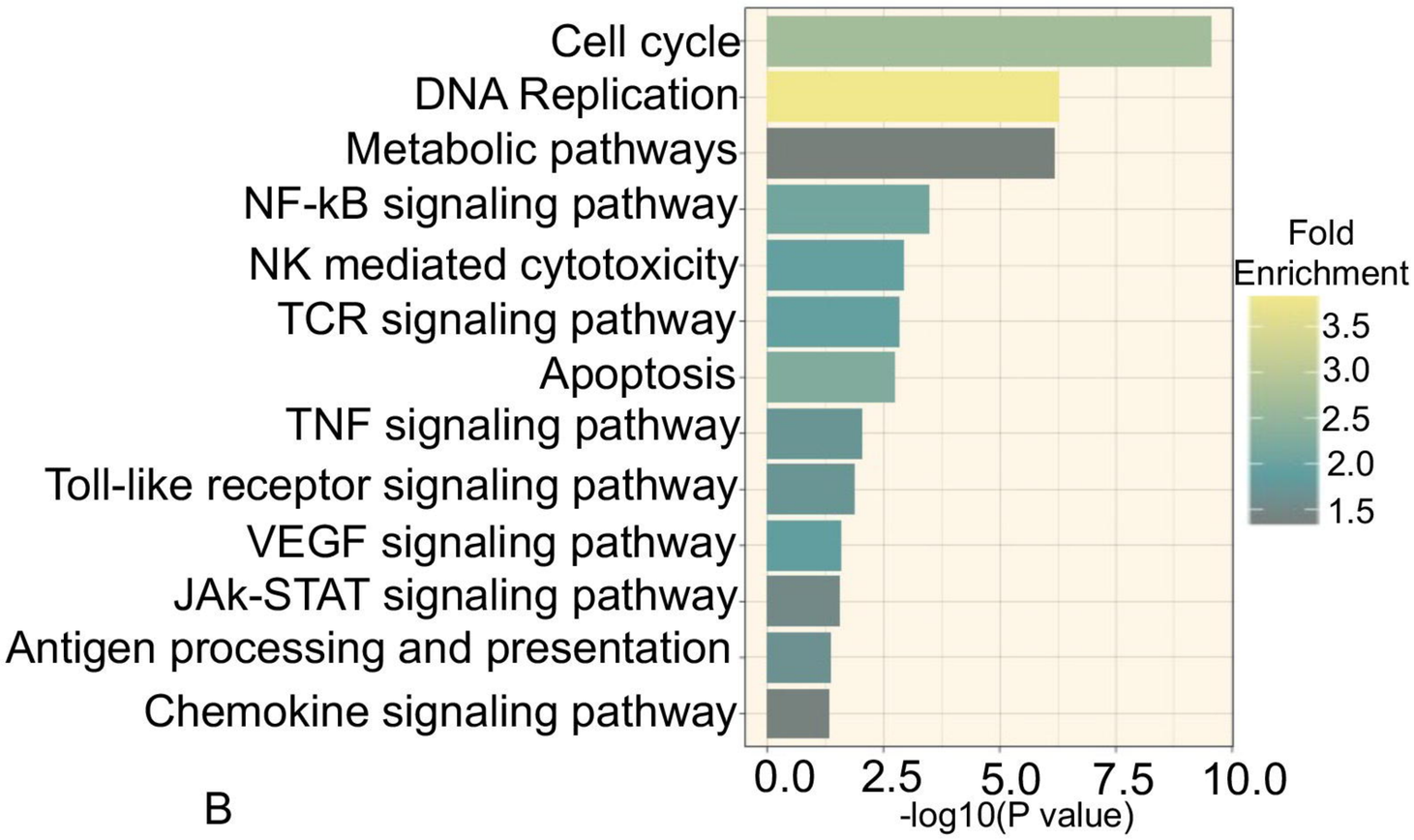
A
Cell cycle
DNA Replication
Metabolic pathways
NF-kB signaling pathway
NK mediated cytotoxicity
TCR signaling pathway
Apoptosis
TNF signaling pathway
Toll-like receptor signaling pathway
VEGF signaling pathway
JAk-STAT signaling pathway
Antigen processing and presentation
Chemokine signaling pathway
0.0
2.5
5.0
7.5
10.0
-log10(P value)
Fold Enrichment
3.5
3.0
2.5
2.0
1.5

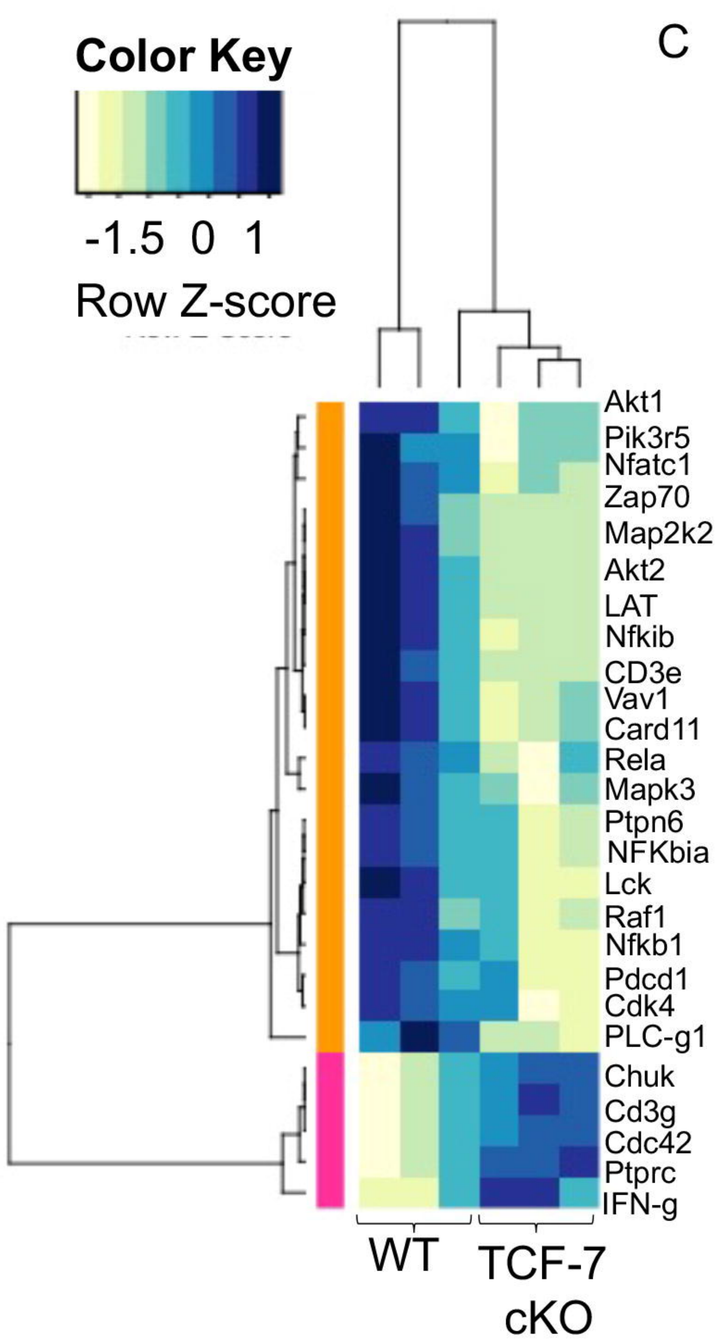
B
Color Key
-1.5 0 1
Row Z-score
Akt1
Pik3r5
Nfatc1
Zap70
Map2k2
Akt2
LAT
Nfkib
CD3e
Vav1
Card11
Rela
Mapk3
Ptpn6
NFKbia
Lck
Raf1
Nfkb1
Pdcd1
Cdk4
PLC-g1
Chuk
Cd3g
Cdc42
Ptprc
IFN-g
WT
TCF-7 cKO

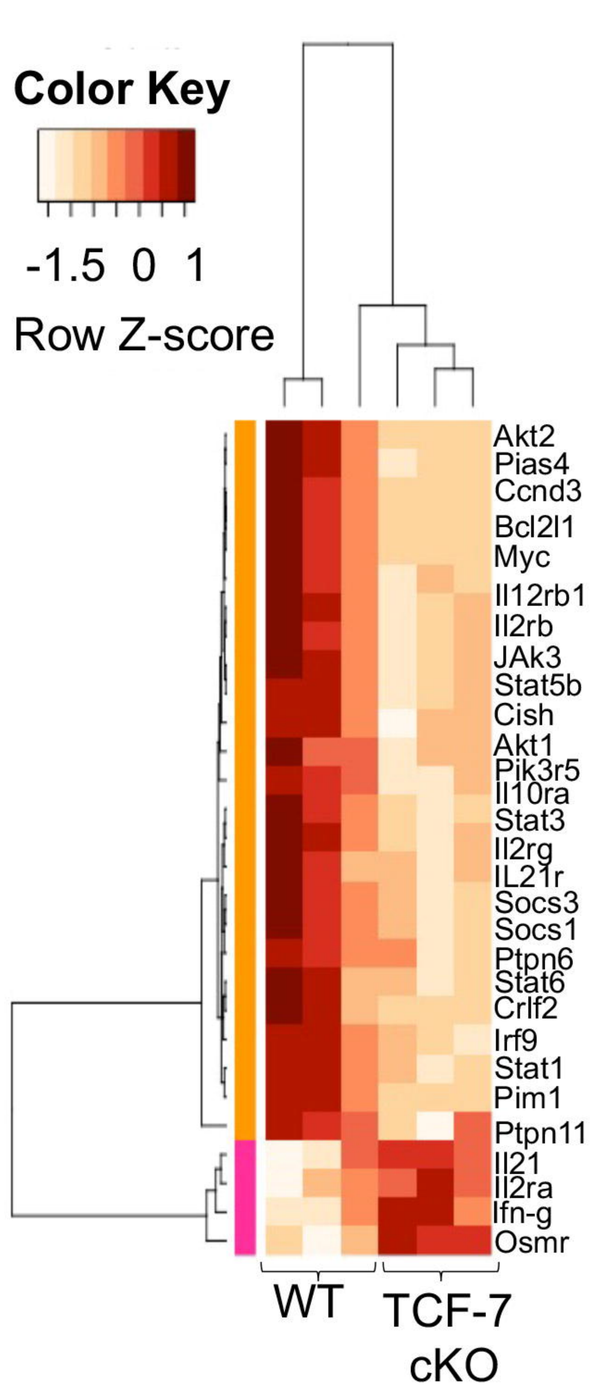
C
Color Key
-1.5 0 1
Row Z-score
Akt2
Pias4
Ccnd3
Bcl2l1
Myc
Il12rb1
Il2rb
JAk3
Stat5b
Cish
Akt1
Pik3r5
Il10ra
Stat3
Il2rg
IL21r
Socs3
Socs1
Ptpn6
Stat6
Crlf2
Irf9
Stat1
Pim1
Ptpn11
Il21
Il2ra
Ifn-g
Osmr
WT
TCF-7 cKO

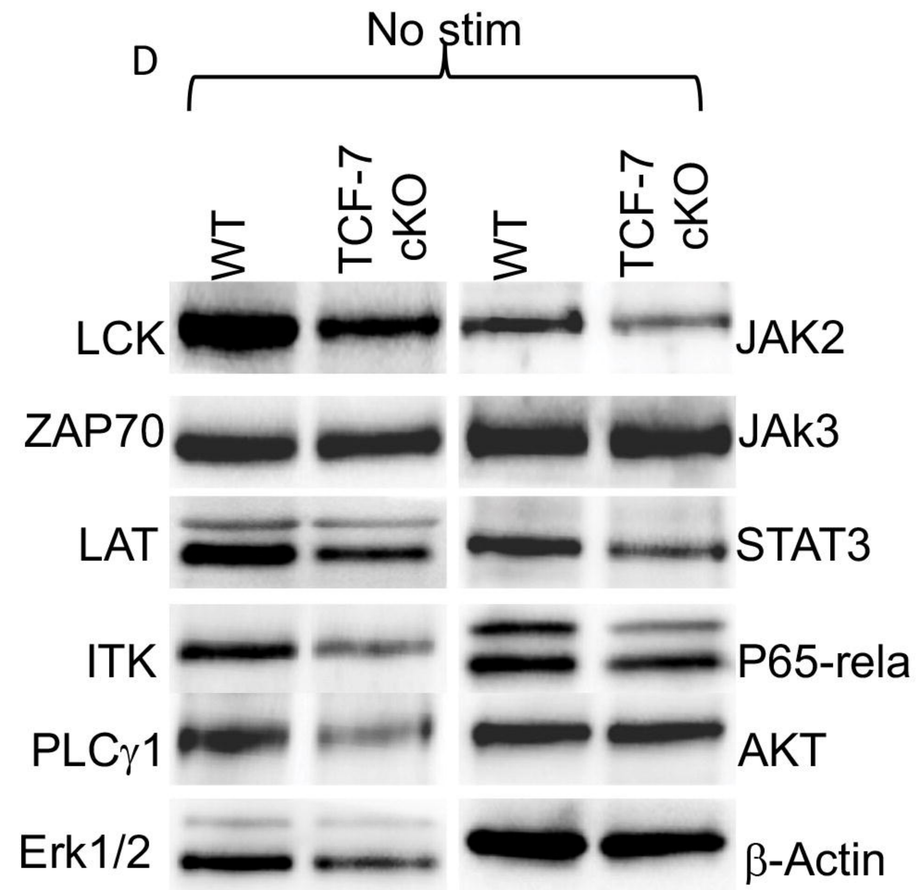
D
No stim
WT
TCF-7 cKO
WT
TCF-7 cKO
LCK
ZAP70
LAT
ITK
PLCγ1
Erk1/2
JAK2
JAk3
STAT3
P65-rela
AKT
β-Actin

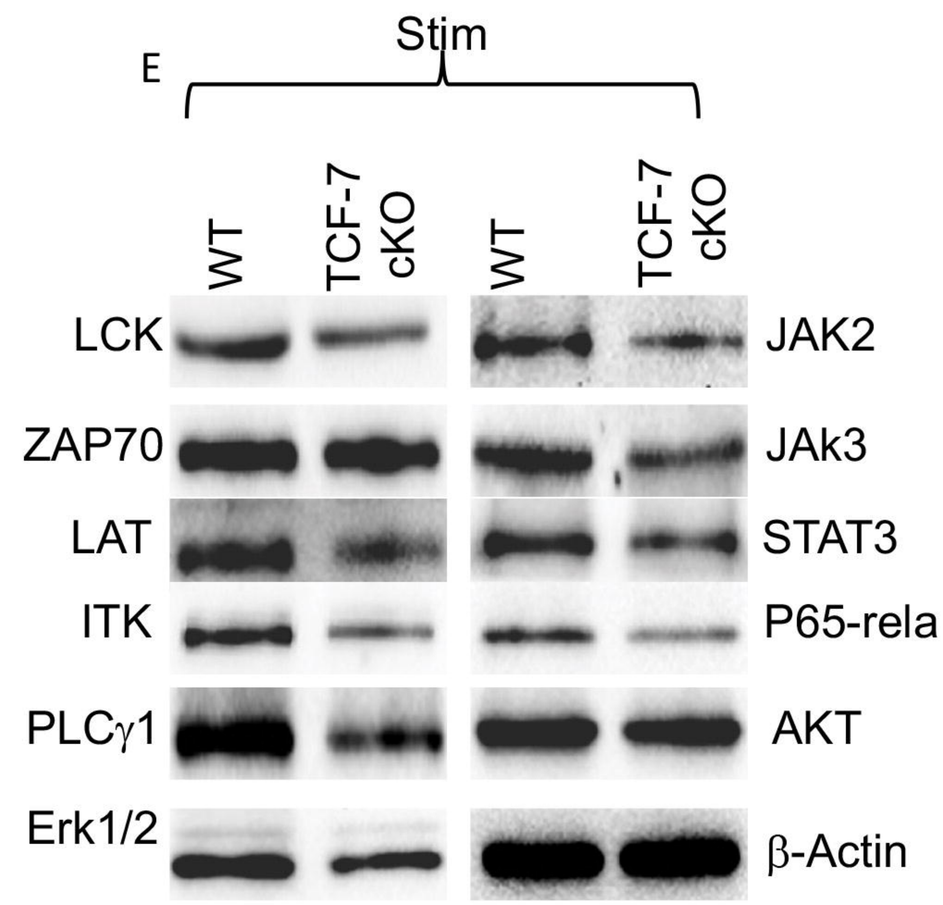
E
Stim
WT
TCF-7 cKO
WT
TCF-7 cKO
LCK
ZAP70
LAT
ITK
PLCγ1
Erk1/2
JAK2
JAk3
STAT3
P65-rela
AKT
β-Actin